

A system perspective on flood risk in polder drainage canal systems

Rikkert, S.J.H.

DOI

[10.4233/uuid:61e6645a-f275-4b69-aa29-1150d3cda2b1](https://doi.org/10.4233/uuid:61e6645a-f275-4b69-aa29-1150d3cda2b1)

Publication date

2022

Document Version

Final published version

Citation (APA)

Rikkert, S. J. H. (2022). *A system perspective on flood risk in polder drainage canal systems*. [Dissertation (TU Delft), Delft University of Technology]. <https://doi.org/10.4233/uuid:61e6645a-f275-4b69-aa29-1150d3cda2b1>

Important note

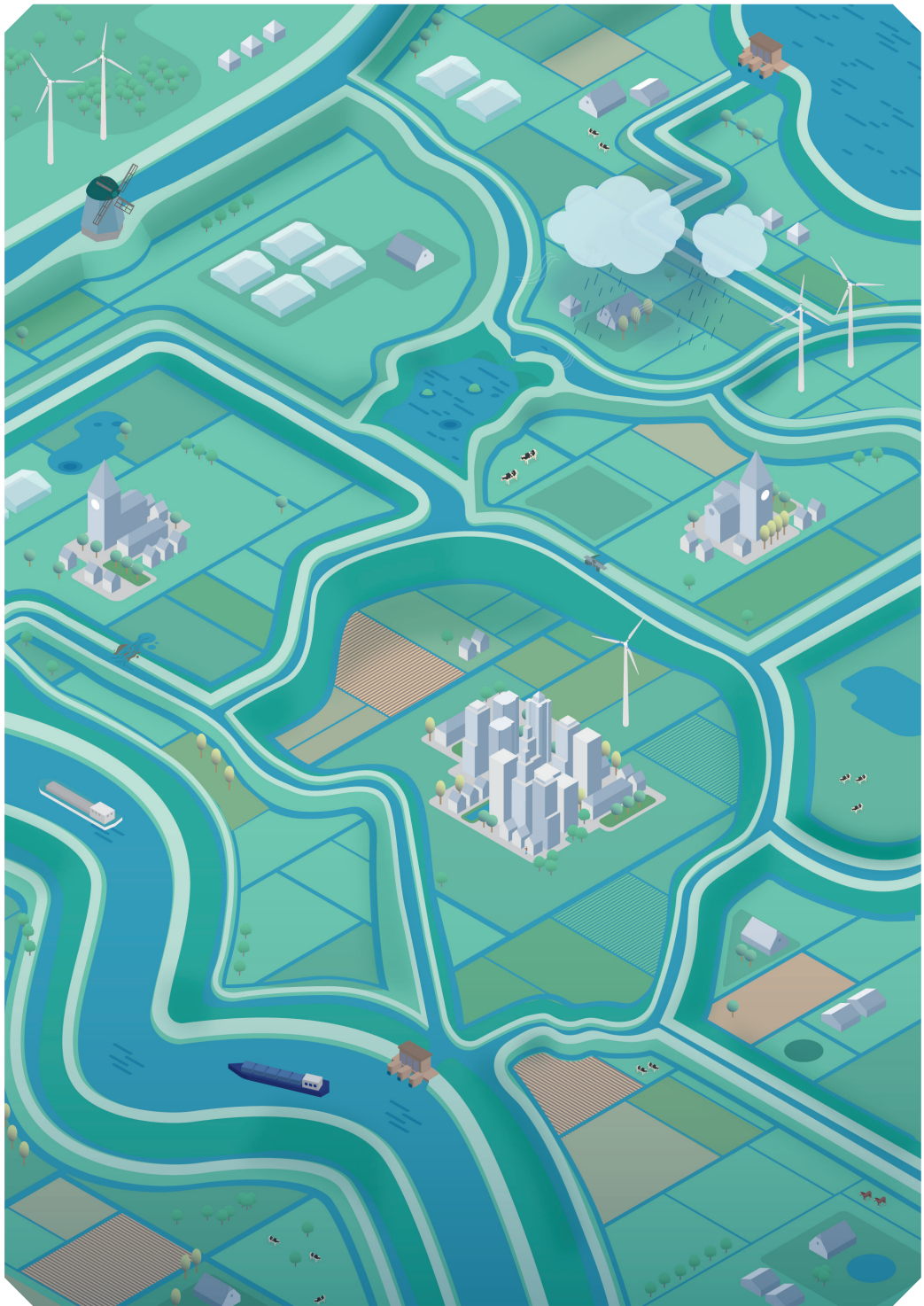
To cite this publication, please use the final published version (if applicable).
Please check the document version above.

Copyright

Other than for strictly personal use, it is not permitted to download, forward or distribute the text or part of it, without the consent of the author(s) and/or copyright holder(s), unless the work is under an open content license such as Creative Commons.

Takedown policy

Please contact us and provide details if you believe this document breaches copyrights.
We will remove access to the work immediately and investigate your claim.



**A system perspective on
flood risk in polder drainage
canal systems**

S. J. H. Rikkert

A system perspective on flood risk in polder drainage canal systems

A system perspective on flood risk in polder drainage canal systems

Proefschrift

Ter verkrijging van de graad van doctor aan de Technische
Universiteit Delft,
op gezag van de Rector Magnificus Prof.dr.ir. T.H.J.J. van der
Hagen,
voorzitter van het College van Promoties, in het openbaar te
verdedigen op woensdag 18 mei om 15:00 uur

door

Stephanus Johannes Hendrikus RIKKERT

Ingenieur in de Civiele Techniek,
Technische Universiteit Delft, Nederland
Geboren te Almelo, Nederland

Dit proefschrift is goedgekeurd door de promotor.

Samenstelling promotiecommissie:

Rector Magnificus, voorzitter
Prof. dr. ir. M. Kok, Technische Universiteit Delft, *promotor*

Onafhankelijke leden:

Prof.dr.ir. R. Uijlenhoet, Technische Universiteit Delft
Prof.dr. J.C.J.H. Aerts, Vrije Universiteit Amsterdam
Priv.Doz.Dr. H. Kreibich, GFZ German Research Centre for Geosciences
Ir. H. van Hemert, Rijkswaterstaat & STOWA
Prof.dr.ir. S.N. Jonkman, Technische Universiteit Delft

Overig lid:

Dr. ir. M.Z. Voorendt, Technische Universiteit Delft

This research was funded by the STOWA



Keywords: flood risk, reliability updating, system behaviour

Printed by: Peter Print

Front and back: Visual of the polder drainage canal system (design by Studio Dirma Janse)

Copyright © 2022 by S.J.H. Rikkert

ISBN: 978-94-6366-543-8

An electronic version of this dissertation is available at

<http://repository.tudelft.nl/>.

Preface

It has been a great journey to work on my dissertation, but especially, to now finish it. I want to thank everyone who has supported me over the years, and I will make a special mention of some key figures, although I am afraid I will forget many.

During the years, I had the chance to work with STOWA and multiple water boards, where I met many friendly and enthusiastic professionals. I want to thank STOWA for their financial support and providing feedback throughout the process. I want to thank the people whom I worked with at the different water boards, with a special mention of the Hoogheemraadschap Delfland and the Hoogheemraadschap Hollands Noorderkwartier for sharing with me their measurement data and the models of their polder drainage canal systems. This was a crucial element in my dissertation.

A big thank you to the TU Delft and my colleagues there. It has been a great pleasure to work in such an ambitious and inspiring environment. A special thanks to Job, Ece, Erik, Orson, and Ermano, with whom I shared the office for many great years. Mark, as my supervisor you spend a lot of your time reading and correcting my work. Thank you for the great discussions we had and the major support you were to me in finalizing the dissertation. Matthijs, you have been a really supportive supervisor and with your positivity you always knew how to inspire me.

I also want to thank my dear friends from Twente. Most of them, I have known for more than 20 years. Along the road, I have met many more great friends, during my years as a student in Delft, but also during my adult life in Dordrecht. Thank you all so much for always being there for me, and for all the great fun we had together.

Dirma, thank you for helping me with the design.

Last, but not least, I want to thank my lovely family, for always being supportive and believing in me. And of course, my wonderful girlfriend Vasileia, for bringing sunshine to my life.



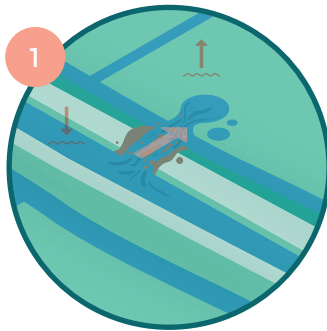
1

2

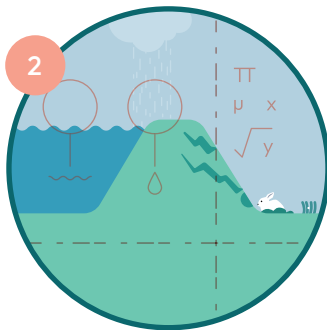
3

Flood risk in polder systems

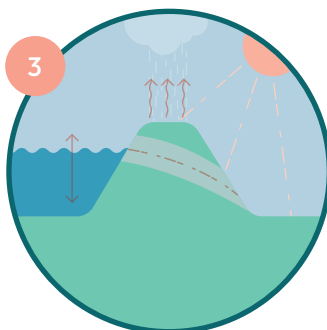
Impression of a polder drainage canal system and the 3 main topics of this dissertation.



Hydraulic load interdependency



Performance-based levee assessment



Rainfall and phreatic lines

Summary

A major part of the Netherlands is prone to flooding: roughly 60%. Therefore, a large system of flood defences protects the country from flooding. These flood defences are divided into primary and regional flood defence systems. Primary flood defences protect areas against catastrophic flooding events from the sea, big lakes and major rivers, whereas regional flood defences protect areas against relatively small flooding events. This dissertation focusses on regional flood defences, and in particular polder drainage canal levees (in Dutch: boezemkaden). These canal levees are located along polder drainage canals (in Dutch: boezemkanalen), which discharge excess water from rainfall and seepage from the polder to the sea or the major rivers. Canal levees play a major role in preventing regional flooding, and are assessed periodically, to keep the risk of levee failure at an acceptable level.

This dissertation focuses on improving flood risk estimations related to regional water systems. More accurate estimations of the risk of flooding support water authorities in spending their resources in a more cost-effective way. This is important, since the outcomes of the levee safety assessments do not reflect well what is observed in practice. Many levees do not meet the required safety level according to the safety assessments, but the number of levee failure cases we encountered over the past decades is very low. For a large part, this discrepancy between the assessments and practice can be attributed to conservatism and simplifications in the current approach for assessment of levee safety. Three aspects of the safety assessment for regional levees are researched in this dissertation. These aspects are:

1. The effect of hydraulic load interdependencies in polder canal systems on levee failure probabilities and flood risk;
2. Inclusion of evidence of survived loads and observations of current levee conditions;
3. The effect of rainfall and evaporation on the phreatic line in, and hence, the stability of levees.

In current flood risk assessments, the levees are assessed individually, neglecting the effects of a levee failure on other parts of the canal system, which leads to overestimation of levee failure probabilities. This dissertation develops a method to quantify effects of hydraulic load interdependency on flood risk in polder drainage canal systems

12

at the system scale. The method consists of modelling the system response to different rainfall events. The levee's ability to resist different water levels was estimated by means of fragility curves and combined with exceedance probabilities of water levels to approximate failure probabilities. The method was applied in two case studies and the outcomes were compared with the current approach. The proposed method allows quantifying the effects of hydraulic load interdependencies on a system scale. This research shows that, by taking into account hydraulic load interdependency, the calculated overall system flood risk significantly decreases, since failure of one levee might mean survival of the other. The inclusion of hydraulic load interdependency also enables different flood risk measures to be assessed on a system level, which makes comparison between measures more complete, potentially leading to different preferred solutions. The effects of hydraulic load interdependence should therefore not be neglected in flood risk assessments of polder drainage.

Many levees have been functioning well for decades, and have survived several relatively high hydraulic loads within their lifetime. However, information on survived load conditions is seldom included in levee safety assessments. Observed degradation from levee inspections is also not taken into account. That way, information that is useful to improve the accuracy on estimations of the actual strength of the levee remains unexploited. This dissertation proposes a pragmatic approach to include observations of survived loads and levee degradation in the levee safety assessment. This approach consists of 3 steps: 1) a prior estimation of the failure probability, based on levee characteristics, 2) a posterior estimation of the failure probability, based on observed hydraulic loads, and 3) correction of the posterior failure probability estimation, based on levee inspections. In a case study, the estimated failure probabilities using this approach were much lower than when information on levee performance was not included. This study demonstrates the value of levee performance observations and how they can be included to improve levee safety assessments.

Most levees along polder drainage canals in the Netherlands permanently withstand water. As water levels in these canals hardly vary, changes of the phreatic water level in the levees are mostly dominated by hydrological processes, such as rainfall and evaporation. These processes are not explicitly included in the current safety assessment and design practices of the Dutch water authorities. Rather on the contrary, the assumed 'extreme' phreatic line that is used in safety assessments, is mainly based on extreme canal and polder water levels. Measurement campaigns of groundwater levels inside these levees have shown that during severe rainfall events the measured phreatic line could exceed the assumed 'extreme' phreatic line, as used in the safety assessment.

This means that for these cases the levee reliability is underestimated, when using the current assessment method. Or in other words: the failure probability is underestimated. At other locations, the measured phreatic line was much lower and less responsive to meteorological variations, which could mean that the assumed 'extreme' phreatic line is too conservative, resulting in an overestimation of the levee reliability, when using the current assessment method. Therefore, the current approach for estimating the extreme phreatic line is too generic. This dissertation proposes to apply conceptual hydrological modelling of the levees to better include the internal and external hydrological processes in combination with measurement of groundwater tables in the levees. The developed models are used to predict phreatic lines under varying meteorological conditions. The model results are in accordance to the field measurements; especially when preferential flow was included. As a final conclusion, this chapter showed that for the tested case studies, inclusion of the rainfall and evaporation leads to better predictions of the phreatic line, which in turn may lead to more accurate levee stability assessments.

Samenvatting

14 Een groot deel van Nederland is kwetsbaar voor overstromingen: ongeveer 60%. Een uitgebreid systeem van waterkeringen beschermt daarom het land tegen overstromen. Deze waterkeringen zijn onderverdeeld in primaire en regionale keringen. Primaire keringen beschermen het land tegen grote overstromingen vanuit de grote rivieren, de zee en de grote meren. Regionale keringen beschermen het land tegen relatief kleine overstromingen uit kleinere, regionale wateren. Dit proefschrift richt zich op deze regionale keringen en in het bijzonder op boezemkaden: de keringen die liggen langs boezemkanalen. De primaire taak van deze kanalen is de afwatering van overtollig water dat via kwel en neerslag de polders binnen komt. Via poldergemalen komt dit water in de boezemkanalen, van waaruit het naar de rivier of de zee wordt afgevoerd. Boezemkaden spelen een cruciale rol in het in stand houden van dit boezemsysteem en het voorkomen van overstromingen. De kaden worden periodiek beoordeeld, om zo het risico van dijkfalen en overstromen op een acceptabel niveau te houden.

Dit proefschrift richt zich op het verbeteren van overstromingsrisicoschattingen met betrekking tot boezemsystemen. Meer accurate schattingen van het risico op overstromen ondersteunen waterbeheerders om hun middelen in een meer kosten-effectieve manier in te zetten. Dit is belangrijk, omdat de uitkomsten van de veiligheidsbeoordeling van boezemkaden de praktijk niet goed weerspiegelt. Veel kaden voldoen volgens de beoordeling niet aan de gestelde veiligheidsnorm, terwijl in de praktijk het aantal dijkdoorbraken de afgelopen decennia daarentegen erg laag was. Dit verschil tussen beoordeling en praktijk is grotendeels toe te kennen aan conservatisme en versimpelingen in de huidige beoordelingsmethodiek. Dit proefschrift gaat dieper in op drie aspecten van deze beoordelingsmethodiek voor veiligheid van regionale keringen, namelijk:

1. Het betrekken van onderlinge afhankelijkheden van de hydraulische belastingen binnen boezemsystemen bij de berekening van de faalkans van individuele boezemkaden en het bijbehorende overstromingsrisico;
2. Het meenemen van overleefde belastingen en observaties van de huidige toestand van een kering bij bepalen van de faalkans van boezemkades;
3. Het effect van neerslag en verdamping op de freatische lijn in

keringen, en daarmee op de stabiliteit van keringen.

In de huidige veiligheidsbeoordelingsmethodiek worden keringen individueel beoordeeld: effecten van dijkfalen elders in het boezemsysteem, en de daarop volgende waterstandsaling worden niet meegenomen, met als gevolg dat de faalkans van een kering vaak wordt overschat. In dit proefschrift is een methode ontwikkeld om de effecten van onderlinge afhankelijkheden van hydraulische belastingen in boezemsystemen te betrekken bij faalkansberekeningen van lokale boezemkaden en het daarbijbehorende overstromingsrisico. De methode bestaat uit het modelleren van de reactie van het systeem op extreme neerslaggebeurtenissen. Het vermogen van de boezemkade om verschillende waterstanden te keren is geschat en gecombineerd met de overschrijdingskansen van die waterstanden om uiteindelijk de faalkans van de boezemkade in te schatten. De methode is toegepast op twee case studies en vergeleken met de huidige beoordelingsmethode. Dit onderzoek toont aan dat het totale geschatte overstromingsrisico op systeemniveau significant afneemt, wanneer deze effecten van belastingafhankelijkheden worden meegenomen, omdat het falen van een kering mogelijk leidt tot overstroming van de achterliggende polder en een waterstandsaling in het boezemsysteem. Dit heeft tot gevolg dat de hydraulische belasting op andere keringen afneemt. Meenemen van deze effecten maakt het ook mogelijk om de effectiviteit van overstromingsrisico-reducerende maatregelen te beoordelen op systeemniveau. Zo kan er een meer complete afweging worden gemaakt tussen maatregelen, wat mogelijk leidt tot andere voorkeursoplossingen. Onderlinge afhankelijkheden in hydraulische belasting in boezemsystemen mogen daarom niet worden verwaarloosd bij de beoordeling van de veiligheid van boezemkaden en afweging van risico-reducerende maatregelen.

Veel boezemkaden functioneren al decennia naar behoren, en hebben in die periode ook al relatief hoge hydraulische belastingen succesvol weten te doorstaan. Echter, informatie van zulke overleefde belastingen wordt maar zelden gebruikt bij de veiligheidsbeoordeling van keringen. Ook informatie over de huidige toestand van dijken uit inspecties wordt niet direct gebruikt in de beoordeling. Dit betekent dat nuttige informatie, die de nauwkeurigheid van schattingen van de actuele sterkte van de kering kan vergroten, veelal onbenut blijft. Dit proefschrift stelt een pragmatische aanpak voor om observaties van zowel overleefde belasting als mogelijke degradatie direct mee te nemen in de veiligheidsbeoordeling. Deze aanpak bestaat uit 3 stappen: 1) een initiële schatting van de faalkans, gebaseerd op karakteristieken van de kering, 2) een verbeterde schatting, gebaseerd op overleefde belastingen, en 3) een correctie van de verbeterde schatting, waarbij ook de huidige toestand van de kering (geobserveerde degradatie) wordt meegenomen. Middels een praktijkvoorbeeld is aangetoond dat faalkansen van keringen

die met deze aanpak worden gevonden significant lager zijn dan wanneer informatie over dijksterkte niet wordt meegenomen. Het onderzoek toont de waarde van observaties van dijksterkte en hoe deze informatie kan worden gebruikt om de veiligheidsbeoordeling te verbeteren.

16

Boezemkaden in Nederland keren permanent water. Door middel van pompen wordt er gestuurd op een streefpeil, en varieert de waterstand nauwelijks. Veranderingen in de ligging van de freatische lijn in boezemkaden worden voornamelijk gedomineerd door hydrologische processen in de dijk zelf, door lokale neerslag en verdamping, en veel minder door de waterstand in de boezem. Deze processen worden niet expliciet meegenomen in de huidige methode voor de veiligheidsbeoordeling. Sterker nog, voor een veiligheidsbeoordeling wordt de ligging van de 'maatgevende' freatische lijn in de kering geschat op basis van de maatgevende waterstand in de boezem en de polder. Meetcampagnes van freatische lijnen in keringen toonden echter aan dat tijdens hevige regenbuien de gemeten freatische lijn de 'maatgevende' freatische lijn soms zelfs overschrijdt. Dit betekent dat voor deze gevallen de hoogte van de freatische lijn wordt onderschat, en daarmee de berekende stabiliteit van de keringen met de huidige methode wordt overschat. Op andere locaties lag de gemeten freatische lijn lager en reageerde deze minder sterk op neerslag, wat voor die locaties kan duiden op een te conservatieve aanname van de freatische lijn in de beoordeling, en daarmee een onderschatting van de stabiliteit. De huidige methode voor de beoordeling van de stabiliteit van boezemkaden is daarom te generiek. Dit proefschrift stelt conceptuele hydrologische modellen voor om hydrologische processen in een boezemkade en de effecten ervan op de freatische lijn beter te representeren. De ontwikkelde modellen voorspellen de freatische lijn onder variërende meteorologische condities en vereisen kalibratie op basis van lokale grondwatermetingen. De modellen gebruiken enkel neerslag en verdamping als invoer, en de voorspellingen komen in redelijke mate overeen met de gemeten freatische lijn, vooral als preferente stroming door de kade is meegenomen. Het meenemen van neerslag en verdamping bij het voorspellen van de freatische lijn in boezemkaden leidt tot betere voorspellingen van de ligging van de freatische lijn, wat op zijn beurt kan leiden tot een meer accurate beoordeling van de stabiliteit van de kering, vooral ook als deze wordt verbonden met de aanpak om ook overleefde belastingen mee te nemen.

Table of contents

| | |
|--------------|----|
| Preface | 7 |
| Summary | 11 |
| Samenvatting | 14 |

| | | |
|----------|---|-----------|
| 1 | Introduction | 20 |
| 1.1 | Motivation for the present research | 21 |
| 1.2 | Background of polder canal levees | 21 |
| 1.3 | Problem analysis | 22 |
| 1.4 | Research objective and research questions | 26 |
| 1.5 | Research approach and report outline | 27 |
| 2 | Flood protection for regional flood defences in the Netherlands | 30 |
| 2.1 | Polder drainage canal levees | 31 |
| 2.2 | Failure mechanisms | 34 |
| 2.3 | Flood safety standards | 35 |
| 2.4 | Levee safety assessments | 36 |
| 2.5 | Dealing with uncertainties in levee safety assessments | 38 |
| 3 | Hydraulic load interdependencies in polder drainage canal systems | 42 |
| 3.1 | Introduction | 43 |
| 3.2 | Development of a flood risk estimation method | 45 |
| 3.3 | Case study 1: Part of a polder drainage canal system (Hoogheemraadschap Delfland) | 47 |
| 3.4 | Case study 2: An entire polder drainage canal system (Hoogheemraadschap Hollands Noorderkwartier) | 59 |
| 3.5 | Discussion | 67 |
| 3.6 | Conclusions and recommendations | 68 |

| | | |
|----------|--|------------|
| 4 | Hydraulic load interdependencies in polder drainage canal systems | 70 |
| 4.1 | Introduction | 71 |
| 4.2 | State-of-the-art of levee safety assessment | 72 |
| 4.3 | Including observed levee strength | 79 |
| 4.4 | Case study | 81 |
| 4.5 | Discussion | 88 |
| 4.6 | Conclusions and recommendations | 90 |
| 5 | Conceptual hydrological modelling of phreatic water levels in polder drainage canal levees | 92 |
| 5.1 | Introduction | 93 |
| 5.2 | Approach | 95 |
| 5.3 | Measurement data | 96 |
| 5.4 | Hypothesis testing: establishing the relation between meteorological, canal water level and the phreatic line measurements | 98 |
| 5.5 | Hydrological modelling of the phreatic line | 100 |
| 5.6 | Discussion | 107 |
| 5.7 | Conclusions and recommendations | 108 |
| 6 | Conclusions and recommendation | 110 |
| 6.1 | Conclusions | 110 |
| 6.2 | Recommendations for future studies | 111 |
| 6.3 | Recommendations for current practice | 113 |
| | Appendix A - Derivation of fragility surfaces | 116 |
| | Appendix B - Results of cross-correlation analysis | 118 |
| | References | 122 |
| | Curriculum Vitae | 128 |
| | List of publications | 129 |

1



Introduction

1.1

Motivation for the present research

Worldwide, the population of people at risk from floods is expected to increase from 1.2 billion in 2012 to 1.6 billion in 2050. Annually, 100 to 200 million people are victim of flooding and economic losses are estimated to range between USD 50 to 100 billion (OECD, 2012). Flood risk is defined by two components: the probability of a flood event, and the consequences of the event. Following the classification of the multi-layer safety approach, measures to reduce flood risk can be divided into 3 safety layers: 1) prevention, 2) spatial planning, and 3) disaster management (Ministry I&E, 2009). The prevention measures often consist of building and strengthening flood defence structures. The spatial design considers developing land in a way that consequences of flooding are limited. Disaster management focuses on measures to take during a flood that limit the consequences (Kok et al., 2017). This dissertation focuses on the first layer: prevention.

Several failure mechanisms can cause flood defence structures to fail, potentially leading to catastrophic flood events (CIRIA, 2013). Building and strengthening of flood defence structures is very costly. Therefore, to be effective, the risk reduction should outweigh the costs of the measure. A fair comparison between flood risk reduction measures requires an accurate estimation of the actual failure probability. This dissertation aims at improving the way to estimate levee failure probabilities, hence improving the accuracy of flood risk estimations.

1.2

Background of polder canal levees

The Netherlands is a densely-populated delta, and prone to flooding from several directions. From the east and the south, rivers enter the country, while in the north and the west, the country is bordered by the sea. Especially in the low-lying areas, rainfall and seepage create an excess of water. In these areas, a continuous effort is needed to discharge excess water towards the rivers, the lakes and the sea. Without its extensive system of flood defences, about 60% of the country can be flooded by water from the major rivers, lakes and sea, with water depths up to 5 meters as a consequence (Kok et al., 2017). Figure 1.1 shows which areas in the Netherlands are prone to flooding.

Flood defences in the Netherlands are divided into two categories: primary and regional flood defences. The former protect the country against large scale floods from the sea, the main rivers and lakes, whereas the latter can be found along regional rivers, canals and smaller lakes. Figure 1.2 shows a map of both categories. As can be seen, both systems look very different in terms of total length and density. Primary flood defences follow the major waters, and have a total length of approximately 3,400 km (Waterveiligheidsportaal). Regional flood defence systems are mainly situated in low lying parts in the north and west, and consist of long and dense networks. Altogether, they have an approximate length of 11,500 km (Pleijster & Van der Veeken, 2015). According to the Dutch Water Law, the primary flood defences should provide protection against flooding and a reduction of the potential consequences. Therefore, the primary flood defences need to provide the minimum safety level that is stated in the Dutch Water

Law. The provinces determine the required safety level for the regional flood defences. The north and west of the Netherlands consists to a large extent of polders.

Hoes and Van de Giessen (2018) define a polder as “a level area which has originally been subject to a high groundwater or surface water level, and is separated from the surrounding hydrological regime, to be able to control the water levels in the polder”.

The majority of the regional flood defences consist of polder drainage canal levees (Dutch: boezemkades) situated along polder drainage canals (Dutch: boezemkanalen). A simplified representation of the polder system is shown in Figure 1.3. In the remainder of this dissertation, these polder drainage canal levees and polder drainage canals are referred to as canal levees and canals. Canal levees ensure that the water from the canals does not flow into the polders and that excess water can be drained away from these polders. These canal systems can consist of hundreds of kilometers of canals, receiving water from hundreds of adjacent polders. The canal levee system exist of levee sections, that are distinguished based on potential economic consequences of a flood. To keep flood risk below acceptable levels, levee sections are assigned flood protection standards. These levee sections are periodically assessed on multiple failure mechanisms to evaluate if they still meet the required safety level. Usually, a characteristic cross-section is assessed in such an assessment. However, if the levee characteristics vary a lot over the length of the levee section, the section can be divided into smaller sub-sections, and these sub-sections are assessed separately.

1.3 Problem analysis

Dutch canal levees hardly ever fail in practice. We define levee failure as the hydraulic load exceeding the levee's resistance, consequentially leading to flooding. In the 60 years between 1959 and 2019, there have been only two cases of levee breaches that eventually led to flooding of the polder. Based on these observations, the annual failure probabilities of individual levee sections appear to be small: not larger than 1/600 on average (Rikkert and Kok, 2019). However, canal levees often do not meet the safety requirements, according to the calculations performed in safety assessments. To illustrate, roughly one third of 3,100 km of regional levees in South Holland did not pass the safety assessment in 2012 (Province of South Holland, 2019). As financial resources are limited, it is important that levee safety assessments are accurate, to ensure that money is spent where it is most effective. This dissertation addresses 3 problems that are important to improve the reliability estimation of polder levees. The remainder of this section briefly introduces these problems.

Problem 1: system behaviour neglected in safety assessments

Individual canal levee sections are elements of a larger system of levees. Failure in one element affects also the other elements. However, this system behaviour is not included in flood risk assessments: levees are assessed per individual section. Several studies have shown that, at least for river systems, the effects of hydraulic system behaviour on flood risk are significant (De Bruijn et al., 2014; Vrouwenvelder, 2010; Klerk et al., 2014). This system behaviour means that events in one location in the catchment affect the situation at other locations. For example, if a levee along the upstream part of the river breaches, part

of the river discharge will flow through the breach. This affects the river discharge downstream, and hence the failure probabilities of the levees downstream. Polder canal systems are different to river systems, as there is not always a clear upstream and downstream part. Another important difference with river catchments is that the storage volume of polders is relatively large compared to the total water volume in the canals. This means that a breach of a canal levee can have a large impact on the canal water level, and hence on other levees in the flood defence system. Not taking into account hydraulic load interdependencies leads to incomplete, and possibly even inaccurate results of safety assessments.

Problem 2: evidence of survived loads and information about current levee conditions is unexploited

Most canal levees have been functioning well for decades, sometimes even centuries. During their lifetime, they have experienced and successfully withstood multiple extreme hydraulic loads. Observations of survived loads are a valuable source of information. If the survived loads are included in the safety assessment, this could greatly reduce the uncertainty in the assessment outcomes, often leading to lower failure probabilities (see for example Schweckendiek, 2014). But not only the loads can vary over time, also the resistance might vary. Water authorities perform regular inspections, to ensure the integrity of levee structures. The inspection results contain important information about the actual condition of a levee. The current levee safety assessment method does not allow for inclusion of this evidence on survived loads and the current levee state, which leaves important information unexploited.

Problem 3: levee response on meteorological conditions is not known

To properly estimate flood risk on the system scale, it is important to understand

how individual levee sections behave under certain hydraulic loading conditions. In current safety assessments, the canal water level is considered to cause the main hydraulic load. Effects of rainfall are only implicitly included in the stability calculations, by assuming a convex shape of the so-called phreatic line. However, recent measurement campaigns show that rainfall has a considerable effect on the hydraulic head in some individual levee sections, while in other locations the effects of rainfall are hardly noticeable (Flanagan and Tigchelaar, 2016). At the same time, canal water level variations are very small (centimeters to decimeters). Several studies attempted to model the phreatic line in levees, but without satisfactory results (Ten Bokkel Huinink, 2016; De Loor, 2018; Dorst, 2019). The large uncertainty in the estimation of the phreatic water level in a levee could lead to an over- or underestimation of the actual failure probability, leading to inadequate measures.

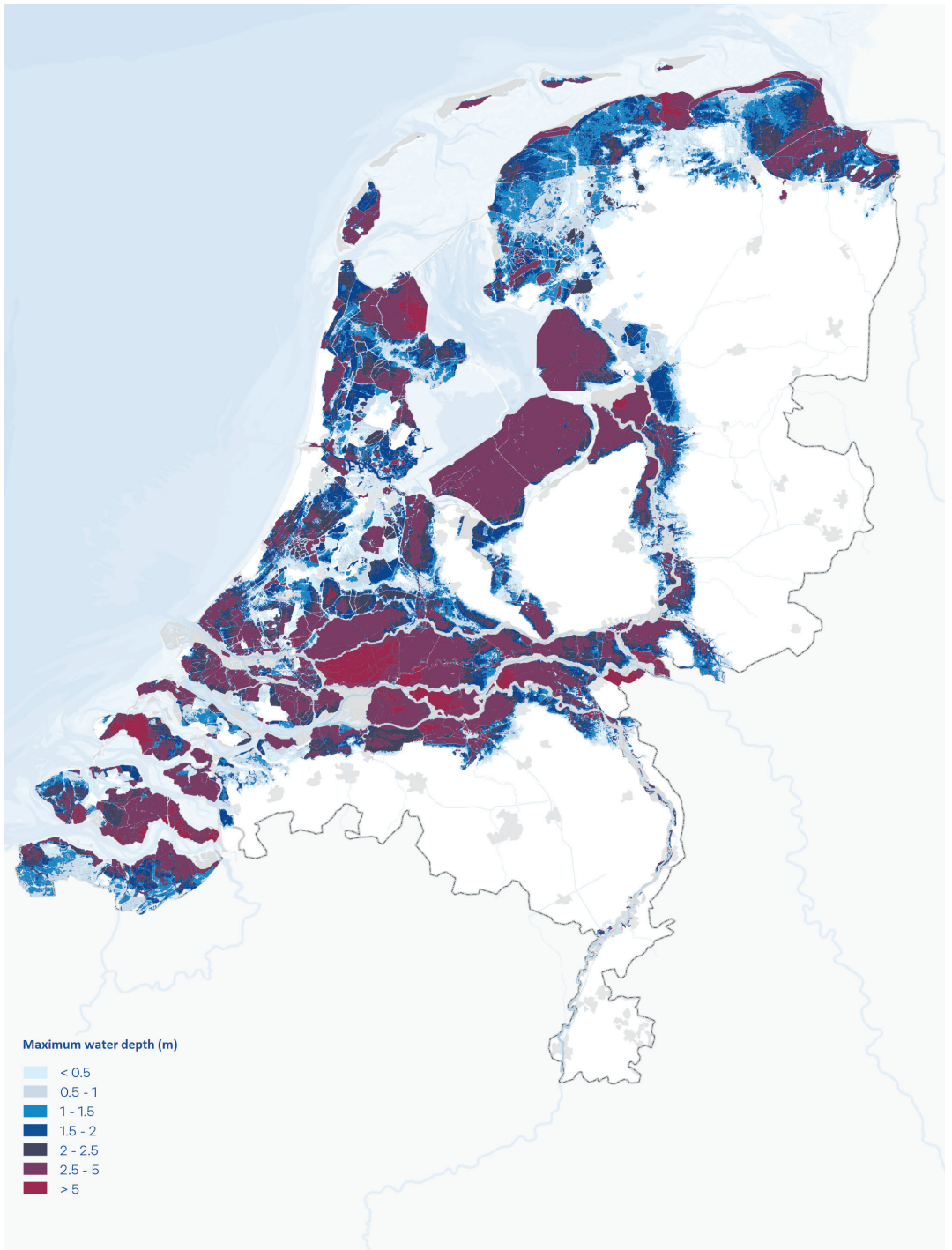


Figure 1.1
Map of the Netherlands, which indicates the area prone to flooding, including maximum water depths (Kok et al., 2017).



LEGEND

- Primary flood defences
- Regional flood defences

Figure 1.2

Map of the Netherlands, showing the primary flood defences (dark green) and regional flood defences (light green) (source data primary flood defences: Waterveilighedsportaal, source data regional flood defences in the Netherlands: Pleijster & Van der Veeke, 2015).

50 km

1.4 Research objective and research questions

The objective of this dissertation is to improve flood risk estimations of polder canal levee systems.

The three problems identified in Section 1.3 lead to three consecutive research questions:

1. The neglected system behaviour in safety assessments of regional levees leads to the first research question: How do hydraulic load interdependencies in polder systems influence flood risk?
2. Evidence of survived loads and information about current levee conditions is currently unexploited in levee reliability estimations. This valuable information, that can be obtained from observed loads, and from observations on the actual condition of the levee from inspections,

increases the accuracy of levee reliability estimations. This leads to the second research question: How can evidence of survived loads and observations of the actual levee condition be included in safety assessments of polder canal levees?

3. The response of the levee to meteorological conditions is not known. Each levee section is unique and therefore levee sections can respond differently to similar extreme meteorological events. The phreatic line in one levee section might hardly be affected by a rainfall event, while in another levee section it responds strongly. This is important, since the phreatic line plays a role in the levee's stability. The effects of rainfall and evaporation are, however, not explicitly taken into account in current levee stability estimations. The third research question therefore is: How do meteorological inputs influence the phreatic line in polder canal levees?

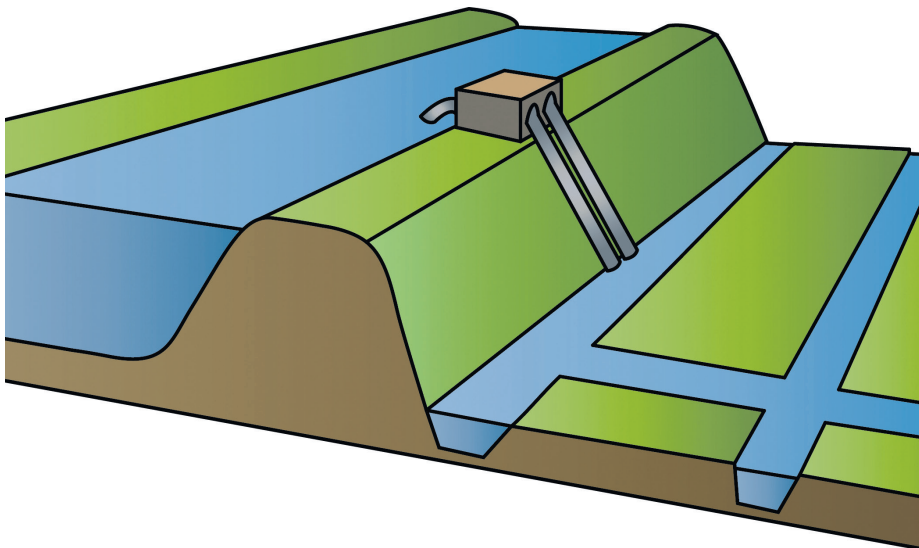


Figure 1.3
Visualization of a polder drainage canal system.

1.5 Research approach and report outline

This dissertation is divided into multiple chapters. Chapter 2 gives a general background on flood protection for regional flood defences in the Netherlands. Chapters 3, 4 and 5 each answer one of the research questions. Figure 1.4 shows the overall outline of this dissertation.

Flood protection for regional flood defences (Chapter 2)

This chapter contains the background information that is necessary to set the context of this dissertation. It explains how polder drainage canal systems work and why they are necessary. Chapter 2 also introduces the concepts on which current safety standards and safety assessments are based.

Hydraulic load interdependencies in polder drainage canal systems (Chapter 3)

To answer research question 1, a method is developed that determines the effects of hydraulic load interdependencies in polder systems. The method is applied to two different case studies to demonstrate that including hydraulic load interdependencies leads to improvement of levee reliability analysis. These case studies consist of parts of the polder system of two different water boards: Delfland and Hollands Noorderkwartier. A comparison is made between flood risk assessments without and with taking into account hydraulic load interdependencies. The effect of multiple flood risk reducing measures were assessed on the system scale.

A pragmatic, performance-based approach to levee safety assessments (Chapter 4)

Observations of survived loads or the current condition of a levee are a valuable source to increase the accuracy of levee

reliability estimations. In Chapter 4, a method is developed that includes this information in levee reliability estimations, answering research question 2. This method consists of a probabilistic assessment of the levee's stability. The method allows for iteratively updating the estimated failure probability by including observations of survived loads and observations of the current condition of the levee. Then, both the developed method, as the current assessment method are applied on a case study. Finally, the results of both methods are compared.

Conceptual hydrological modelling of phreatic water levels in polder canal levees (Chapter 5)

To answer research question 3, a hydrological model is developed that makes it possible to include effects of rainfall on the hydraulic head in canal levees. Second, the developed hydrological model configurations are tested on a case study. Using measurement data obtained in a campaign of hydraulic head measurements, the hydrological models are calibrated and validated.

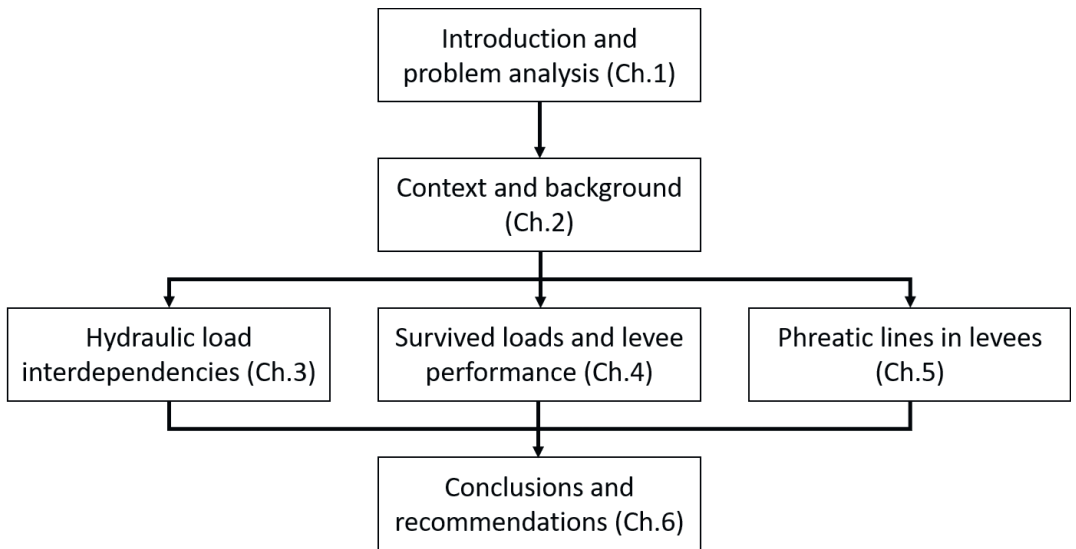


Figure 1.4
Outline of this dissertation.

2



**Flood protection for
regional flood defences in
the Netherlands**

2.1 Polder drainage canal levees

The Netherlands is a low-lying country that is protected against flooding by an extensive flood defence system, distinguished in primary and regional flood defences. The primary flood defence system protects the country against flooding from the main rivers, large lakes and the sea, whereas the regional flood defence system protects the country against flooding from regional rivers, canals and smaller lakes. There are more than 11.500 km of these regional flood defences (Rikkert and Kok, 2019), of which the bulk consists of polder drainage canal levees (Dutch: *boezemkaden*). A large part of the Netherlands is prone to flooding, as there are nearly 4,000 polders in the Netherlands (Geuze and Feddes, 2005). Polders are low-lying areas, protected against flooding by surrounding flood defences. Due to the low surface elevation of polders, rainfall and seepage leads to an increase of the groundwater level. While part of this water evaporates or is stored in open water bodies, such as ditches and ponds, the remaining water cannot be discharged through natural gravity flow. This excess water must therefore be pumped away into polder drainage canals (in Dutch: *boezems*), referred to as drainage canals in the remainder of this dissertation. Water is discharged through these canals by additional pumping stations and sluices to an adjacent river or to the sea. The local water authorities regulate the water level in drainage canals and aim to keep it at a constant level. The water level in the canal is almost completely controlled by pumping stations, which on one hand pump the water into the canal, and on the other hand pump the water from the drainage canal to main rivers or the sea. Wind setup influences the water level as well, but in the daily practice, the water levels in the canals hardly vary. A schematization of how this system functions is shown in Figure 2.1.

Even though the drainage canals are necessary to discharge excess water, they pose a constant threat of flooding to the polders because the flood protection system can fail, and the water level in these canals is often higher than the surface level of the surrounding polders. Breaching in levees along such canals has resulted in flooding of the adjacent polder causing local economic and social disruption, as occurred in Tuindorp Oostzaan (1960) and Wilnis (2003). Therefore, the levees along these canals require a continuous effort of safety assessment, inspection, maintenance, and, if necessary, strengthening. Figure 2.2 shows a picture of a canal levee and a schematic representation of such a levee.

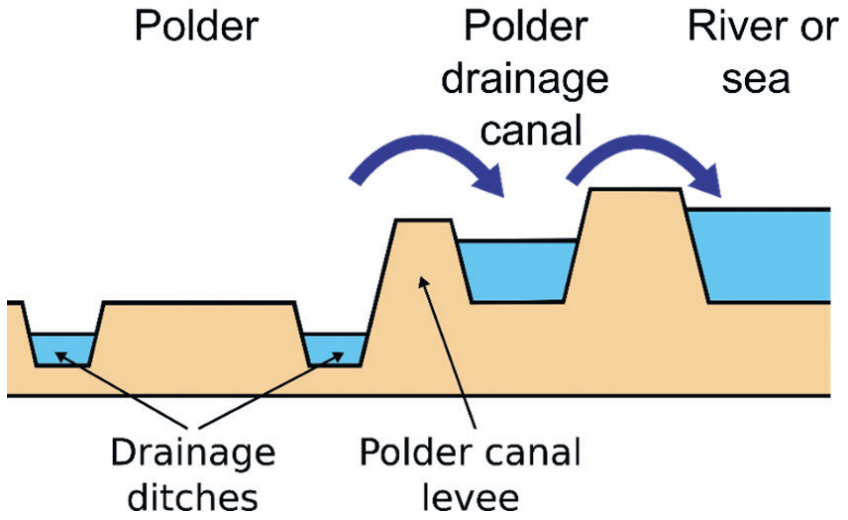


Figure 2.1
Schematization of a polder drainage canal system, showing the polder in which water is collected through drainage ditches. Excess water is pumped to the polder drainage canal, through which it is discharged towards a river or the sea. Note that the horizontal and vertical scale are not identical.

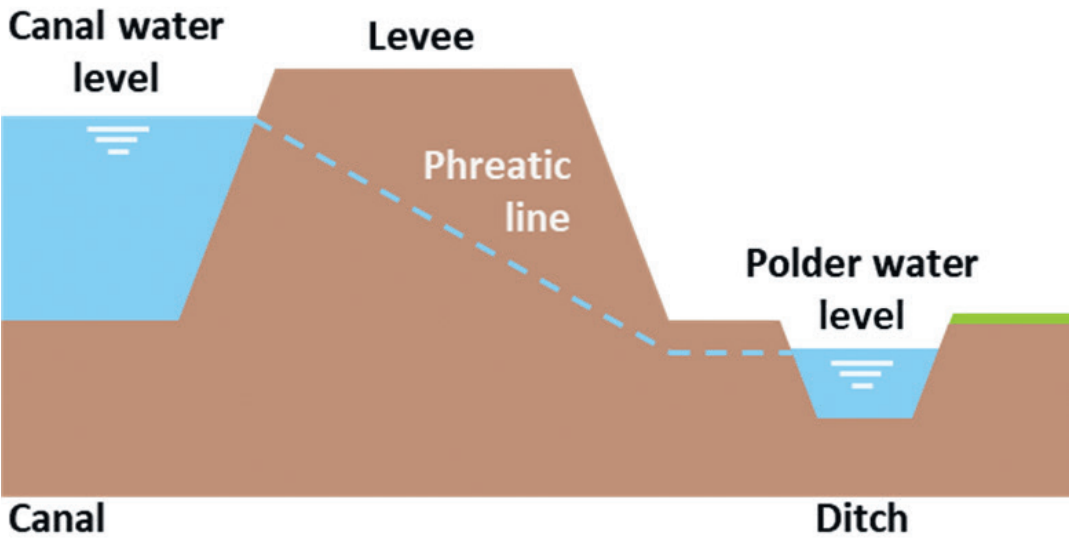


Figure 2.2

Upper: picture of a regional levee along the Rotte, near Rotterdam (picture by Mark Voorendt).

Lower: a cross-section of a canal levee, showing the hydraulic loads (canal water level and phreatic line) that act on the levee.

2.2 Failure mechanism

There are many mechanisms that can cause a levee to fail. As mentioned by Lendering (2018), the dominant failure mechanisms for canal levees are continuous overflow, macro-instability of the landslide slope and uplift and piping. An overview and explanation of these mechanisms is shown in Figure 2.3, 2.4 and 2.5. Interestingly, the

failure cause of the breach at Tuindorp Oostzaan (1960) was never found. It is assumed that it is caused by combination of factors, such as increased use by heavy military vehicles and leakage of a water pipe (Hieselaar, 2010). The failure at Wilnis in 2003 was most likely caused by horizontal instability due to drought (Van Baars, 2005). The causes of the failure are not explicitly considered in current safety assessments for canal levees.

Figure 2.3
Continuous overflow: occurs when the canal water level exceeds the levee crest height, which leads to a continuous flow of water over the levee, potentially damaging the crest, landside slope and landside toe.

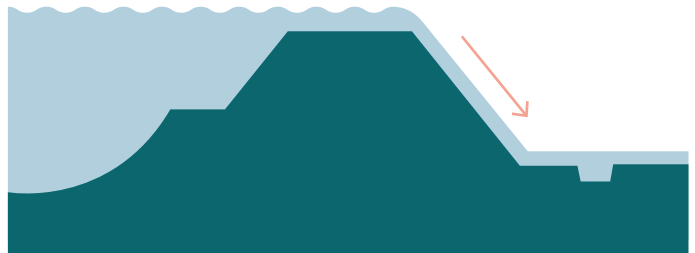


Figure 2.4
Macro-instability of the landside slope: occurs when the inner landside slope slides, due to water pressure exerted against the structure and increased pore pressure in the subsurface.

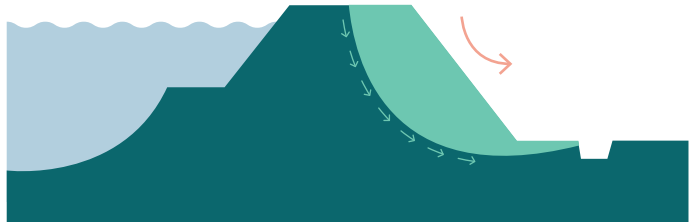
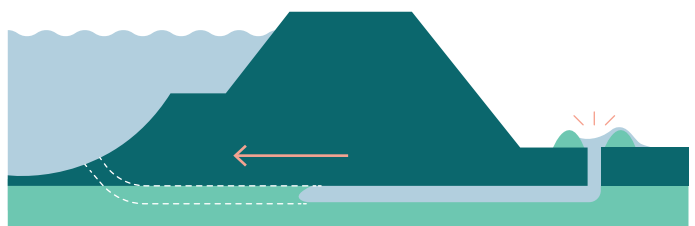


Figure 2.5
Piping: occurs when the head difference over a levee causes internal erosion during which shallow pipes are formed in the direction opposite to the flow underneath the levee as a result of the gradual removal of sandy material by the action of water (Van Beek, 2015).



2.3 Failure mechanism

To get more insight in the condition of the canal levees in the Netherlands, a first systematic assessment of their safety was finished in 1992. This assessment focused on the 200 most important polders in the Netherlands, using for the first time a uniform approach. The height and stability of the levees were considered with respect to one extreme canal water level (in Dutch: maatgevend boezempeil). Out of the 1,730 km of levees that were assessed, over 20% was considered unsafe (TAW, 1993). One of the important conclusions of that report was that there was not yet a required level of safety provided for the regional flood defences. Flood protection standards for primary flood defences have already been used since 1960, after the flooding of the South West of the Netherlands (STOWA, 2004). Protection standards came decades later for regional flood defences. Assigning flood protection standards to the regional flood defences became a task of the provinces (IPO, 1999). Regional levees were divided into levee sections, based on the possible consequences of levee failure. If a breach in location A and B both lead to similar floods in the same area, they can be considered as the same levee section. Based on the severeness of the potential flood in terms of economic damage, each levee section is assigned a flood protection standard. The higher the potential damage, the higher the required level of safety the levee should provide. The risk of loss of life is not considered in determining safety standards for regional flood defences, as flooding of the polder goes relatively slow, and flood depths are relatively low (IPO, 1999). Table 2.1 gives an overview of the 5 different classes of flood protection standards, and the corresponding allowed exceedance probabilities of the water level. This means that the levee should provide sufficient safety for the water level

that is exceeded with the given annual probability corresponding with the levee section's safety class. This is the so-called "exceedance probability approach".

The flood protection standard in the exceedance probability approach prescribes the hydraulic conditions that should be considered in the levee safety assessment. For example, a levee section with safety class 1 should provide sufficient safety for the water level with an annual exceedance probability of 1/10. A levee section with safety class 5 should provide sufficient safety for the water level with an annual exceedance probability of 1/1,000. For primary flood defences, flood protection standards were expressed in terms of annual exceedance probabilities of water levels as well. Since 2017, however, the safety standards are expressed in terms of probability of flooding due to failure, or the "failure probability approach". This refers to the probability that "for all possible loads, the flood defences loses their water retaining capacity at one or more places, allowing flooding to occur" (Kok et al., 2017). Both approaches are directly linked to each other, the main difference is how uncertainties are dealt with (Maaskant, 2021). An important benefit of the failure probability approach is that it gives more opportunities to improve the risk assessment, for instance through reliability updating. Whereas the exceedance probability approach makes use of more conservatism and generalizations in the assessment. This becomes more clear in the remainder of this dissertation.

2.4 Safety assessment for regional flood defences

2.4.1 Guidelines for the Safety Assessment of Regional Flood Defences

Local water authorities (in Dutch: waterschappen) are responsible for periodically assessing the main part of the regional levees to ensure that levees meet their safety requirements. The current procedure for the assessment of regional flood defences is described in the Guidelines for the Safety Assessment of Regional Flood Defences (Dutch: Leidraad Toetsen op Veiligheid Regionale Keringen) (STOWA, 2015a). For specific and technical details these guidelines refer to several background reports. As mentioned by Lendering (2018), the dominant failure mechanisms are continuous overflow, macro-instability of the landside slope and piping. Other mechanisms, such as instability of the revetment or wave overtopping typically have a negligible effect to the failure probability. The importance of the dominant failure mechanisms becomes also clear through the failure budget. Through this failure budget it is suggested how the allowable overall levee failure probability can be divided over the different failure mechanisms. Depending on the safety standard, a levee needs to be able to withstand a water level with a specified

exceedance probability. It is suggested that the overall failure probability of a levee is a factor 5 smaller than this exceedance probability of the water level (Fugro, 1998). For example, a levee with IPO safety standard 3 should be able to withstand an extreme water level with an annual exceedance probability of 1/100 (see Table 2.1. Given that the levee meets the required level of safety, the overall failure probability is assumed to be at least a factor 5 lower. In this example, this results in an annual failure probability of 1/500. Now, from this overall failure probability 80% is reserved for instability of the landside slope, 10% for failure due to continuous overflow and wave overtopping, and 10% for other failure mechanisms, such as piping (IPO, 1999). The following subsections give a brief explanation of how the failure mechanisms are assessed for regional flood defences. For macro-instability and piping, the guidelines make a distinction between a simple, detailed and advanced assessment (STOWA, 2015a). The assessment usually starts with a simple assessment, which rules out the probability of the failure mechanism, based on relatively simple levee characteristics. If the simple assessment is not sufficient, a detailed assessment is necessary. This requires more effort and information and makes use of more advanced calculation methods. The advanced assessment is very specific to the assessed case, and is usually carried out by specialists (STOWA, 2015a).

Table 2.1

The 5 classes of flood protection standards with corresponding required probabilities of exceedance of the water level (IPO, 1999) and potential damage (price level 2019) (Nieuwjaar, 2020).

| Flood protection class | Annual exceedance probability | Potential damage [10 ⁶ €] |
|------------------------|-------------------------------|--------------------------------------|
| 1 | 1/10 | < 12.5 |
| 2 | 1/30 | 12.5 – 40 |
| 3 | 1/100 | 40 – 125 |
| 4 | 1/300 | 125 – 400 |
| 5 | 1/1,000 | > 400 |

2.4.2

Continuous overflow

The procedure for assessing overflow is based on the extreme water level in combination with a local water level increase, and a safety margin. If the levee crest height is lower than the extreme water level plus the local water level increase plus a safety margin, the levee does not meet the required safety level, and the levee is considered unsafe. The local water level increase is usually caused by wind set-up. The safety margin is 0.1 m for canals and lakes with a controlled maximum water level, and 0.2 m for canals and lakes with a limited controlled maximum water level (STOWA, 2015a). Levee heightening is a common measure in this case.

The extreme water level, and local water level increases, can be determined based on statistical analysis of historical data. However, the water level data collection is often not long enough for accurate extreme value predictions. Therefore, hydraulic and hydrological models are often used to simulate the canal water levels under extreme conditions. The water levels are highly regulated, so when canal water levels become too high, the drainage of excess water from polders into the canals is stopped: the so-called ‘drainstop’ (Lendering, 2018).

2.4.3

Macro-instability of the landside slope

The first question in the simple assessment for levee stability is if the levee meets the safety requirement in an earlier assessment, or has been strengthened based on the recent design standards, and hydraulic loading conditions and other levee characteristics have not changed. If this is the case, the levee can be considered safe. If this is not the case, the levee might still pass the simple assessment, if the levee has a “safe” dimensions, which can be the case for over-dimensioned levees (STOWA, 2015a).

The detailed assessment consists of stability calculations. Usually, these calculations follow the Bishop method (Bishop, 1955). Important hydraulic load conditions in these calculations are the canal water level, the phreatic line in the levee and traffic loads on the levee, in case a road is present. The phreatic line under extreme conditions is usually estimated following a one-size-fits-all approach, in which rainfall is not explicitly taken into account. This approach determines the phreatic line, based on levee characteristics and the canal water level (Expert Workshop, 2008). For the traffic loads, a conservative approach is used. If a road is present, the weight of a heavy truck is considered: 30 kN/m² over a width of 2.5 m (STOWA, 2015a).

Interestingly, based on the stability calculations, the canal levees are often considered unsafe, even though the extreme water level hardly varies from the daily water level. This is illustrated by the results of the safety assessment for the Starnmeer (HHNK, 2015) and the Eilandspolder (HHNK, 2019a), where respectively 50% and 61% of the levees were found insufficiently safe for macro-instability.

2.4.4

Piping

The simple assessment is performed by checking the sensitivity of the levee and the subsoil to piping. This failure mechanism can be ruled out if one of the following criteria is met:

- The levee consists of sand and is built on a sand layer;
- An entrance point is lacking;
- An exit point is lacking;
- Vertical transport of sand (heave) does not occur.

The detailed assessment of piping follows the equations for piping, as formulated by Sellmeijer et al. (2011).

2.5 Dealing with uncertainties in levee safety assessments

One of the major challenges in the safety assessment is dealing with uncertainties. As mentioned by Kok et al. (2017), in hydraulic engineering, uncertainty is generally categorized into:

- Aleatory uncertainty, which refers to natural variability. This type of uncertainty arises from pure randomness that cannot be reduced by doing additional measurements.
- Epistemic uncertainty, which is uncertainty resulting from a lack of knowledge. This type of uncertainty can be reduced by doing further analysis or additional measurements.

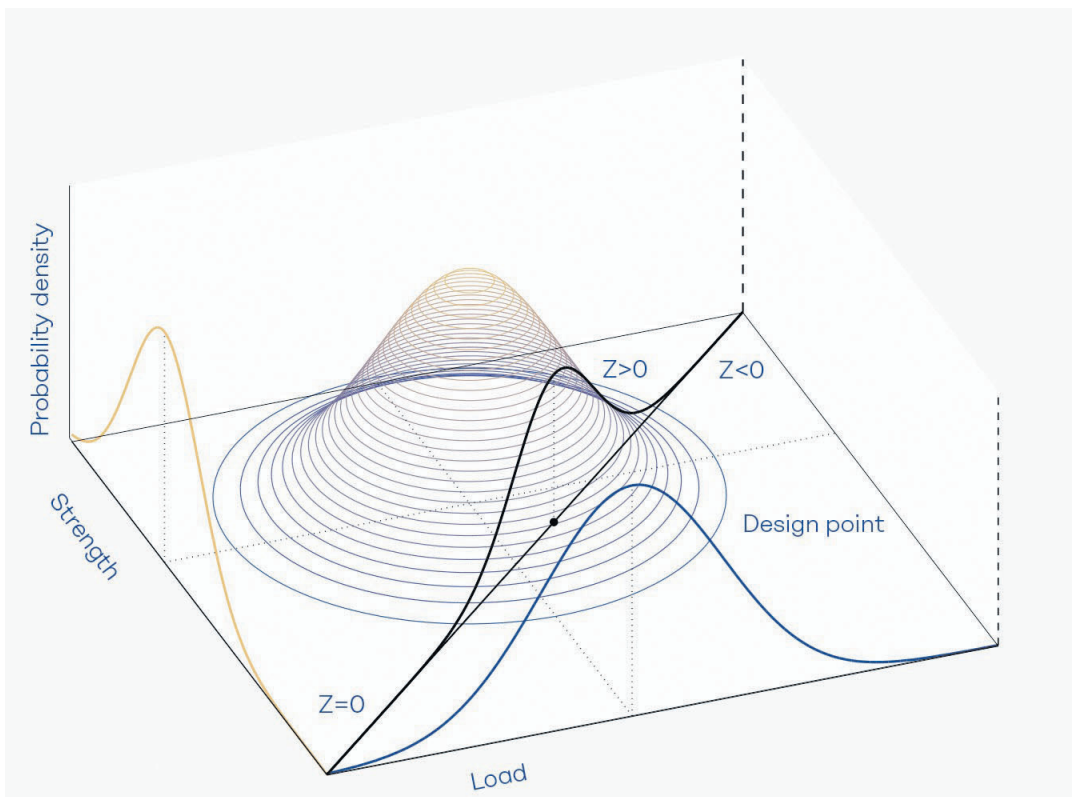
Full-probabilistic levee safety assessment methods take these uncertainties of the load and strength parameters into account and calculate a failure probability, which is the probability that an uncertain load will exceed the uncertain strength of a flood defence structure and cause flooding. This is usually expressed in a limit state function Z :

$$Z = R - S \quad (\text{Eq. 2.1})$$

R is the resistance, or strength, and S is the load. Failure of a levee occurs when $Z < 0$. In a full-probabilistic approach, uncertainties are included through probability distributions of input parameters (such as R and S) for the failure mechanism models (Kok et al., 2017). Figure 2.6 shows a joint probability density function of strength and load.

Figure 2.6

The failure probability and the joint probability density function of strength and load (Kok et al., 2017).



Currently, safety assessments of regional flood defences follow a semi-probabilistic approach, based on exceedance probability of the hydraulic load. The levees are designed to withstand a specific, governing hydraulic load condition (i.e., a water level) with a maximum annual exceedance probability, prescribed by flood protection standards. The semi-probabilistic approach uses design values rather than probability distributions as input for modelling a failure mechanism. These design values are a combination of characteristic values and a partial safety factor. The design values are determined as follows:

$$S_d = S_{char} \times \gamma_s \quad \text{(Eq. 2.2)}$$

$$R_d = \frac{R_{char}}{\gamma_R} \quad \text{(Eq. 2.3)}$$

S_d and R_d are the design values of a load and a resistance variable, respectively, while γ_s and γ_R are partial safety factors for the load and resistance variable, respectively, and are both larger than 1. Finally, S_{char} and R_{char} are characteristic values of load and resistance.

Semi-probabilistic methods are often simpler and easier to use than full-probabilistic methods. However, they tend to be conservative, because the partial factors need to be relatively strict to be widely applicable. In theory, full-probabilistic methods lead to more accurate outcomes than the semi-probabilistic methods, since full-probabilistic methods take into account all possible combinations of loads and strengths, and the probability of these combinations, whereas semi-probabilistic methods consider one extreme event. In addition, actual field observations hardly have any place in these analyses. This is unfortunate, since actual observations of

levees surviving specific load conditions can improve failure probability estimations by reducing uncertainties in the levee's strength (Schweckendiek, 2014). The effect of this reliability updating approach has been demonstrated for individual failure mechanisms, such as piping (Schweckendiek, Vrouwenvelder and Calle, 2014), and slope instability (Schweckendiek et al., 2016; Lendering et al., 2018), as well as for the overall levee failure probability (Kanning et al., 2017; Lendering, Schweckendiek and Kok, 2018).

Moving towards a more full-probabilistic approach not only provides opportunities for including survived loads, but also for taking real life observations of levee inspections into account. Examples of such inspection observations, called 'levee performance indicators', include subsidence, cracks and animal burrows. Including these effects directly in the safety assessment contributes to a more representative estimation of the actual levee safety (USACE, 2015; Kwakman and Van Loon, 2019).

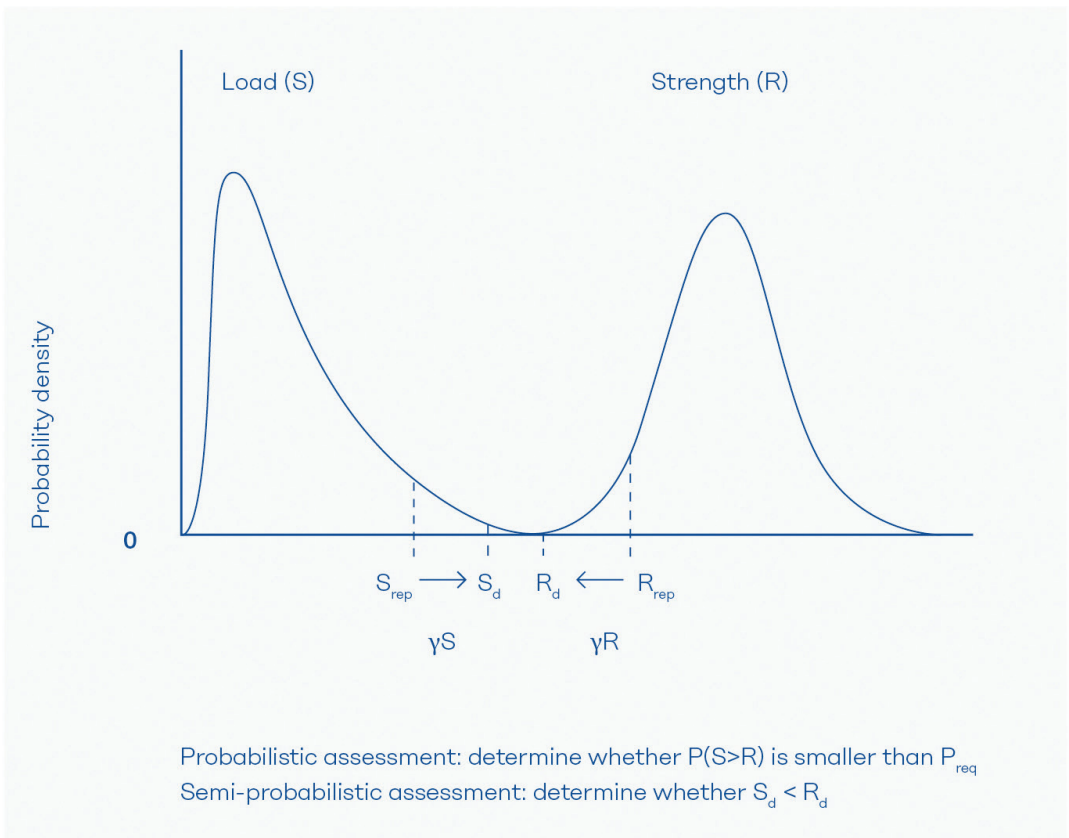


Figure 2.7
 Schematic representation of the difference between a probabilistic and a semi-probabilistic assessment (Kok et al., 2017).

The semi-probabilistic safety assessment determines whether or not a levee meets the required safety standard, but does not provide insight in the extent to which it performs well. Lendering, Jonkman & Kok (2015) have shown that performing a full probabilistic safety assessment on regional flood defences gives quantitative insight in failure probabilities of levee sections. Figure 2.7 further illustrates the difference between a full-probabilistic and a semi-probabilistic assessment. A full probabilistic approach, calculating actual failure probabilities, provides opportunities to assess the failure probability and corresponding risk of a flood defence system, and prioritize interventions based on their (cost) effectiveness in terms of risk reduction.

Length effects

The failure probability of a levee is length-dependent, due to the spatial variability of stochastic variables. This means that the longer a levee section is, the more likely it is that loading conditions exceed the levee's strength conditions locally (Jongejan et al., 2013). Such "length-effects" are considered in the assessment methods for primary flood defences, but not yet for regional flood defences. One reason for that, is that it is difficult to implement in the semi-probabilistic approach used for the assessment of regional flood defences.

3



**Hydraulic load
interdependencies in
polder drainage canal
systems**

3.1 Introduction

3.1.1 Problem analysis

Current flood risk assessments of canal levee systems focus on individual levee sections, even though these individual levee sections are part of a large system of connected levees. Therefore, effects of a levee breach on the hydraulic load in other parts of the canal system are not considered. In this dissertation, these effects are referred to as hydraulic load interdependency. Not taking into account the hydraulic load interdependency leads to an incomplete and incorrect assessment of levee failure probabilities, which in turn affects the estimated overall flood risk in the system.

The importance of these effects has been shown in several studies. These studies showed that, for example, the river discharge in the Rhine at Lobith, where the river enters the Netherlands, has an upper bound, because extreme discharges will lead to overflowing of levees and flooding upstream of Lobith (Vriend et al., 2016). This flooding upstream reduces the hydraulic load on downstream levees. Apel, Merz and Thieken (2006) reached a comparable conclusion for a more upstream section of the Rhine. Besides reducing the hydraulic load downstream, hydraulic load interdependency can lead to increased hydraulic loads elsewhere in the system, if river water flows through a levee breach, through the hinterland, and enters the same or another river at a different location (Courage et al., 2013; De Bruijn, Diermanse and Beckers, 2014; Klerk et al., 2013). However, these studies only focused on river systems, which are quite different from the polder drainage canal systems. First, river systems have a clear upstream and downstream end, whereas this is often not the case in polder drainage canal

systems. Second, canal systems often have a limited quantity of water, and therefore the water level drop due to a levee breach is relatively large in polder drainage canal systems compared to river systems. These differences make it difficult to quantify the effects of hydraulic load interdependency in polder systems, using existing methods. Figure 3.1 shows schematically how hydraulic load interdependency works for drainage canals.

3.1.2 Objective

The aim of this chapter is to assess the effects of hydraulic load interdependency on flood risk in polder systems. This resolves in the following research question:

How do hydraulic load interdependencies in polder systems influence flood risk?

In order to answer this question, a method is developed with which this effect can be quantified. The added value of including hydraulic load interdependency in the flood risk calculation was demonstrated by applying the method to two cases.

3.1.3 Approach and chapter outline

The research consists of two research parts. In the first part, a method is developed to estimate the flood risk on a system scale. By not focusing on the individual levee section scale, effects of hydraulic load interdependency can be included. The method is developed in Section 3.2. In the second part, the method is applied to two case studies. In the first case study (Section 3.3), the method is applied to part of a drainage canal system to assess the effects of hydraulic load interdependency, how it affects flood risk and what it means for potential risk reduction measures. In the second case study (Section 3.4), the method is applied to an entire drainage canal system.

Figure 3.1
Visualization of hydraulic load interdependency
in a drainage canal system.



1. Hydraulic load exceeds levee resistance;
2. Levee breach initiates;



3. Water enters the polder;
4. Levee breach develops;



5. Hinterlying polder fills with water;
6. Canal water level drops;
7. 'Surviving' levees 'relieved'.

3.2

Development of a flood risk estimation method

A flood risk estimation method is developed that includes the effects of hydraulic load interdependency in flood risk assessments. The method consists of the following 7 steps:

1. define the system of polders and drainage canals;
2. model the polder system;
3. simulate extreme meteorological events in the model;
4. determine the resistance of individual levee sections;
5. determine the failure probabilities;
6. determine the consequences of levee failure
7. calculate the flood risk.

By following these 7 steps, the overall flood risk within a system can be assessed with and without hydraulic load dependencies. In the remainder of this section, each of the steps is explained in more detail.

Step 1

Define the system

Systems of Dutch polders are connected to each other through pumps and drainage canals and protected from flooding by canal levees. Because of these connected elements, any change within the system (e.g. levee failure, adjustments to pump configuration) has consequences for other parts of the system. It is therefore necessary to find the boundaries of the system and to understand how the system works. Thus, the first step is to make an overview of the various elements that characterize the system and their connections. Several general elements are polders, levees, canals, pumping stations, and rainfall and wind conditions. Other important elements are polder characteristics (e.g., imperviousness, area and elevation) and levee characteristics (e.g., geometry, and subsoil stratification).

Various hydraulic and hydrologic models exist to model polder system. It depends on the level of complexity of the chosen models how much information is actually needed as model input.

Step 2

Model the polder system

Studies focusing on hydraulic load interdependency in river systems have used river discharges and river and sea water levels as input variable for hydraulic loads (Apel et al., 2004; Courage et al., 2013, De Bruijn et al., 2014). However, in polder systems the amount of water that is pumped out into the canals, heavily depends on local meteorological conditions, as heavy rainfall causes more water to be pumped away from the polders, and wind effects can cause water level differences within the system. At the same time, the canal inflow is largely controlled through pumping stations. For that reason, it is necessary to understand how the system works and how meteorological conditions influence the canal water level so that it can be included properly in a model. Polder pumping stations pump excess water from the polder into the canals to maintain the polder target level. Drainage canal pumps pump the water out of the drainage canal system, to maintain the target canal water level. With a model of the canal system, containing both functions for the hydrologic and hydraulic response to meteorological conditions, the water level at each location in the system can be calculated.

Step 3

Simulate extreme meteorological events

Once the relationship between rainfall, wind and canal water level is established in a model, extreme weather scenarios can be simulated. Different combinations of rainfall with varying intensity, duration, patterns and return periods, in combination with wind from varying directions, with varying speeds and return periods, lead to varying water levels within the canal

system. Since it is impossible to simulate all possible events, a selection should be made that to a large extent represents all possible scenarios. This selection can be based on the probability of events, or on the severity of the consequences.

Step 4

Determine levee resistance

Several failure mechanisms can cause a levee to fail, such as erosion due to overflow or overtopping, internal backward erosion, and macro-instability (CIRIA, 2013). The strength of a levee depends on different characteristics that influence the resistance of a levee against these failure mechanisms, such as geometry and soil composition of the levee body. These characteristics are levee-specific, and are usually not exactly known, due to natural variations, but also due to lack of data. These uncertainties affect the outcome of a reliability assessment. In this step, the resistance of a levee to hydraulic loads is determined, based on limit state functions. In this paper, we choose to express the ability of a levee to resist varying hydraulic loads in fragility curves. As explained by Kok et al. (2017), these fragility curves show the trend in the failure probability of a levee section as a function of a load parameter. Often, the water level is used as a load parameter. The fragility curve depends on location-specific strength properties of the levee section and differs per failure mechanism.

Step 5

Determine failure probabilities

If hydraulic load interdependency is not considered, as is the case in the current approach, the levee failure probability $P_{f, no\ hli}$ of an individual levee section is determined by combining extreme water level statistics with levee resistance (or the fragility curve). In order to assess the failure probability of the system, the dependency between levees has to be considered. There are two extremes: complete independence or complete dependence between the levee

sections. If hydraulic load dependencies are included, the system failure probability lies somewhere between the two extremes. To include these effects, the entire system should be exposed to event-specific hydraulic loads simultaneously to calculate the failure probability $P_{f, hli}$ of each levee section. A simulation of extreme meteorological events is necessary to determine the water level in the canal, since these loads can differ throughout the system. This way, possible effects of levee failure to the hydraulic loads elsewhere are included. Important in this step is that in case of a failure, the surviving levees are assessed again under the changed hydraulic loads, to investigate whether more levees will fail.

Step 6

Determine the consequences of levee failure

The characteristics of the flood (such as water depth and flow velocity) are derived to estimate the potential (economic) damage of flooding in a polder. These flood characteristics serve as input for the damage model that considers to which extent different land use types are affected. A damage function describes how a specific land use type (such as arable land, housing, or industry) is affected by flooding as a function of the flood characteristics, such as water depth and flood duration. Besides flood damage, levee failure and flooding lead to a lower water level in the canal system, which reduces the hydraulic load on levee sections elsewhere in the system. Therefore, it is necessary to estimate the effect of a levee failure on the water level in the canals in the system. In turn, this reduced water level can affect potential damage.

Step 7

Determine the flood risk

The final step is to determine the flood risk in a polder, which is found by summing the products of the failure probability of

each levee section with the corresponding potential consequences of that levee failure. The risk calculation is the same for both the case where hydraulic load interdependency is included, as where it is not included. However, failure probabilities and estimated potential damage might differ.

The flood risk is determined as follows:

$$R_i = P_{f;i} \times D_i \quad \text{(Eq. 3.1)}$$

with:

R_i = the annual flood risk as a consequence of failure of levee section i [€].

$P_{f;i}$ = the annual failure probability of levee section i [-].

D_i = the estimated damage as a consequence of failure of levee section i [€].

$$R_{total} = \sum_{i=1}^n R_i \quad \text{(Eq. 3.2)}$$

With n is the total number of potential breach locations in the canal system. In theory, this amount is infinite, which is why a weakest spot should be identified per levee section.

3.3

Case study 1: Part of a polder drainage canal system (Hoogheemraadschap Delfland)

In this section, the developed flood risk estimation method is applied to a small part of the polder drainage canal system of the Water Board Delfland.

3.3.1

Overall flood risk assessment

Step 1: Define the system

This case is located in Zuid-Holland, and focuses on a part of the Schie canal and a smaller side branch, named the Berkelse Zweth (see Figure 3.2). Five potential breach locations were defined in such a way that each branch has at least a breach. The Berkelse Zweth contains a compartmentalization structure, which can be closed to compartmentalize the canal system in case of emergency (see Figure 3.3).

Only levee failure due to overflow was considered in the first case study. Therefore, levee crest height is the main parameter determining the levee strength. The crest height was determined using a recent elevation map (AHN3). While in this case study we zoomed in on a small part of the system, the whole system contains hundreds of kilometers of canals. For realistic simulation results, the hydraulic model we used, includes the entire system of canals. However, we did not consider failure in other parts of the system than our case study area. Levees in other parts of the system were thus assumed to not fail.

Step 2: Model the system

This step was performed by the local water authorities (Hoogheemraadschap van Delfland), so that in our study we could work with their water level predictions.

For the breach calculations we used an existing model of the system that was developed in 3Di (Nelen & Schuurmans, 2020), which is hydrodynamic simulation software that allows for high resolution integral 1D/2D flow modelling. In this model, the entire system of canals was modelled, so also the part outside of the very limited boundaries of this case study.

Step 3: Simulate extreme events

In this step we focused only on the water level, since we were only interested in levee failure due to overflow. In Figure 3.4 the water level is shown as a function of the return period. Water levels in this graph were slightly increased with respect to the actual estimations by the water authorities, for the sake of the assessment. In extreme cases, the polder pumps that pump the water from the polders into the canals can be switched off to minimize further water level rise (in Dutch: maalstop). However, these ‘maalstop’-effects are not included in Figure 3.4.

Step 4: Determine levee resistance

The crest level at each breach location was determined, based on elevation data. The crest heights were obtained from cross-sectional profiles every 100 meters. From these cross-sectional profiles, a minimum crest height was derived. In this case study, we only consider failure due to wave overtopping and overflow. The probability of failure increases with an increasing water level, if the load on the levee increases. We assumed that the failure probability increases linearly from 0, when the minimum crest height is exceeded, to 1, when the minimum crest height is exceeded by 10 cm, to take into account that the increasing amount of water overtopping or overflowing the levee. This was summarized in fragility curves (Figure 3.5). These curves are derived from the fragility curves where hydraulic load interdependency is not taken into account. For each water level, it is determined how likely each levee fails. The

assumption is that as soon as a levee fails, the water level will not increase further, and the other levees will remain intact. The fragility curves in Figure 3.5 are described by the following equations:

$$P_f = 0, \text{ where } h < h_{min} \quad (\text{Eq. 3.3})$$

$$P_f = \frac{h - h_{min}}{0.1}, \text{ where } h_{min} \leq h < h_{min} + 10 \text{ cm} \quad (\text{Eq. 3.4})$$

$$P_f = 1, \text{ where } h \geq h_{min} + 10 \text{ cm} \quad (\text{Eq. 3.5})$$

With h is the canal water level [in m+NAP], and h_{min} the minimum crest height [in m+NAP].

These individual fragility curves were used to derive the fragility curve where hydraulic load interdependencies are included (see Figure 3.6).

Step 5: Determine the levee failure probabilities

For this step, the outcomes of step 3 and 4 were combined. The water level was incrementally increased with dh , and for each increasing step the corresponding change in probability of occurrence $dP(h)$ was determined. The failure probability was determined by the sum of the failure probability conditional to the water level and the probability of occurrence of the water level. This step was performed both for the case without hydraulic load interdependencies, and with hydraulic load interdependencies. With hydraulic load interdependencies, it was assumed that all surviving levees are safe after the breach of another levee.



Figure 3.2

Overview of the case study area, covering a part of the Schie canal and a smaller side branch, named the Berkelse Zweth. A, B1, B2, C, and D as potential levee breach locations and the red areas are potential flooding areas. The yellow star (BWO-kering) indicates a compartmentalization structure, meant to close of a part of the canal system.



Figure 3.3

Compartmentalization structure at the Berkelse Zweth, near Delft, the Netherlands. This structure is meant to compartmentalize the canal, by lowering eight steel beams in place with a crane, to block the flow in the canal. In this picture closure of the structure was practiced. (Picture taken by Stephan Rikkert, 2018).

The calculated failure probabilities are shown in Figure 3.7. As can be seen, the failure probabilities for all levees, except the lowest (B2), drop significantly, if hydraulic load interdependency is taken into account. The failure probability at levee A even drops to zero. It is higher than the other levees, and water levels will never be high enough to cause enough overtopping or overflow of levee A; one of the other levees will always fail earlier.

Step 6: Determine the consequences

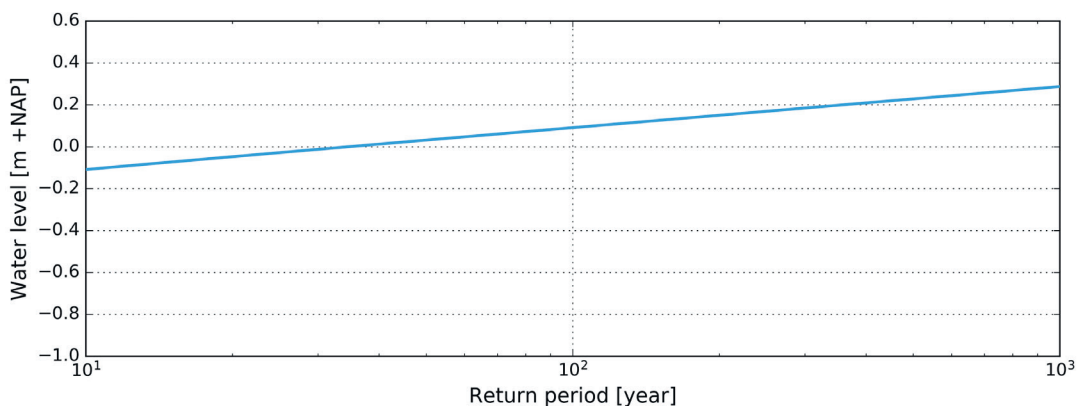
The consequences of a levee breach were determined in terms of economic damage only. An existing model of the canal system, 3Di, was used for inundation modelling. 3Di uses the formula of Verheij and Van der Knaap (see Verheij, 2003) for breach growth. The initial breach width was assumed to be 10 m and this breach was assumed to reach to the polder surface level within 10 minutes (De Bruijn et al., 2018). Based on the calculated inundation map, the economic damage was calculated, using the Water Damage Predictor (Dutch: Waterschadeschatter). Three damage scenarios were calculated per breach location, in which the duration

of flooding (time until excess water has disappeared from the polder), duration of repairs of infrastructure and duration of repairs of buildings is varied (see Table 3.1). As can be seen in Figure 3.7, the estimated damage increases significantly for breach location A, B1, and C, if the repair time to infrastructure and buildings increases. This is mainly caused by the presence of highway and train tracks in the flooding polders. However, for short repair times (1d), the estimated damage are relatively close (within a range between 1.8 – 5 million euros). To acknowledge the importance of the repair time, the mean damage was used in the risk calculations that follow (see Table 3.2).

Step 7: Determine flood risk

The results of the flood risk calculation are shown in Figure 3.7. The total calculated annual flood risk without hydraulic load interdependencies is about €510,000. If hydraulic load interdependencies are taken into account, the calculated annual flood risk is approximately 68% lower: about €160,000.

Figure 3.4
Water level as function of the return period, Gumbel fit to predictions of water levels with 10, 100 and 1000 year return periods.



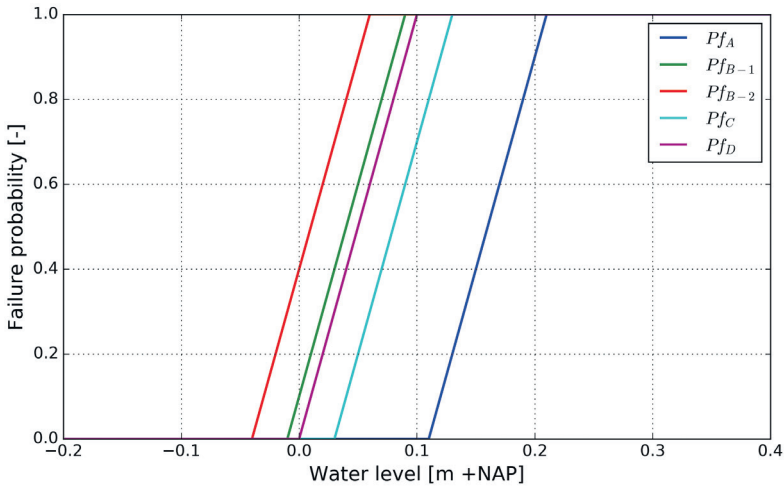


Figure 3.5
Fragility curves for each individual levee for the failure mechanisms overtopping and overflow (without consideration of hydraulic load interdependencies).

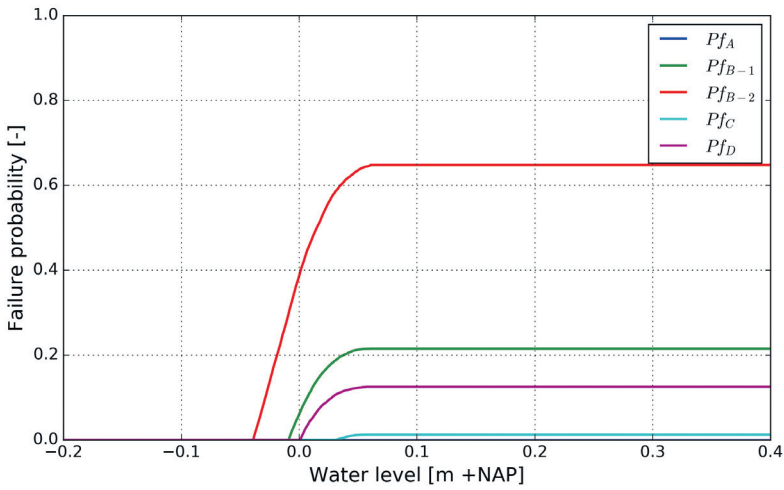


Figure 3.6
Fragility curves for each individual levee for the failure mechanisms overtopping and overflow (with consideration of hydraulic load interdependencies).

Table 3.1
Scenarios used in damage predictions.

| Scenario | Duration of flooding [days] | Duration of repairs on infrastructure [days] | Duration of repairs on buildings [days] |
|-------------|-----------------------------|--|---|
| <i>Low</i> | 1 | 1 | 1 |
| <i>Mid</i> | 1 | 5 | 5 |
| <i>High</i> | 1 | 10 | 10 |

Table 3.2
Overview of estimated consequences of levee breach per breach location (in million euros).

| Breach location | Mean damage [in 10 ⁶ €] |
|-----------------|------------------------------------|
| <i>A</i> | 17.2 |
| <i>B1</i> | 10.5 |
| <i>B2</i> | 4.67 |
| <i>C</i> | 5.81 |
| <i>D</i> | 1.80 |

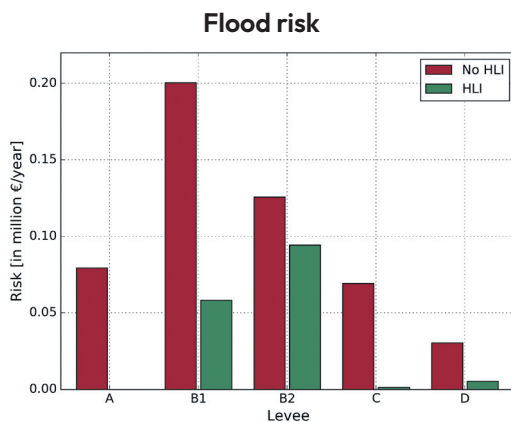
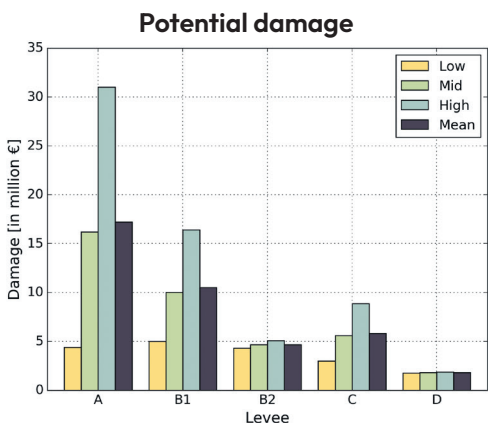
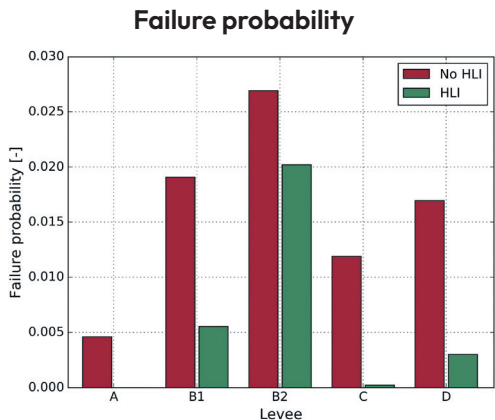


Figure 3.7
 Top left: Estimated failure probabilities without (red) and with hydraulic load interdependencies (green). Top right: Overview of the case study area, showing the potential breach locations in levee sections A, B1, B2, C, and D. Bottom left: Estimated economic damage of a levee breach per location for different scenarios. Bottom right: Flood risk at each breach location without (red) and with hydraulic load interdependencies (green).

3.3.2

Flood risk reduction measures

Next, the effect of 3 different flood risk reduction measures were assessed with and without hydraulic load interdependencies:

- Levee heightening;
- Levee lowering (controlled overflow);
- Compartmentalization of the canal system.

Levee heightening

This measure concerns heightening of the levee with the highest failure probability, in this case the levee with the lowest crest height: levee B2. At the lowest point this levee is -0.04 m+NAP. It has a total length of 1500 m, in which the height was derived from a cross-section every 100 m. The levee heightening was applied as follows:

- The minimum crest level was determined;
- Every 100 m cross-sections were derived from the height map for each levee section;
- For each cross-section it was determined if the crest height was above or below the required height;
- If the crest height of a cross-section was found lower than the required height, this 100 m stretch was heightened.

Table 3.3 shows the number of levee segments to be increased, depending on the required height. The increased levee height resulted in changes in failure probabilities. The annual flood risk was determined by multiplying the updated failure probabilities with potential flood damage. The result is shown in Table 3.4. Without taking into account hydraulic load interdependency, the higher the levee, the larger the flood risk reduction, although this additional flood risk reduction becomes less significant as the levee becomes higher. If hydraulic load interdependency is included, the overall flood risk is lower, but heightening hardly has a significant effect on overall flood risk. On the contrary, after a certain height, the overall flood risk in the system increases, as it becomes more likely that another levee will fail.

Table 3.3

Number of 100 m-levee segments to be increased, and to which extent.

| | Required levee height for levee B2 in m+NAP | | | |
|---|---|------|------|------|
| | 0.0 | 0.10 | 0.20 | 0.30 |
| <i>Levee segments that require a 0.1 m increase</i> | 2 | 3 | 1 | 7 |
| <i>Levee segments that require a 0.2 m increase</i> | 0 | 2 | 3 | 1 |
| <i>Levee segments that require a 0.3 m increase</i> | 0 | 0 | 2 | 3 |
| <i>Levee segments that require a 0.4 m increase</i> | 0 | 0 | 0 | 2 |
| Total strengthened levee segments | 2 | 5 | 6 | 13 |

Table 3.4
Annual flood risk [10^6 €] for different levee height increase steps.

| | | Required levee height for levee B2 in m+NAP | | | |
|---|-------|---|-------|-------|-------|
| | | reference | 0.0 | 0.10 | 0.20 |
| Height increase step | 0 | 1 | 2 | 3 | 4 |
| Annual flood risk (without HLI) [10^6 €] | 0.505 | 0.458 | 0.404 | 0.387 | 0.381 |
| Annual flood risk (with HLI) [10^6 €] | 0.159 | 0.151 | 0.153 | 0.153 | 0.153 |

Cost benefit-analysis levee heightening

The investment costs for levee heightening increase with the required height of the levee. A distinction was made between fixed and variable costs, where fixed costs are independent and variable costs are dependent of the extent levee strengthening. Several assumptions regarding costs by Nicolai et al (2017) were used for this study. They are shown in Table 3.5.

The net present value of the investment costs, flood risk and total costs are presented in Figure 3.8. The investment costs are equal, regardless of hydraulic load interdependency is included or not, as the same amount of levee segments have to be heightened. The optimal levels of heightening are shown by the diamonds, and the optimum is different when hydraulic load interdependency is included. The reason for this is that the probability of failure decreases with increasing the height of one levee. Even though the overall

system failure probability decreases, the failure probability can increase at a location with a potential high damage, and as a consequence the overall flood risk can increase.

Controlled overflow by lowering a levee locally

A way to reduce the flood risk in a polder is to relocate the probability of flooding from areas where potential damage is high to areas where potential damage is low. Therefore, the height of the levee along the polder with the lowest potential damage, levee D ($\text{€}1.8 \times 10^6$), was locally lowered, by adjusting the fragility curve, so controlled overflow could take place. Levee D was lowered to -0.05 , and -0.10 m +NAP. Although lowering of a dike section can be designed in such a way, that overflow can take place without breaching, leading to a lower amount of water and lower damage, the same damage was used for each case. The total calculated system flood risk is shown in Table 3.6. These results

Table 3.5
Assumptions used in cost calculation (based on Nicolai et al. (2017)).

| Parameter | Value |
|--|-----------------|
| Costs per 0.1 m levee height increase [$\text{€}/\text{km}$] | 5×10^6 |
| Ratio fixed costs/variable costs | 0.75/0.25 |
| Design lifetime [year] | 50 |
| Discount ratio [%/year] | 2.5 |

show that without taking hydraulic load interdependency into account, the total risk increases, since the risk in polder behind levee D increases, while the risk in other polders stays the same. On the other hand, if hydraulic load interdependency is taken into account, the system flood risk reduces. The probability of failure of a levee where consequences are high are shifted to a levee where consequences are much lower.

Compartmentalization of the canal system

The polder drainage canal system of Delfland contains several structures that can be closed in case of emergency. By closing these structures, the canal system is divided into compartments. This reduces the water volume that can flow through a breach, resulting in lower flood levels. At the same time, this compartmentalization ensures that the rest of the system stays intact and can continue functioning.

The compartmentalization structure in this study area (see Figure 3.2 for its location and Figure 3.3 for an impression of the structure) consists of beams that can be lowered in position by a crane to close off

the canal. Closing this structure during a breach consists of the following processes. An indication of the estimation time of the closure process is given:

- Detect the breach. During extreme conditions the inspection frequency is high, and levees are monitored closely, so that a breach can be detected in an early stage (1 hour).
- Call emergency response team. It is assumed that the emergency response team can be at the crisis centre in 30 minutes.
- Prepare material and equipment. Beams are brought up from the storage (next to the structure) and the crane is brought into position (30 minutes).
- The beams are lowered in the canal one by one and should fit neatly into recesses on both sides of the canal. High flow velocities during a breach will make this process difficult (4 hours).

This amounts to a total closing time of 6 hours. This is in line with the expectations of experts from the water authorities.

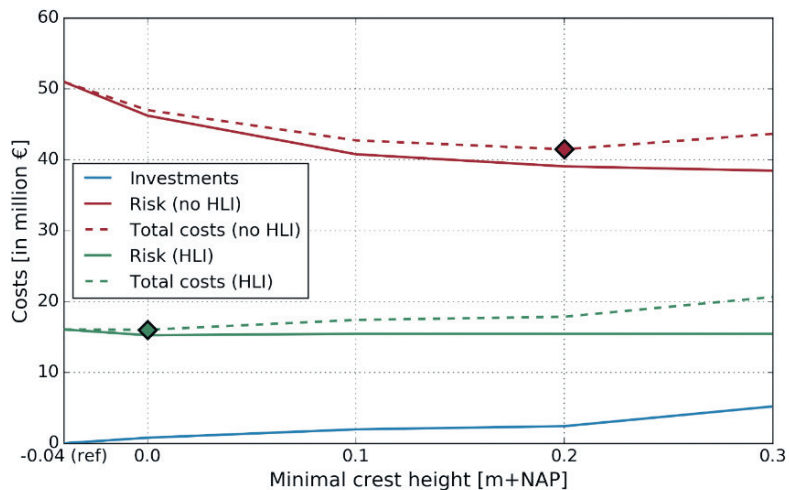


Figure 3.8

Overview of net present value of the investment costs (blue), overall flood risk (red and green solid lines), and total costs (red and green dashed lines) for heightening of levee B2 so that the entire levee meets the minimal crest height. The diamonds indicate the optimal solution when hydraulic load interdependency is not included (red) and when it is included (green).

Table 3.6
Flood risk [$10^6\text{€}/\text{year}$] for levee lowering scenarios.

| | | Minimal crest height levee D [m+NAP] | |
|---------------|----------------|--------------------------------------|-------|
| | | -0.05 | -0.10 |
| | Reference case | | |
| Lowering step | 0 | 1 | 2 |
| Without HLI | 0.505 | 0.529 | 0.572 |
| With HLI | 0.159 | 0.121 | 0.108 |

To estimate the damage in case of a closed compartmentalization structure, again several damage scenarios were taken into account, and from these scenarios the average damage was derived. Results are shown in Table 3.7. For comparison, the average damage for the reference case without compartmentalization (as presented in Table 3.2) is included in this table as well. It becomes clear that closing the structure hardly has any effect on the total damage, especially when a levee breach occurs along the Schie (levee A, B1 and B2). The structure closes off the Berkelse Zweth from the Schie. However, the dimensions of the Berkelse Zweth are relatively limited, and therefore the effect on the damage is negligible.

When combined with the failure probabilities, as derived in step 5, this leads to an overall flood risk of $\text{€}1.53 \times 10^5/\text{year}$ (with hydraulic load

interdependency). Compared to not closing the compartmentalization structure (overall flood risk of $\text{€}1.59 \times 10^5/\text{year}$), the flood risk reduction is small.

Comparison effectivity of measures

In this section, 3 flood risk reduction measures were applied:

- Levee heightening;
- Levee lowering (controlled overflow);
- Compartmentalization.

The effects on the overall flood risk for the reference cases without and with hydraulic load interdependency are shown in Table 3.8. The table also includes the total risk for the risk reduction measures, where hydraulic load interdependency was taken into account. The lowest flood risk was obtained by locally lowering the levee, resulting in controlled overflow, at the location where flood damage is the lowest.

Table 3.7
Damage without and with compartmentalization.

| Breach location | Potential damage without compartmentalization [10^6€] | Potential damage with compartmentalization [10^6€] |
|-----------------|--|---|
| A | 17.2 | 17.1 |
| B1 | 10.5 | 10.7 |
| B2 | 4.67 | 4.41 |
| C | 5.81 | 5.44 |
| D | 1.80 | 1.04 |

3.3.3

Discussion

In this case study, we have demonstrated the effect of hydraulic load interdependency through the failure mechanisms wave overtopping and overflow. The case study focussed only on a part of the water system, and assumed that the rest of the canal system, outside of the study area, does not contribute to the risk of the system. However, the system is larger than the area considered, meaning that levees can fail at more locations. This would decrease failure probabilities even further.

For the closure of the compartmentalization structure, a closure time of 6 hours was assumed. This closure time was based on expert judgement, but can vary in practice, due to conditions that make closure more

difficult, such as an inaccessible site, or extreme weather conditions. If the actual closure time is shorter, the amount of inflow into the polder is reduced, resulting in less flood damage. However, this also reduces the relieving effect of the canal water level drop elsewhere in the system. If the closure time is longer, the inflow into the polder, and hence the damage, is larger than estimated now. At the same time, the water level drop elsewhere in the system is also larger. An optimal closure time is likely site-specific, but has not been researched in this study.

Table 3.8
Results of risk calculations for all scenarios.

| | Total flood risk [in €10 ⁶ /year] | |
|--|--|----------|
| | Without HLI | With HLI |
| <i>Reference</i> | 0.505 | 0.159 |
| <i>Levee B2 heightened to 0.2 m +NAP</i> | 0.387 | 0.153 |
| <i>Levee D lowered to -0.10 m +NAP</i> | 0.572 | 0.108 |
| <i>Compartmentalization</i> | 0.484 | 0.153 |

3.4

Case study 2: An entire polder drainage canal system (Hoogheemraadschap Hollands Noorderkwartier)

The second case study focusses on an entire polder drainage canal system at the Water Board Hollands Noorderkwartier.

3.4.1

Overall flood risk assessment

Step 1: Define the system

In this second case study, we focused on the Schermer polder drainage canal system, which consists of roughly 670 km of levees, 175 polders and 2 outlet structures (pump/sluice). The total area of all polders in this system is about 80,000 ha. An overview of the system is shown in Figure 3.9. The target canal water level is -0.50 m+NAP. In extreme cases, a drain stop (Dutch: maalstop) is used, which minimizes further increase of the canal water level by disabling polders from pumping their excess water into the canals. The drain stop level for this system lies at -0.15 m+NAP. The polder surface levels are generally lower than this canal water level.

Step 2: Model the system

To determine the water level throughout the canal system under varying rainfall and wind conditions, an existing SOBEK model (version from 2017) was used that was developed by the local water authorities (Hoogheemraadschap Hollands Noorderkwartier). This SOBEK model (Deltares, 2018) uses the modules IDFLOW (Rural) and RR (Rainfall-Runoff). The used RR-module is a hydrological model, which simulates the effects of rainfall and evaporation on polders, to predict how much water should be pumped out of the polder into the canal system. The IDFLOW-module is the hydraulic model that is used to calculate the flow

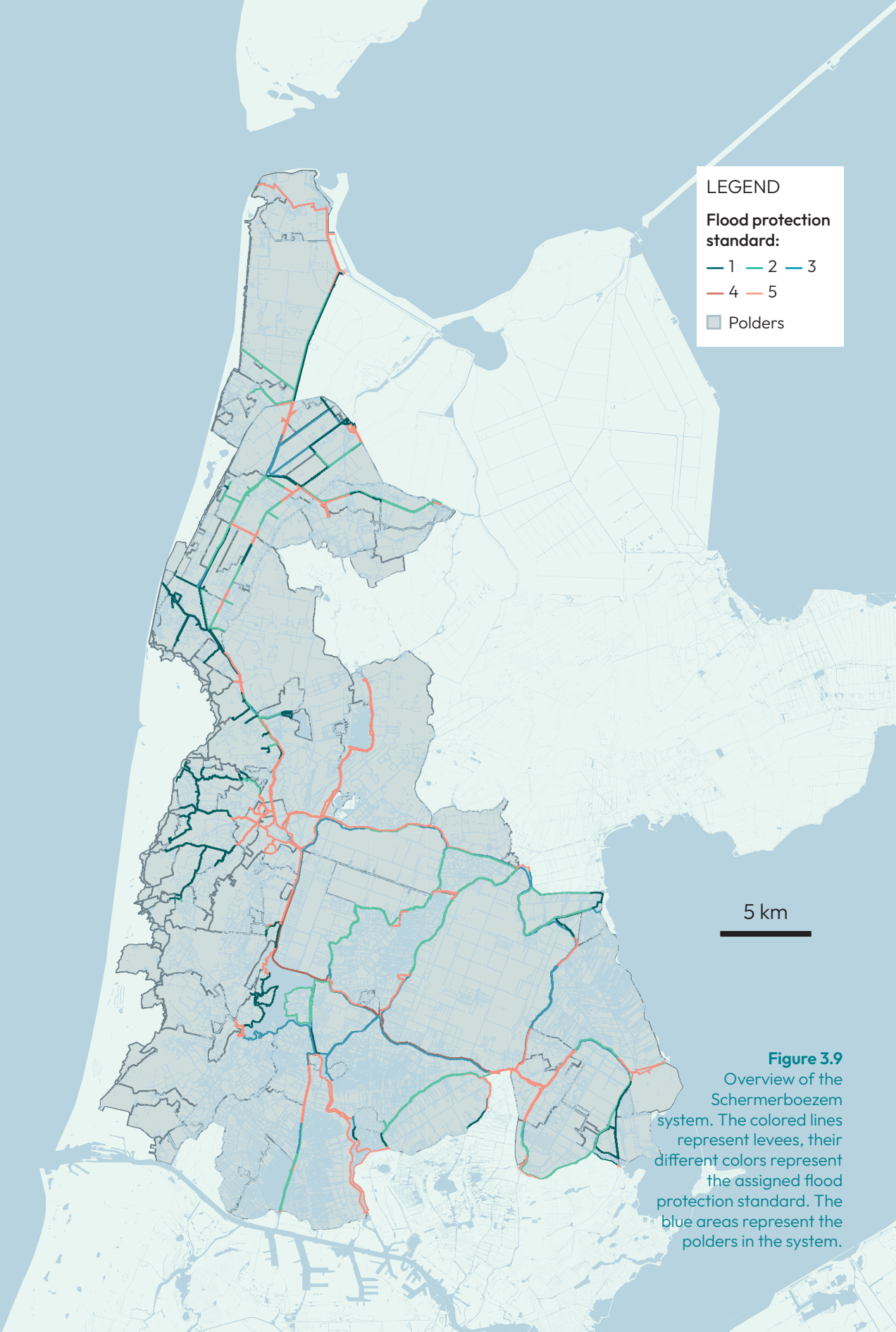
through the canal system. The model was validated by Hoogheemraadschap Hollands Noorderkwartier, and showed good resemblance between measured and modelled pump discharges at the outlets of the system. To simulate the effects of a levee breach on canal water levels as well, the Overland Flow (2D) module is included.

Step 3: Simulate extreme events

Rainfall and wind conditions can vary in time in space, resulting in an infinite number of possible events. For pragmatic reasons, the authors have decided to include only a limited number of storm conditions: 3 possible conditions for rainfall are used in this study: rainfall events with a return period of 10, 100 and 1000 years, following a common rainfall pattern, derived from Smits et al. (2004). 24 hour rainfall events were used, and the rainfall pattern is shown in Figure 3.10. This is a rainfall event with 1 peak, in which 62.5% of the total rainfall is concentrated.

The total amount of rainfall was determined, following rainfall statistics at the location the Bilt, which is centrally located in the Netherlands (STOWA, 2015b) and is expected to be fairly similar to the project location. Figure 3.11 shows the total cumulative rainfall for varying return periods and rainfall durations. We focus on 24h-rainfall events, with return periods of 10, 100 and 1000 years, resulting in rainfall amounts of 58.1, 85.2, and 116.8 mm, respectively.

Besides rainfall, other stochastic variables in this case study are wind velocity and wind direction. We know that these three stochastic variables are not independent, and in this proof of concept we take rainfall and wind velocity completely dependent. Four different wind directions are simulated: North, East, South and West, and each wind direction has a known probability of 0.13, 0.20, 0.36, and 0.30, respectively (based on wind statistics at Schiphol, derived from



LEGEND

Flood protection standard:

- 1 — 2 — 3
- 4 — 5
- Polders

5 km

Figure 3.9
Overview of the Schermerboezem system. The colored lines represent levees, their different colors represent the assigned flood protection standard. The blue areas represent the polders in the system.

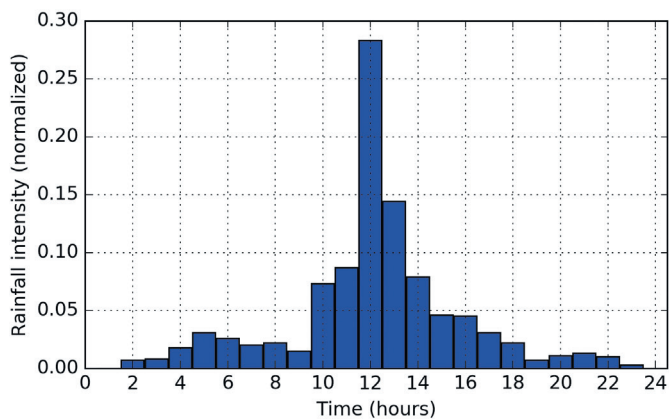


Figure 3.10
 Pattern of a 24 hour rainfall event, based on a typical 1-peak pattern, as presented by Smits et al. (2004). 62.5% of the total rainfall is concentrated in the peak.

(Deltares, 2015)).

During the rainfall event, the calculated water level and cumulative rainfall change in time and space. The maximum water levels at different locations could be reached at different moments. For simplicity reasons, we have only considered the maximum water level at each location, and the total amount of rainfall, regardless of the timing.

Step 4: Determine levee resistance

The Schermer polder drainage canal system consists of about 670 km of levees. To reduce the number of levee safety analyses, only the relatively weak spots in the system were included. In the context of this dissertation, weak spots mean locations with a relatively high failure probability, where under increasing hydraulic loads the

levee system is most likely to fail. Based on insights from experts of the water authority, 18 of those locations were identified. These experts have much experience with the levees in the study area and the weak spots were derived from the safety assessments of these levees. The identified weak spots are presented in Figure 3.12. As can be seen, all weak spots are located in the southern part of the system. This has to do with the system’s topography. In the southern part, the polders have surface levels meters below the canal water level, whereas in the northern part the polder surface levels are much higher and closer to the canal water level. The levees in the northern part are relatively robust with respect to their water retaining height, while this is less the case in the southern part of the system.

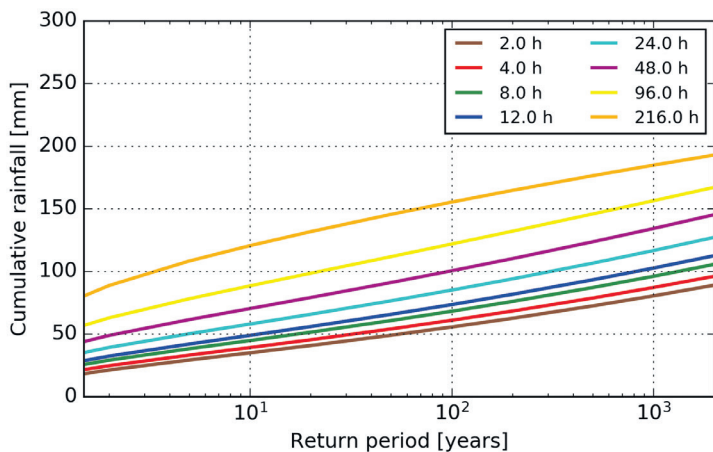


Figure 3.11
 Cumulative rainfall for varying return periods and rainfall durations at the Bilt (STOWA, 2015b).

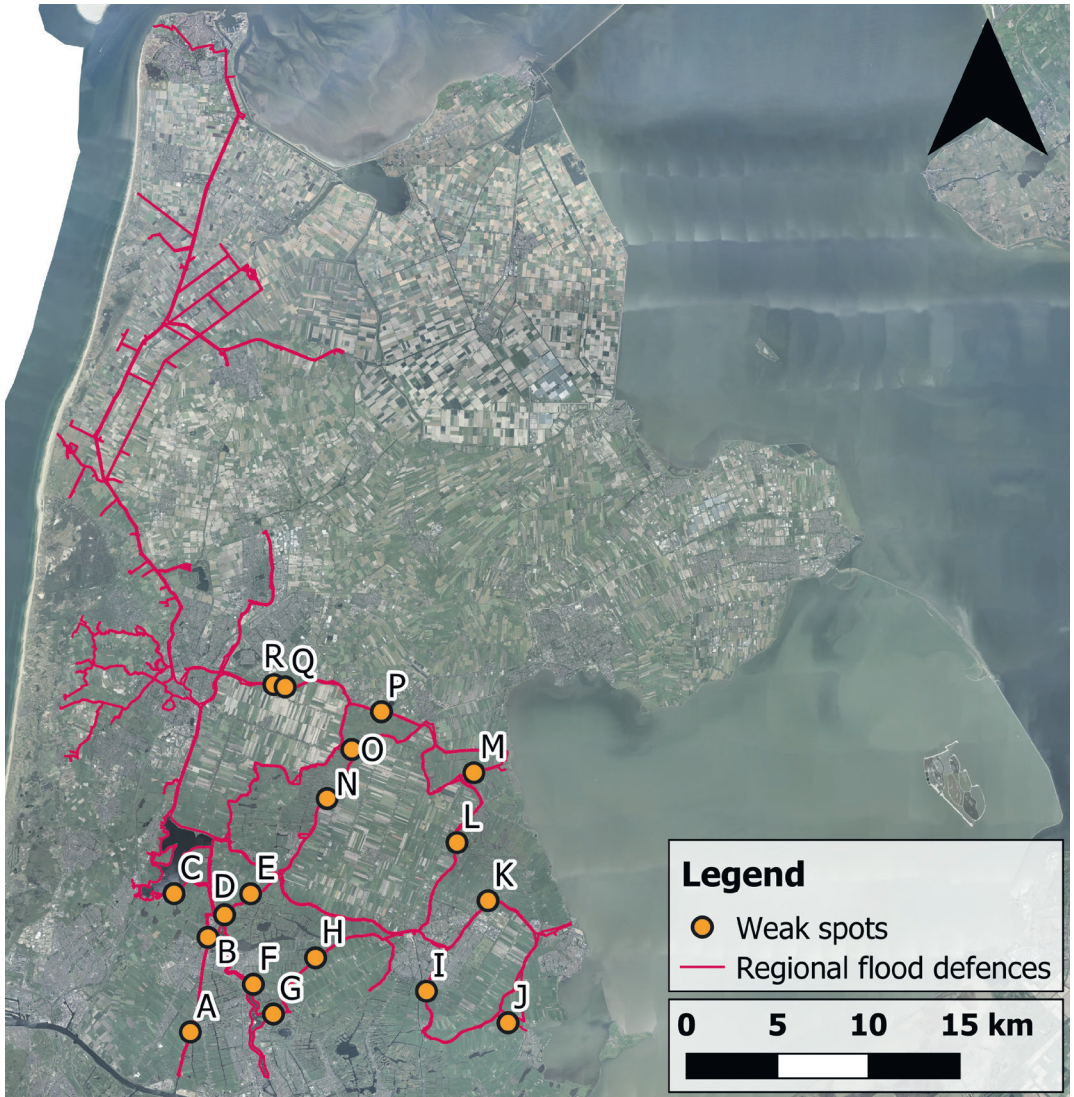


Figure 3.12
Overview of levees in the Schermer polder drainage system, with 18 weak spots (identified by experts from the water board).

Table 3.9

Categories for levee resistance, where the color gives an indication of the levee resistance: the category with the weakest levees is indicated in red, the strongest in green. Yellow is in between.

| | Hardly sensitive to rainfall | Strongly sensitive to rainfall |
|-----------------------------------|-------------------------------------|---------------------------------------|
| Hardly sensitive to water level | Wide, consistent clay cover layer | Wide, inconsistent clay cover layer |
| Strongly sensitive to water level | Narrow, consistent clay cover layer | Narrow, inconsistent clay cover layer |

The phreatic line in a canal levee responds to rainfall, and this response is location-dependent. Research has shown that the phreatic line is difficult to predict (see for instance Dorst, 2019). Often, fragility curves are used to express the failure probability as a function of the water level. But due to the influence of rainfall on the phreatic line, we chose to use a fragility surface, rather than a fragility curve. This way, two hydraulic loads can be included: the canal water level and the cumulative rainfall that occurred during one rainfall event. This is different than in case study 1, because we focused on overflow and wave overtopping, while in this case study we focus on levee instability.

The fragility surface was assumed, based on location specific levee characteristics: geometry and subsoil. For now, 4 surfaces for four typical cross sections were defined, that distinguishes in sensitivity to water level changes and to rainfall (influencing the phreatic line within the levee). These 4 categories are shown in Table 3.9. Levees are considered wide, and hardly sensitive to water level changes, when their crest width is more than 5 m. If the crest width is smaller than 5 m, the levee is considered narrow and strongly sensitive to water level changes. The levee is considered hardly sensitive to rainfall, when it has a clay cover layer thicker than 1.5 m. If the clay cover layer is smaller than 1.5 m, or not present at

all, the levee is considered strongly sensitive to rainfall.

The fragility surface expresses the conditional failure probability of a levee as a function of both the canal water level and the cumulative rainfall (Table 3.10). The derivation of these fragility surfaces is further elaborated in Appendix A. With these fragility surfaces, the failure probability can be determined, if the canal water level and the cumulative rainfall during an event are known. In this paper, 4 fragility surfaces were distinguished:

1. Hardly sensitive to water level and hardly sensitive to rainfall;
2. Hardly sensitive to water level and strongly sensitive to rainfall;
3. Strongly sensitive to water level and hardly sensitive to rainfall;
4. Strongly sensitive to water level and strongly sensitive to rainfall;

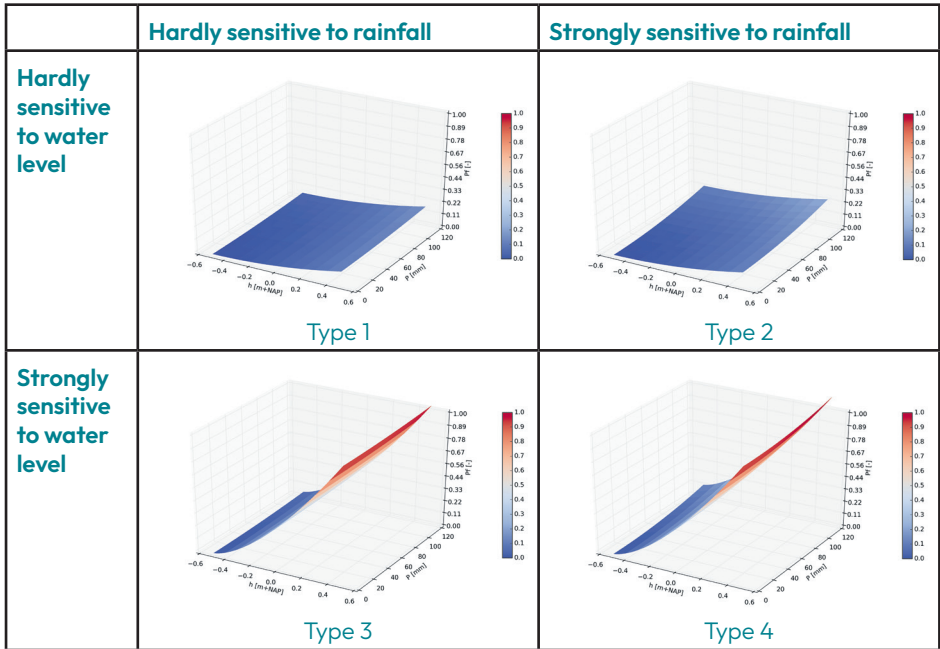
Step 5: Determine the levee failure probabilities

The levee section's failure probability is determined for both with and without hydraulic load interdependencies. The approaches are described as follows:

Without hydraulic load interdependency

Per event, the cumulative rainfall and water level at each levee section were determined. In this case study, the SOBEM model was

Table 3.10
Fragility surfaces which show per levee the failure probability as function of the outer water level and the cumulative precipitation.



used to determine the canal water level at each potential breach location in the canal system, following a rainfall event that is uniform over the study area. Subsequently, the conditional levee failure probability was determined from the fragility surface. The total failure probability per levee section was determined as follows:

$$P_i(F) = \sum_{j=0}^N P_i(F | h, r, w) \times P_j(h, r, w) \tag{Eq. 3.6}$$

Where i indicates the i^{th} levee, and j indicates the j^{th} event. h, r and w represent the water level, rainfall and wind conditions, respectively. $P_i(F|h,r,w)$ describes the probability of failure for levee i , given the water level, rainfall and wind conditions. $P_j(h,r,w)$ describes the probability of the combination of water level, rainfall and wind.

With hydraulic load interdependency

For the situation with hydraulic load interdependency, a number of samples N was drawn for each levee location between 0 and 1 (uniformly distributed). From the fragility surface, the maximum water level that the levee can withstand was derived using the value from the sample.

Example of a failure probability calculation with the fragility surface

A rainfall event with an accumulative rainfall of 70 mm results in a canal water level of -0.15m +NAP at location A. According to the fragility surface, the conditional failure probability is 0.3. N samples between 0 and 1 were drawn. Every time the conditional failure probability exceeded the sample value, this resulted in a failure. The estimated failure probabilities are shown in Table 3.11. The table includes failure probabilities for both exclusion and inclusion of hydraulic load interdependencies, followed by the relative reduction in failure probability by inclusion of hydraulic load interdependencies.

Table 3.11

Failure probabilities without and with hydraulic load interdependence (HLI) of the 18 beach locations A till R.

| Breach location | Without HLI [-] | With HLI [-] | Change [%] |
|-----------------|-----------------------|-----------------------|------------|
| A | 1.26×10^{-3} | 1.04×10^{-3} | -17% |
| B | 3.08×10^{-3} | 2.88×10^{-3} | -6% |
| C | 3.09×10^{-3} | 2.89×10^{-3} | -6% |
| D | 7.95×10^{-3} | 5.64×10^{-3} | -29% |
| E | 6.11×10^{-3} | 3.59×10^{-3} | -41% |
| F | 6.24×10^{-3} | 3.86×10^{-3} | -38% |
| G | 3.08×10^{-3} | 2.87×10^{-3} | -7% |
| H | 1.39×10^{-3} | 1.09×10^{-3} | -22% |
| I | 8.10×10^{-3} | 4.76×10^{-3} | -41% |

| Breach location | Without HLI [-] | With HLI [-] | Change [%] |
|-----------------|-----------------------|-----------------------|------------|
| J | 3.25×10^{-3} | 2.94×10^{-3} | -9% |
| K | 1.30×10^{-2} | 9.23×10^{-3} | -29% |
| L | 1.42×10^{-2} | 1.06×10^{-2} | -25% |
| M | 8.91×10^{-3} | 5.74×10^{-3} | -36% |
| N | 1.15×10^{-2} | 7.77×10^{-3} | -32% |
| O | 1.45×10^{-2} | 1.07×10^{-3} | -26% |
| P | 1.35×10^{-2} | 9.46×10^{-3} | -30% |
| Q | 1.17×10^{-2} | 7.88×10^{-3} | -33% |
| R | 1.16×10^{-3} | 7.80×10^{-3} | -33% |

Step 6: Determine the consequences

To determine the consequences, results of earlier studies have been used. Nelen & Schuurmans (2015) determined the damage in a polder based on water depths up to a maximum of 2.50 m. The damages calculated in their report were based on the WaterSchadeSchatter (WSS). The WSS calculates damage based on land use maps and calculated water depths, using damage functions (see Nelen & Schuurmans, 2019). These damage functions express the damage as a function of the water depth and are dependent of the land use. The damage in a polder is sensitive to water depth, and therefore to the moment after the formation of the breach. This sensitivity is shown in Table 3.12. In this study, we assumed that inflow into the polder can be stopped in 24 hours, similar to case study 1.

Step 7: Determine flood risk

The total flood risk was calculated by the sum of the product of the potential damage and the failure probability for each failure location. The total annual flood risk without hydraulic load interdependencies is about €810,000. When hydraulic load interdependencies are taken into account, the annual flood risk is approximately 31%

lower: about €560,000. Table 3.13 shows the annual flood risk per breach location without and with inclusion of hydraulic load interdependencies.

3.4.2

Flood risk reduction measures

Several flood risk reduction measures are qualitatively explored in this section.

Locally strengthening of a levee

Strengthening of one levee section, will locally reduce the flood risk, but increases the flood risk elsewhere. This measure is therefore only beneficial if the overall risk reduction outweighs the investment costs. This effect can only be calculated if hydraulic load interdependency is taken into account.

Controlled overflow

The increase of the canal water level during extreme conditions can be minimized by assigning dedicated areas as water retention basins. Depending on the event, and because the levee system is extensive, critical water levels can occur at multiple locations within the system simultaneously. Besides, controlled overflow at one location in the system might not be sufficient to

Table 3.12

Potential flood damage [x million €]
polder X hours after breach initiation of
the 18 beach locations A till R.

| | A | B | C | D | E | F | G | H | I |
|------------|-------|-------|-------|-------|-------|------|------|------|------|
| 6h | 0.00 | 0.00 | 0.00 | 0.21 | 0.22 | 0.01 | 0.01 | 0.01 | 0.01 |
| 12h | 0.20 | 0.37 | 0.44 | 19.53 | 9.59 | 0.29 | 0.16 | 0.06 | 0.14 |
| 24h | 2.96 | 5.15 | 5.84 | 33.26 | 19.59 | 4.18 | 3.01 | 0.23 | 0.28 |
| 36h | 8.28 | 12.12 | 12.71 | 47.67 | 22.11 | 6.28 | 5.02 | 0.70 | 0.56 |
| 48h | 12.41 | 16.26 | 16.79 | 51.19 | 24.83 | 7.58 | 6.40 | 2.37 | 1.25 |

| | J | K | L | M | N | O | P | Q | R |
|------------|------|------|------|------|------|------|------|------|-------|
| 6h | 0.01 | 0.21 | 0.21 | 0.02 | 0.02 | 0.31 | 0.01 | 0.00 | 0.01 |
| 12h | 0.15 | 1.14 | 1.08 | 0.10 | 0.32 | 0.52 | 0.30 | 0.02 | 1.17 |
| 24h | 0.27 | 1.95 | 1.94 | 1.39 | 2.00 | 1.00 | 1.13 | 0.30 | 20.50 |
| 36h | 0.46 | 2.27 | 2.27 | 1.88 | 3.25 | 1.59 | 2.81 | 1.15 | 60.20 |
| 48h | 0.99 | 2.46 | 2.48 | 1.88 | 4.88 | 2.92 | 4.08 | 2.24 | 74.31 |

Table 3.13

Annual flood risk per breach location
without and with inclusion of hydraulic
load interdependencies.

| Breach location | Without HLI [€10 ³ /year] | With HLI [€10 ³ /year] |
|-----------------|--------------------------------------|-----------------------------------|
| A | 3.73 | 3.09 |
| B | 15.87 | 14.85 |
| C | 18.02 | 16.89 |
| D | 264.28 | 187.65 |
| E | 119.74 | 70.34 |
| F | 26.09 | 16.15 |
| G | 9.27 | 8.64 |
| H | 0.32 | 0.25 |
| I | 2.27 | 1.33 |

| Breach location | Without HLI [€10 ³ /year] | With HLI [€10 ³ /year] |
|-----------------|--------------------------------------|-----------------------------------|
| J | 25.4 | 18.01 |
| K | 27.46 | 20.62 |
| L | 12.38 | 7.97 |
| M | 23.01 | 15.54 |
| N | 1.45 | 1.07 |
| O | 15.28 | 10.69 |
| P | 3.5 | 2.36 |
| Q | 237.87 | 159.82 |
| R | 25.4 | 18.01 |

reduce the canal water levels at other parts of the system. To be effective as a risk reduction measure, multiple locations should be appointed for water retention, so that controlled overflow could be implemented at the location where the situation requires it. Polders with a large storage capacity and low economic value are most suitable for this measure.

Compartmentalization of the canal system

To reduce the consequences of a breach, the canal system could be compartmentalized near the breach. This way, the amount of water that can enter the polder through the breach is limited, which will limit the breach growth, limit the rate at which the water level in the polder rises and limit the final water level in the polder. However, compartmentalizing reduces the effect the breach has on the water level in some parts of the system, while in the compartmentalized part, the water level drops faster. Compartmentalization should therefore be considered only in case of breaching of a polder with high economic value.

3.5 Discussion

In this case study, we have identified 18 weak spots in the system that are susceptible to levee failure. This implicitly assumes that the other levees in the system have a very small failure probability compared to those 18 weak spots. However, the other levee sections can still significantly contribute to the overall flood risk as well, if the potential damage is high. If these sections would be included in the assessment, including the hydraulic load interdependency might even have a larger effect on flood risk on the system scale compared to not including these effects. Because these locations are not included in the assessment in this study, this risk reduction does not become apparent. To calculate the flood on the system scale more accurately, all levees that significantly contribute to the flood risk in the system should be included in the calculations.

When taking into account hydraulic load interdependency, levees become connected through the hydraulic load in the system. An inaccurate estimation of the failure probability (or the fragility curve or surface) would therefore also have consequences for the other levees in the system. However, the exclusion of hydraulic load interdependencies could lead to costly and unnecessary strengthening of levees that in practice are sufficiently safe.

In this case study, 12 extreme events were used, in which rainfall amounts, wind speeds and wind directions were varied. Because of the variability in time and space of the conditions that cause extreme hydraulic loads in the canals (e.g., rainfall amounts, wind speeds), there is an infinite number of possible events. Finding a representative set of scenarios is challenging, and becomes even more challenging with an increasing size of the system.

3.5 Conclusions and recommendations

3.5.1 Conclusions

In this study, a method was developed that assesses flood risk in controlled canal systems, while taking hydraulic load interdependencies into account. To compare these effects to current practice, it was applied on two case studies: a partial system and an entire system. The conclusions are presented here:

- If the levees are assessed at the individual levee section scale, as is the case in current practice, the overall flood risk at the system scale is overestimated. As a consequence, the effects of risk reduction measures are overestimated, as measures often have a contra-effect at other locations. These effects are not neglected, when hydraulic load interdependency is included.
- Strengthening of vulnerable levee sections will reduce the probability of failure of that specific levee section, but will also reduce the probability of hydraulic load reduction on levee sections elsewhere in the system. The increased hydraulic loads on other sections make them more likely to fail. While strengthening locally leads to a local risk reduction, the increased vulnerability elsewhere might lead to an increased overall flood risk if flood damage is higher at one breach location compared with another breach location. On the contrary, strengthening of less vulnerable levee sections, which can occur if levees are assessed on the individual levee section scale, might lead to minimal risk reductions, which makes them less cost-effective. The effects on the system scale can

only be assessed when hydraulic load interdependency is taken into account in the flood risk assessment.

- The current system of safety standards for flood protection is based on potential flood risk: the required reliability increases with increasing potential flood damage. So, levees protecting areas with low economic value get a low safety standard, whereas levees protecting areas with high economic value have a high safety standard. Strengthening a levee section better than the prescribed safety standard could lead to an increased flood risk elsewhere. The decision of further strengthening a levee section should not be based on the local risk reduction, but on the overall risk reduction at the system scale in relation. The measure is only cost-effective, if the overall risk reduction is lower than the strengthening costs.
- Overall, including hydraulic load interdependency brings down the estimated overall risk of the system, 68% in case study 1 and 31% in case study 2. It should be noted that these case studies only included a part of the system (case study 1) or only the identified weak spots (case 2). This is however, still a conservative estimate. If all levees that contribute significantly to the overall flood risk of the system are included, the effects of hydraulic load interdependency will become even larger. Including these effects can also lead to different preferred solutions compared to the estimation with no interdependency.

3.5.2 Recommendations

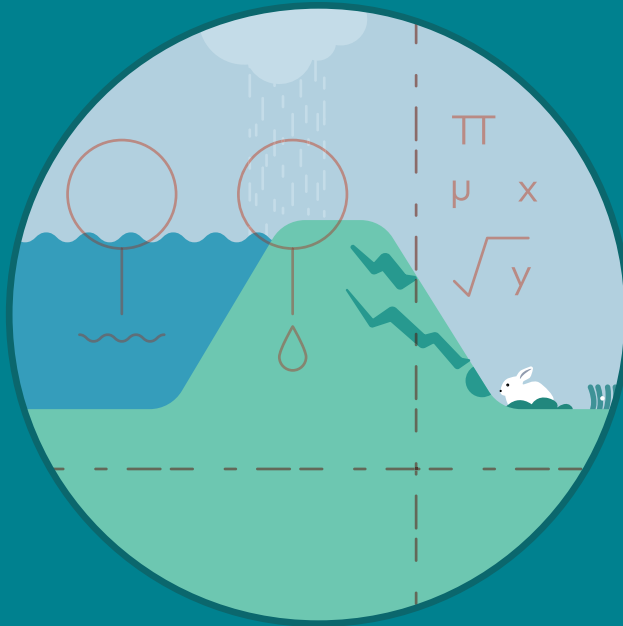
As this study showed, hydraulic load interdependency plays a significant role in the failure probability estimation. However, to further improve the estimation of its

effects, the following improvements are suggested:

reliability updating.

- Enrich the set of possible load scenarios with the following stochastic variables: wind speeds, wind directions, rainfall durations and rainfall intensities. These variables should also include spatial variations and differences in magnitude.
- Do not only include the weak spots in the system, but include all levees that contribute significantly to the overall flood risk of the system. Significant contributions to the overall flood risk do not have to come from levee sections with high failure probabilities only. Sections where the failure probabilities are low, but the potential consequences of a breach are high, also contribute to the overall flood risk. By including them, a better prediction of the flood risk on the system scale can be done.
- Use local conditions and characteristics rather than generic parameters to optimally predict the strength of a levee section.
- Controlled overflow or controlled levee breaching can be adopted as a flood risk reduction strategy to reduce the hydraulic loads elsewhere and relieve other levees in the system, if the hydraulic loads in the system become critical. This could be achieved by including designated 'weak' spots in the design of the system at locations where consequences of inundation are minimal. Additional measures can help to reduce potential damage in the designated retention basin further.
- More accuracy can be obtained by focusing on the substantiation of the fragility surfaces. If a levee survives certain extreme conditions, the fragility surface can be improved through

4



A pragmatic,
performance-based
approach to levee safety
assessments

4.1 Introduction

4.1.1 Problem analysis

The current safety assessment of regional canal levees is a costly affair, due to their large number and their total length. These assessments often result in that a large portion of levees do not meet the safety standards, leading to expensive reinforcements, which can be an order of magnitude larger than safety assessment costs (HHNK, 2019b). To illustrate, of all regional levees maintained by the water boards in the province of South Holland, 953 km out of approximately 3,100 km, roughly one third, did not meet the safety standards in 2012. Through extensive levee reinforcement works and additional research, this number was reduced to 571 km in 2018 (Province of South Holland, 2019). Water Authority HHNK (Hoogheemraadschap Hollands Noorderkwartier), in the Province North Holland, has strengthened about 200 km of almost 1,100 km of regional levees between 2008 and 2018 (HHNK, 2019b).

Rikkert and Kok (2019) concluded that the average annual failure probability of all canal levees is around 1/600 or lower, which is much lower than the results of the safety assessment calculations suggest. The estimation is based upon a statistical analysis of historical failure cases between 1960 and 2020. Their analysis focused on observed levee behaviour over a longer time span of 60 years. This means that survived loads and variations of levee performance were implicitly taken into account. In other words, the large number of levees which do not fulfil the safety standard does not seem to match the actual observed strength of the levees. This mismatch can be ascribed, at least to some extent, to conservatism in the current approach, which could lead to unnecessary

and costly levee reinforcements. While conservatism in safety assessments is acceptable to some extent, a more accurate estimation of the actual failure probability of the levee can be achieved, by including survived loads and levee inspection results in the safety assessment. This supports more cost-effective strengthening of levees and management of funds.

4.1.2 Objective

The current approach of assessing the safety of canal levees neglects performance observations of these levees and may lead to conservative results and unnecessary reinforcements. Utilizing information from inspections could reduce uncertainties in and improve accuracy of levee safety assessments. Therefore, the aim of this chapter is to develop a new approach to assess the safety of canal levees, which utilizes both the information from observed survived loading conditions, as well as observations of levee performance indicators resulting from recent levee inspections. Important to note is that, while the current approach is based on exceedance probability of the hydraulic load, the new approach is a pragmatic method to do a full probabilistic assessment, that is able to calculate levee failure probabilities.

4.1.3 Approach and chapter outline

The approach that is developed in this chapter aims to assess the safety of canal levees and could therefore provide an alternative to current levee safety assessment practices. Section 4.2 presents background information on a semi-probabilistic and a full-probabilistic method for levee safety assessments. In Section 4.3, a method is presented to include information on actual levee performance in the safety assessment. The developed approach is validated by means of a case study: the Eilandspolder (Section 4.4).

In this case study, the applicability of the approach is demonstrated and the outcomes are compared to the outcomes of the current approach. We have restricted ourselves to one failure mechanism: inner slope instability, since this is the dominant stability-related failure mechanism for which canal levees are not fulfilling the safety standard in the levee stability assessment (see for example: HHNK, 2015; De Leau, Bijnen & Fila, 2019).

4.2 State-of-the-art of levee safety assessment

In Section 4.2.1 the current, semi-probabilistic exceedance probability approach for a levee slope stability assessment is explained, while Section 4.2.2 focuses on the probabilistic approach. In Section 4.2.3, we explain important elements on how to include observations in levee slope stability assessments.

4.2.1 Current safety approach to inner slope stability assessment

Flood protection standards for regional flood defences are based on the potential economic damage of a levee breach, in which the levee is divided into sections in which a breach leads to similar flooding (STOWA, 2008; IPO, 1999). The classification system for flood protection standards distinguishes between 5 safety standard classes (called IPO classes), all with their own annual exceedance frequency. This annual exceedance frequency refers to the hydraulic load (i.e., the water level) that the levee should be able to withstand. For slope instability, the driving load factors are the canal water level and the phreatic surface, and traffic loads. The water level associated to the prescribed exceedance probability is obtained through a statistical analysis

Table 4.1
Flood protection standards with corresponding required probabilities of exceedance and failure.

| Flood protection class | Annual exceedance probability | Annual failure probability |
|------------------------|-------------------------------|----------------------------|
| 1 | 1/10 | 1/50 |
| 2 | 1/30 | 1/150 |
| 3 | 1/100 | 1/500 |
| 4 | 1/300 | 1/1,500 |
| 5 | 1/1,000 | 1/5,000 |

of historical water level measurements or through predictions of a model that simulates the behaviour of the polder canal system. The ‘extreme’ phreatic surface is often derived based on a set of general rules, in which the phreatic surface is a function of the canal water level (see for instance Leau, Bijnen & Fila, 2019). The importance of traffic loads on failure probability was already presented in earlier studies (e.g., Lendering et al., 2015). However, we are interested in the impact of degradation, and for the sake of simplicity, we leave traffic loads out of the analysis. The possible effects of this simplification are included in the discussion chapter.

It is reasonable to assume that the failure probability, which is defined as the probability that a levee breaches and consequently leads to flooding, is much lower than the exceedance probability. This is explained because these levees are designed and assessed in a conservative way: if the design water level will occur, the levee will not immediately fail. An estimate of a factor 5 (following Fugro, 1998) between the exceedance probability and the failure probability is given in Table 4.1. For comparison, levees with IPO class 1, 2 and 3 have allowable annual failure probabilities of 1/50, 1/150 and 1/500, respectively, while, according to Rikkert and Kok (2019) the average annual failure

probability of a levee section is 1/600 or smaller.

Levee stability assessments are often performed with D-Geo Stability, which is a limit equilibrium slope stability package (Deltares, 2016). With D-Geo Stability, a factor of safety (SF) can be calculated using different slip circle methods. In the slip circle method of slices, a potential rotational sliding soil body mass is divided into a number of finite vertical slices and the equilibrium of each slice is considered in determination of the factor of safety (Tsuchida & Athapaththu, 2014). In this study, we limit ourselves to Bishop’s method of slices, in which the assumption is made that the forces acting on the sides of each slice have a resultant of zero kiloNewton in the vertical direction (Bishop, 1955). The required factor of safety for canal levees depends on the safety standard, and is determined based on the following requirement (STOWA, 2015a):

$$SF = \gamma_n \times \gamma_{mod} \times \gamma_s \times \gamma_{mat} \quad \text{(Eq. 4.1)}$$

In which SF is the required factor of safety, γ_n is the damage factor (which is based on the required safety standard), γ_{mod} is the model factor (default for Bishop’s method of slices is 1), γ_s is the schematization factor, which takes into account for uncertainties in

| Flood protection class | Damage factor γ_n | Factor of safety (SF) |
|------------------------|--------------------------|---------------------------|
| 1 | 0.8 | 1.06 |
| 2 | 0.85 | 1.12 |
| 3 | 0.9 | 1.19 |
| 4 | 0.95 | 1.25 |
| 5 | 1.0 | 1.32 |

Table 4.2
Flood protection standard, damage factor γ_n and required Factor of safety, based on an average material factor γ_{mat} of 1.2, a model factor γ_{mod} of 1 (Bishop), and a schematization factor γ_s of 1.1.

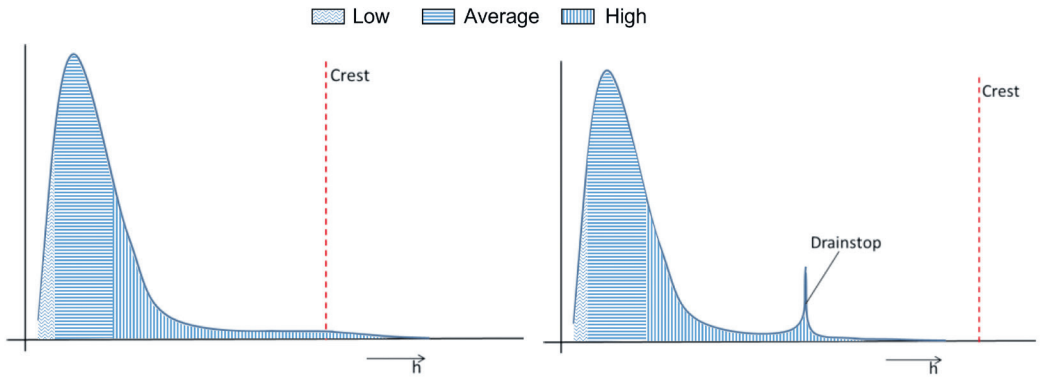


Figure 4.1

Probability density function of water level h in a normal river (left), and in a polder canal (right) (from Lendering et al., 2015), with an indication of how the low, average and high water level can be discretized.

the schematization and typically has a value between 1.0 and 1.2 (STOWA, 2015a), γ_{mat} is the material factor, and depending on the soil material and soil properties typically has a value between 1.1 and 1.35 (STOWA, 2009). An example of how the flood protection class in combination with the different factors translates into a required Factor of Safety is shown in Table 4.2.

4.2.2

Probabilistic approach to inner slope stability assessment

While the semi-probabilistic approach is based on only one load combination, the probabilistic approach accounts for the entire range of possible load combinations. This can be either done through using the continuous probability density function of the load, or by discretizing the continuous probability density function, to limit the amount of load combinations.

The probability density function of the canal water level is usually derived from water level measurements. Since water levels are controlled, a drain stop is applied if the canal water level exceeds the so-called drain-stop level. At that point, no more water will be pumped from the polders into the canals. For that reason, the probability density function for canal water levels has a different shape than the probability

density function of the water level in normal rivers (see Figure 4.1). More specifically, the probability density function of the regulated water levels contains a high probability density at the drain-stop level, as (most of) the probability density of higher water levels is reduced due to the regulation of water levels at this point. The continuous statistical distribution of these water levels could be discretized to limit the number of possible load combinations and hence the number of necessary stability calculations. Figure 4.1 also gives an example of how the continuous function can be discretized into a low, average and high water level.

A probability density function of the phreatic line can be discretized in a similar way. However, measurement data of the phreatic line is usually lacking, and at the same time the phreatic line is very location specific (Flanagan and Tigchelaar, 2016; Rikkert et al., forthcoming). Lendering et al. (2018) discretized the phreatic line into three possible conditions: 1) average, under normal conditions; 2) high, under wet conditions, and; 3) low, under dry conditions. Under normal conditions, the phreatic surface is interpolated linearly between crest and toe. Under dry conditions, the phreatic surface is assumed to have a concave shape, whereas, during wet conditions, the schematized phreatic

surface is expected to have a more convex shape. These possible (discretized) conditions of phreatic lines are shown in Figure 4.2.

The failure probability can be determined, as follows:

$$P(F) = \sum_{i,j} P(F | h_i, S_j) \times P(h_i, S_j)$$

(Eq. 4.2)

Where $P(F)=1-\Phi(\beta)$, and $P(F|h_i, S_j)$ is the conditional failure probability given water level h_i and phreatic surface level S_j , and $P(h_i, S_j)$ is the probability of occurrence of the combination of water level h_i and phreatic surface level S_j . This failure probability is called the a-priori failure probability as it is calculated prior to applying reliability updating.

4.2.3 Including observed condition in slope stability assessment

This section explains how real-life field observations can be included in slope stability assessments to reduce uncertainty and conservatism in levee stability analysis. It also elaborates how different forms of degradation of a levee might influence its stability.

Reliability updating to calculate the posterior probability

Reliability updating means that the a-priori failure probability is updated by including information on survived loads. Applicability of the ‘reliability updating’ method strongly depends on the availability of accurate and reliable observations of hydraulic loads that a levee has successfully withstood in the past (STOWA, 2009). We explain reliability updating through one loading variable: the canal water level.

The base of the reliability updating approach is Bayes’ theorem:

$$P(F | \varepsilon) = \frac{P(F \cap \varepsilon)}{P(\varepsilon)}$$

(Eq. 4.3)

In which $P(F|\varepsilon)$ is the probability of failure, given observation ε , $P(F \cap \varepsilon)$ is the joint probability of failure and observation ε , and $P(\varepsilon)$ is the probability of observation ε . This is illustrated in Figure 4.3: the failure probability is determined by the probability density of the load (in red) and the probability density of the resistance (in green). When the levee resistance is constant in time, a survived load (at dashed vertical black line) serves as evidence that the probability of failure for that load (and smaller loads) equals zero. The probability density under that load is then redistributed over the probability density above that survived load, reducing the levee’s overall failure probability.

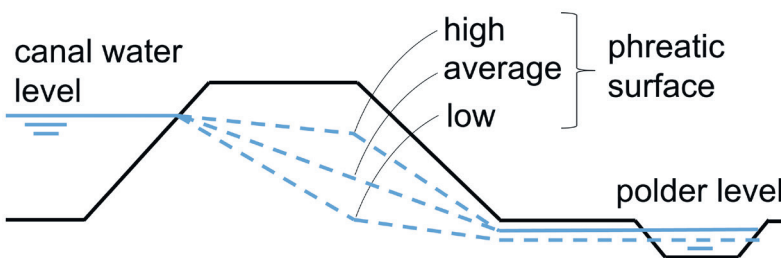


Figure 4.2
Schematic representation of possible phreatic surface levels (high, average, and low).

We follow the ‘direct approach’ for reliability updating, which exploits the definition of the conditional probability of failure from equation 4.3, by defining a new limit state of the intersection (cut set) of failure and the observation ($F \cap \epsilon$), as described by Schweckendiek et al. (2016). We assume that the correlation between the survived load and the current (or future) situation equals one: the strength does not change. In other words, there have been no changes in the levee that might have led to an increase or decrease of its strength properties. This leads to an adjusted probability density of the estimated levee’s resistance (see Figure 4.3). The figure shows there is no probability density left below the observed water level.

In our analysis, we not only take into account the canal water level, but also the phreatic line, which adds a dimension to the reliability updating, as was already done by Lendering et al. (2015; 2018). We use the same combination of canal water levels (low, average and high) and phreatic

surface levels (low, average and high), with each combination having a specific conditional failure probability (Table 4.3) and probability of occurrence.

The probability that a certain load combination occurs, depends on its assumed conditional probability of occurrence of the phreatic surface, given a water level. As measurements of the phreatic line are often lacking, Lendering et al (2018) made an estimate of the conditional probabilities of occurrence of a phreatic line, given the canal water level (see Table 4.4). These conditional probabilities are based on the assumption that during wet conditions, in which a high canal water level is observed, there is a larger chance of observing a high phreatic surface. This is caused by the dependency of the canal water level and the phreatic surface on rainfall. Under normal or dry conditions, when the water level is average or low, the probability of a high phreatic surface is relatively small.

Figure 4.3

The concept of ‘reliability updating’, where the probability density under the survived load is redistributed over the probability density above the survived load (Schweckendiek, 2014).

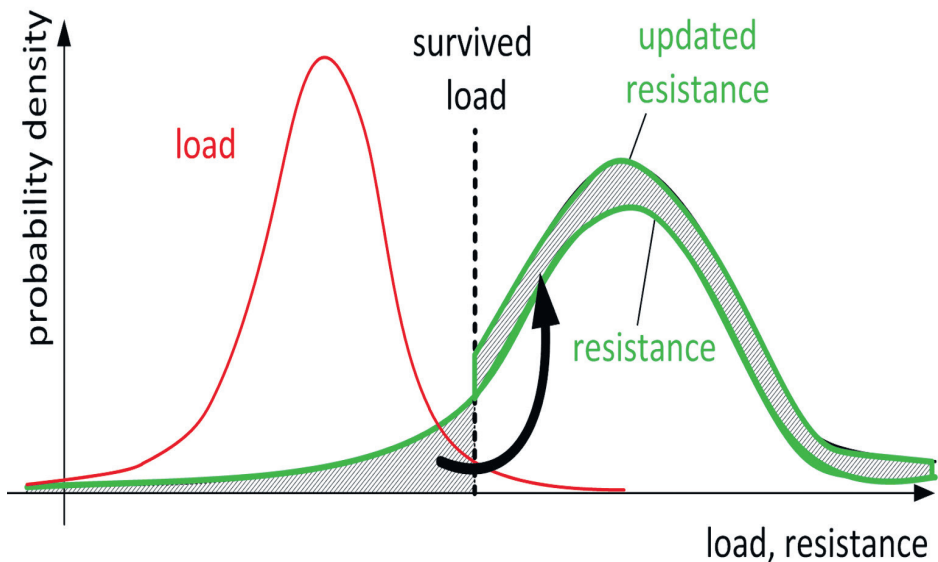


Table 4.3

Conditional failure probability, given a combination of load conditions.

| | Low phreatic surface (S_1) | Avg. phreatic surface (S_2) | High phreatic surface (S_3) |
|----------------------------|--------------------------------|---------------------------------|---------------------------------|
| Low water level (h_1) | $P(F h_1, S_1)$ | $P(F h_1, S_2)$ | $P(F h_1, S_3)$ |
| Avg. water level (h_2) | $P(F h_2, S_1)$ | $P(F h_2, S_2)$ | $P(F h_2, S_3)$ |
| High water level (h_3) | $P(F h_3, S_1)$ | $P(F h_3, S_2)$ | $P(F h_3, S_3)$ |

Even though observations are not always present, the following combinations of loads can reasonably be assumed to have occurred in the past:

1. An average water level with a high phreatic surface: it is reasonable to assume that this combination has occurred in the past, for instance during heavy local rainfall which did not have sufficient volume to raise the water level in the entire canal.
2. A high water level with an average phreatic surface: this assumption is reasonable, if high water levels were observed from historical data of canal water levels, although it is not sure if, for a specific location, the phreatic surface was also raised.
3. An average canal water level and a low phreatic surface: it is reasonable to assume that, during dry conditions, the canal water level was artificially kept at an average level, while the phreatic surface is low.

This means that the following combinations of load conditions from Table 4.3 are assumed to have occurred: h_1 and S_1 , h_2 and S_3 , h_3 and S_2 .

Effects of degradation

Degradation processes of levees negatively influence the levee strength. Examples of such processes are unwanted vegetation on or near the levee (Lanzafame, 2017), subsidence of the hinterland (Kwakman and Van Loon, 2019), cracking of the cover layer (Jamalinia et al., 2020), and animal burrows (Kwakman and Van Loon, 2019). The Levee Screening Tool (USACE, 2015) explicitly uses observable indicators of levee performance, so that results from a levee inspection can be used to improve estimations of levee stability. Figure 4.4 show an example of an observable levee performance indicator: animal burrowing. In this section, we describe degradation effects and how they influence levee stability. We hereby focus on observable levee performance indicators that can be observed in a levee inspection. Further, we limit ourselves to an earlier study that has been performed on regional levees.

In their analysis, Kwakman and Van Loon (2019) calculated the effects of varying levee performance indicators on levee stability. They focused on existing Dutch canal levees with very different

Table 4.4

Example of conditional probabilities of phreatic surface, given a water level (Lendering et al., 2018).

| | Low phreatic surface (S_1) | Avg. phreatic surface (S_2) | High phreatic surface (S_3) |
|----------------------------|--------------------------------|---------------------------------|---------------------------------|
| Low water level (h_1) | 0.01 | 0.98 | 0.01 |
| Avg. water level (h_2) | 0.01 | 0.98 | 0.01 |
| High water level (h_3) | 0.01 | 0.01 | 0.98 |

characteristics, and included the following levee performance indicators:

- Reduction of hydraulic resistance of canal bottom;
- Subsidence of hinterland;
- Lower water level in ditch at levee toe;
- Deepening of the ditch at levee toe;
- Animal burrows.

For each of these performance indicators they used 3 levels of severity:

1. Good (reference case with no reduced performance);
2. Light;
3. Severe.

The performance indicators resulted in changes in geometry, soil structure, the phreatic water level, and the hydraulic head in the aquifer, which was used in their calculations. Their results show that the extent to which performance indicators influence the levee stability varies with levee characteristics.

Konings and Van Hemert (2020) followed the same approach, but they performed

their calculations on a selected set of typical Dutch canal levees, based on combinations of local subsoil characteristics, levee slope, crest width, water retaining height (difference between canal water level and the polder surface level), and the presence of a berm. They also included subsidence as one of the performance indicators in their study and made the same distinction: no subsidence (0 m), light subsidence (0.25 m), and severe subsidence (0.5 m). They have found reductions of up to 25% in the factor of safety for severe subsidence for levees with varying water retaining height, and inner slope, and a crest width of 5 m. Therefore, when levee inspection observations are included in a safety assessment, indicators of reduced levee performance will have a direct influence on the strength and cannot be neglected.



Figure 4.4
Example of a performance indicator: animal burrows (picture by André Koelewijn).

4.3

Including observed levee strength

In this section, we develop a 3-step approach for levee stability assessments, that optimally utilizes evidence of observed levee strength, and results of levee inspections. The proposed method is a pragmatic approach to perform a full-probabilistic stability assessment. It reduces the uncertainty that is initially included in the partial safety factors, by adjusting the relation between factor of safety SF and reliability index β . Figure 4.5 shows a schematization of the proposed approach. The first step of this method is to estimate the failure probability, based on levee specific load and strength parameters. In the two following steps, this estimation is improved by including observed levee behaviour.

1. The first step is to determine the a priori annual failure probability (P_f). Probabilistic stability calculations are performed for each levee section, providing both the safety factor SF and the reliability index β , as explained in section 2.2. This can be done with a slope stability package, such as D-Geo stability. Levees with comparable characteristics, such as inner slope, soil structure and geotechnical parameters, can be grouped into 1 levee type to obtain a specific relation for this type of levee. Based on results for multiple levee sections within the same levee type the relation between SF and β is established through a best fit (see Figure 4.6). Through this SF - β relation the failure probability of other levees can be determined if the safety factor is calculated, without doing the probabilistic calculations.

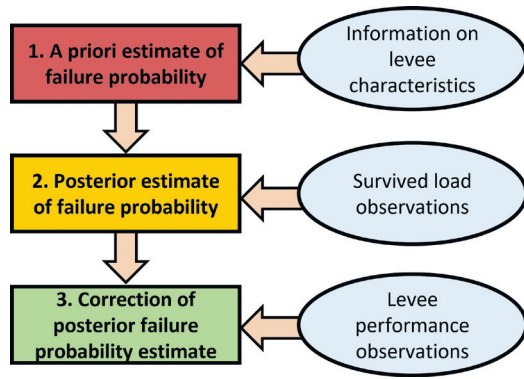


Figure 4.5

Schematization of the proposed method to estimate the failure probability, utilizing information on levee performance under critical conditions and levee inspection results.

Determine relation SF - β

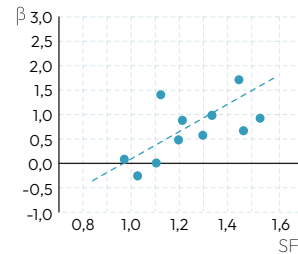


Figure 4.6

Relation between safety factor SF and reliability index β for one levee type, based on probabilistic stability assessments.

2. In the traditional safety assessment, observations of performance of the levee under various circumstances are not taken into account, which means that evidence of the observed strength of the levee is not used. This evidence can be included, using the approach described in section 4.2.3 on reliability updating. The initial relation found in step 1 can be improved, by fitting a line through the points after reliability updating, as is shown in Figure 4.7.

3. The final step is to correct the posterior failure probability by including results of levee inspections in the form of levee performance indicators, in addition to the survived loads from the previous step. These levee performance indicators contain information about the actual condition of the levee, and they influence the stability factor, and hence the probability of failure. Ideally, the same approach as in step 2 would be used here: including the effects of a certain performance observation, based on Bayes theorem. However, in this study a more pragmatic approach is used to limit the processing time of the study. Besides, discretization of the load and resistance in reliability updating makes it difficult to take into account gradual degradation. Therefore, we assume that the effect of an observation (e.g., animal burrows) on the stability factor can be expressed as a reduction factor that is dependent of the levee type, the performance indicator and the level of severeness. Figure 4.8 shows how this works.

To demonstrate the applicability of the proposed method, it is applied in the next section to a case study: the Eilandspolder, which is a polder managed by the Water Authority Hoogheemraadschap Hollands Noorderkwartier (HHNK). For reliability updating, we make reasonable assumptions of loading conditions that the

Update relation SF- β

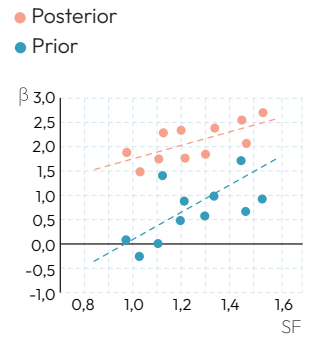


Figure 4.7

Updating the prior relation between safety factor SF and reliability index β for one levee type, based on observations of survived hydraulic loads, with the prior relation in blue and the relation after updating in orange.

Determine degradation effect

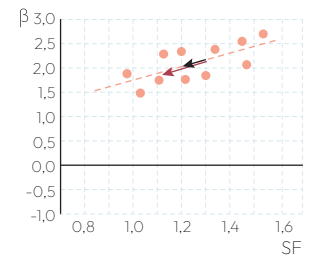


Figure 4.8

The arrows indicates how different degrees of degradation (black: light degradation; red: severe degradation) affect the stability factor, and hence the reliability index, of one levee type that is influenced by levee degradation. The arrows are indicative, and effects on the stability factor depend on levee characteristics and degradation type.

levee has survived in the past. Regarding performance indicators, we limit ourselves to levee inspection results concerning levee subsidence. Finally, our results are compared to the results of the traditional levee safety assessment approach.

4.4 Case study

4.4.1

Description of Eilandspolder

In this section we apply the developed approach to a case study: the Eilandspolder, which is a polder in North Holland, the Netherlands. The polder is surrounded by the Schermer boezem, which is a canal with an average daily water level of $-0.5\text{ m} +\text{NAP}$ (MSL) and an extreme water level of about $-0.2\text{ m} +\text{NAP}$. The results of the proposed method were compared to the outcomes of the traditional approach. Figure 4.9 shows the total of 26.9 km of regional levees protecting the Eilandspolder from flooding, including an indication of the assigned levee safety standard. The assigned safety standards are based on the expected flood damage after a levee breach. The figure also shows the distinction into different levee sections, derived from a recent levee safety assessment, that was finalized in 2019 (IV-Infra, 2019).

Figure 4.10 shows the distribution of different levee safety standards for the levees protecting the Eilandspolder, according to the Dutch IPO classification system (classes 1 to 5).

For the macrostability assessment, the levees were schematized, and several sections were distinguished, based on similarities and differences in geometry (crest height, inner slope, and hinterland surface level), and soil structure. As mentioned in Section 4.3, it is not always possible to derive a single $SF-\beta$ relation for all polder canal levees, hence, a classification is made based on aspects such as inner slope, soil structure, and geotechnical parameters. For the Eilandspolder, however, we assume that all levees can be classified as one levee type, since they have very similar slopes, water retaining heights and subsoil material.



Figure 4.9 Left: map of the Netherlands, with the location of the Eilandspolder. Right: overview of levees protecting the Eilandspolder, the distinction into separate, numbered, levee sections, and their assigned flood protection standard.

Levee safety standards Eilandspolder



Figure 4.10
Distribution of assigned levee safety standards over the levee system for the Eilandspolder. The highest safety standard (5) is assigned to levees protecting urbanized areas, while lower safety standards are assigned to rural areas.

Survived loads

In our analysis, we use the 9 load combinations following Table 4.3. We assume that the following 3 load scenarios have been observed as survived (see section 4.2.3):

- An average water level (-0.5 m +NAP) with a high phreatic surface;
- A high water level (-0.2 m +NAP) with an average phreatic surface;
- An average canal water level (-0.5 m +NAP) and a low phreatic surface.

Inspection of degradation

From the results of levee inspection for the Eilandspolder, in the period July 2014 until June 2020, it is found that the most frequently observed performance indicators at the levee crest, inner slope and inner berm were levee subsidence (38%), followed by wet spots (27%). For each performance indicator a score was indicated: light and severe. In our study, we focus solely on the most observed performance indicator for the Eilandspolder: levee subsidence.

Konings and Van Hemert (2020) studied the effect of levee subsidence on the stability factor for different representative schematizations of the subsoil of levees within the management area of HHNK. We have used one of these schematization that resembles our levee sections best. Besides the schematization for the subsoil, Konings and Van Hemert (2020) also distinguished between other levee characteristics, such as inner slope, crest width, retaining height, and the presence of a berm. While they found that effects of degradation on the safety factor depend on these levee characteristics, we have chosen to average these effects to values that roughly resemble the values calculated by Konings and Van Hemert (2020). The effects on the safety factor relative to a zero subsidence case are shown in Table 4.5. It should be noted that Konings and Van Hemert focused more on subsidence of the hinterland. However, they also included partial subsidence of the berm and the toe of the levee, which also influences the inner slope. Therefore, we assume that the reduction factors from Table 4.5 can be applied to our case, when subsidence on the slope is observed.

| Effect on safety factor relative to reference (zero subsidence) case [%] | |
|--|----------------------------|
| Light subsidence [0.25 m] | Severe subsidence [0.50 m] |
| -7.5% | -15.0% |

Table 4.5
Estimated relative effect of subsidence on safety factor, based on Konings and Van Hemert (2020).

4.4.2

Results of semi-probabilistic approach

Following the levee safety assessment results of the water authority, out of the 26.9 km of levees, 16.1 km (about 60%) do not meet the required levee safety standard for macro-stability. Figure 4.11 and Figure 4.12 give an overview of levees that do not meet the safety standard and the distribution per safety standard class.

In this case study, only levee sections that do not meet the safety standard according

to the current approach were taken into account, to determine if the new approach is less conservative and leads to less rejections. These levee sections are divided into 5 representative schematizations, based on inner slope, subsurface composition and water retaining height (see Table 4.6). This table also includes the results of the stability assessment, using the traditional approach.

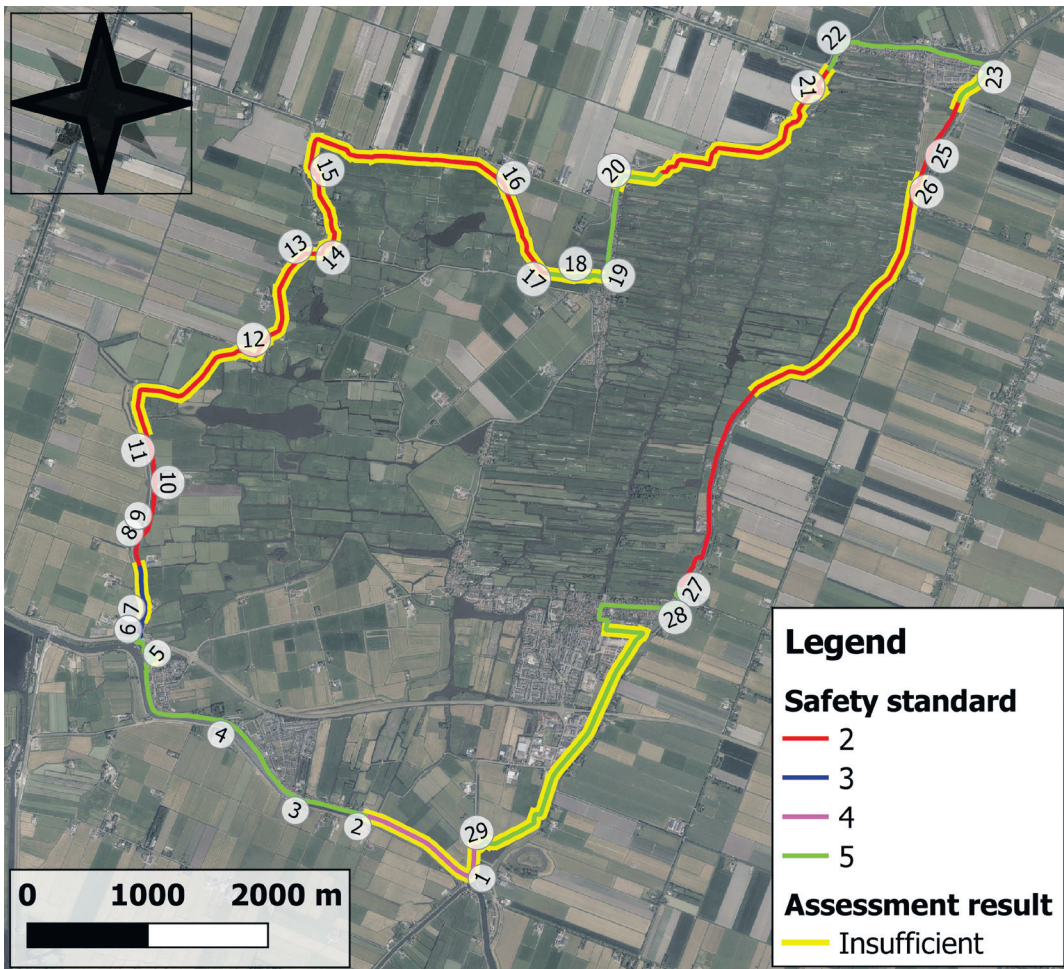


Figure 4.11
Overview of levees that do not meet the required safety standard for the failure mechanism macro-instability.

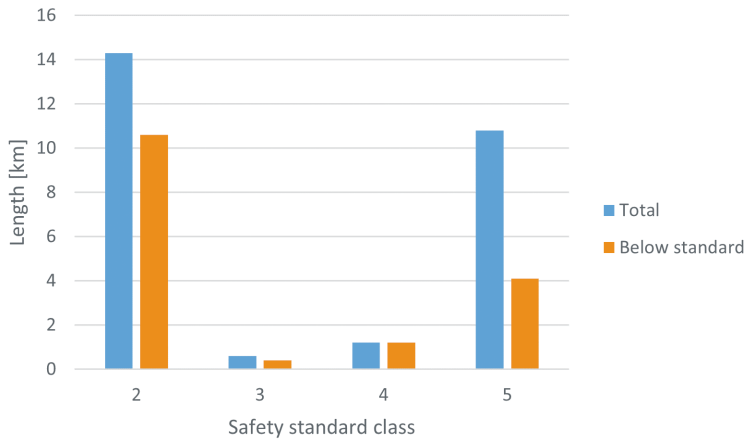


Figure 4.12
Total length of levees per safety standard class and length of levees that do not meet safety standard for macro stability per safety standard class. Out of 26.9 km in total, about 60% does not meet the required safety standard.

4.4.3

A-priori failure probability

In this section, the a-priori failure probability per levee section is estimated. Different than in the current approach, both load and resistance parameters are considered as stochastic variables, rather than using design values.¹

For the water level statistics of the Schermerboezem and the phreatic surface, we applied the distributions as estimated by Lending et al. (2018). Specifically, for the phreatic surfaces, we distinguished between the 3 possible conditions, as assumed by Lending et al. (2018): low, normal and high. The conditional probability of a phreatic water level condition, given a canal water level, were already presented in Table 4.4 as an example, and we consider them as reasonable values in this case study.

By assessing all 9 possible combinations (3 water levels multiplied by 3 phreatic surface levels) in a stability calculation and including the probability of occurrence of each of these combinations, both a (weighted) Stability Factor and a reliability index was

calculated. The results of this probabilistic stability assessment are shown in Figure 4.13. A linear relation provides a good fit ($R^2 \approx 0.97$) between the prior reliability index and the safety factor:

$$\beta_{prior} = 6.43 \times SF - 6.57 \quad (\text{Eq. 4.4})$$

4.4.4

Failure probability after reliability updating

The a-priori failure probability was updated, following the approach as presented in Section 4.2.3. The survived loads that are included in this analysis are:

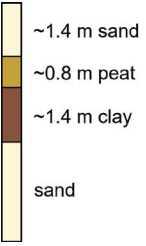
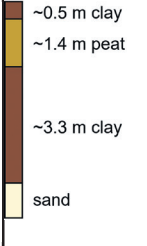
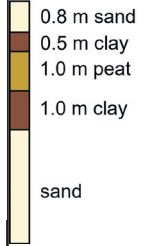
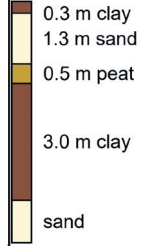
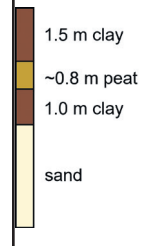
- Low phreatic water level in combination with normal water level (-0.5 m +NAP);
- Average phreatic water level in combination with high water level (-0.2 m +NAP);
- High phreatic water level in combination with average water level (-0.5 m +NAP).

Figure 4.14 shows the results of the stability analysis before and after reliability updating. As the figure shows, including

¹ To perform the probabilistic calculations with D-Geo Stability, an older version of the set of regional geological parameters was used. Using this model, similar safety factors were calculated as were found in the safety assessment done by the Water Board. This check proved that a fair comparison can be made between the results of our approach and the outcomes of the safety assessment done by the Water Board.

Table 4.6

This table shows which 5 levee sections are used as representative levee sections, which levee sections they represent, and some distinctive characteristics.

| Levee section | 7 | 29 | 18 | 26 | 1 |
|---|---|---|---|---|--|
| Represents levee sections | 13, 14, 15, 16, 17 | 12, 21, 24 | 20 | - | - |
| Subsurface composition (the lowest sand layer is where the boring stopped) |  |  |  |  |  |
| Slope [1/x] | ~1:3.8 | ~1:3.6 | ~1:3.3 | ~1:2.7 | ~1:2.4 |
| Berm present | No | No | No | No | Yes |
| SF (Bishop) from semi-probabilistic approach | 0.83-0.87 | 0.87-0.90 | 0.82-0.88 | 0.79 | 0.68 |

observations of survived loads significantly increase the estimated reliability index.

The following linear relation was found between the posterior reliability index and the safety factor:

$$\beta_{posterior} = 1.27 \times SF + 1.94 \quad \text{(Eq. 4.5)}$$

With this posterior $SF-\beta$ relation, an

increased reliability index can be found for the same safety factor, compared to the a-priori $SF-\beta$ relation. This means that the estimated failure probability has decreased, which could result to approving a levee, that was initially rejected. Interesting to note is that the slope of the $SF-\beta$ relation changes after updating. This is further discussed in the discussion chapter.

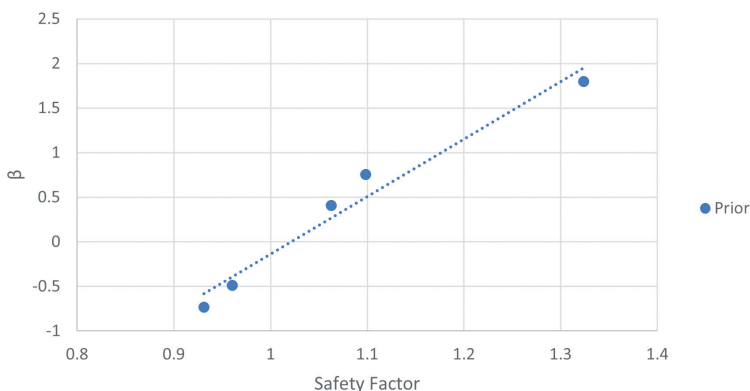


Figure 4.13
Results of probabilistic stability assessment for a priori calculations.

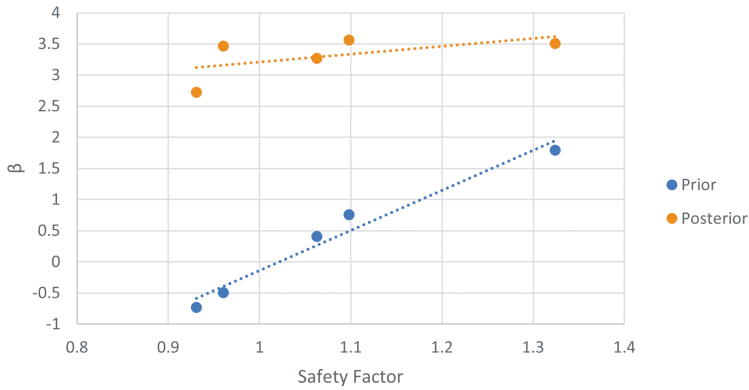


Figure 4.14
Results of probabilistic stability assessment for a priori (blue) calculations and after reliability updating (orange).

4.4.5

Effects of levee degradation on failure probability

Figure 4.15 shows the severity of levee subsidence per location, observed during levee inspections over a course of about 2 years (2016–2018). The figure only includes observations of levees that were unsafe according to the semi-probabilistic safety assessment. A distinction is made based on the degree of severity of subsidence:

- Light subsidence: about 0.25 m subsidence is observed in section 12;
- Severe subsidence: about 0.5 m subsidence is observed in section 1, 26, and 29.

The relative reduction of light and severe subsidence on the safety factor is assumed 7.5% and 15%, respectively. These values were presented earlier in Table 4.5, and are based on Konings and Van Hemert (2020). How these observations influence the reliability index is explained levee section 1 (with severe subsidence). Results for levee section 12, 26 and 29 were derived in the same way and are all presented in Table 4.7.

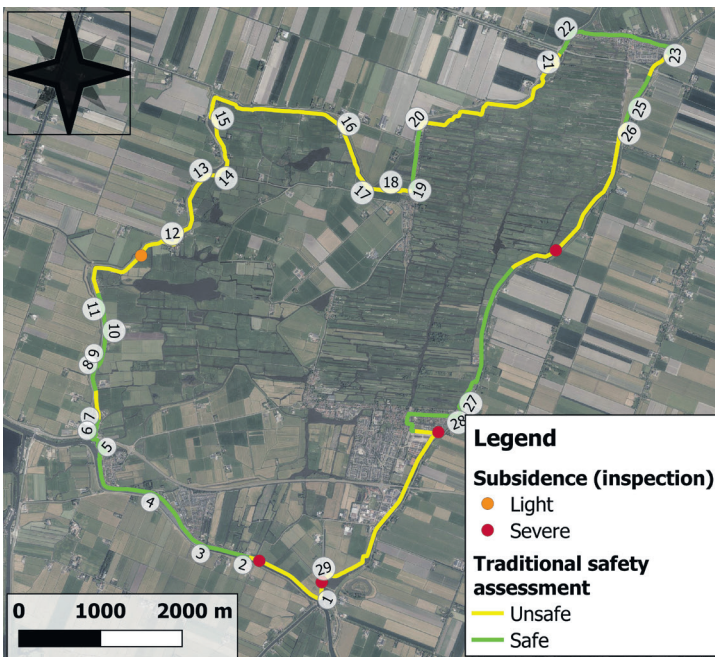


Figure 4.15
Map showing the subsidence observations from the levee inspection. Light subsidence is observed in section 4.5, and severe subsidence is observed in section 1 (on 2 locations), 8.2, and 9.2.

Levee section 1

Step 1. Determining the a-priori reliability index:

Initially, a safety factor of 0.93 was calculated for levee section 1 with the probabilistic approach. Which, according to Eq. 4.4 corresponds to:

$$\beta_{prior} = 6.43 \times 0.93 - 6.57 = -0.59$$

Step 2: Determine the a-posterior reliability index after including information on survived loads:

Through the observations of survived loads, the SF - β relation was updated. When filling in the a priori factor of safety in Eq. 4.5 the β after reliability updating increases from -0.59 to:

$$\beta_{posterior;survivedloads} = 1.27 \times 0.93 + 1.94 \approx 3.12$$

Step 3: Determine the adjusted reliability index from step 2 after including levee inspection observations of degradation

During the inspection, severe subsidence was observed in this levee section. For severe subsidence we expected a reduction of the safety factor of 15% (see Table 4.5). This coincides with a reduction of 5.7% of the reliability:

$$\begin{aligned} \beta_{posterior;observed\ degradation} &= 1.27 \times (100\% - 15\%) \times 0.93 + 1.94 \\ &\approx 2.94 \end{aligned}$$

This equals an annual failure probability of 1.62×10^{-3} (or a return period of about 620 years).

Table 4.7

Overview of effect of including levee performance indicator observations on the reliability index.

| Levee section | 1 | 12 | 26 | 29 |
|--|--------|--------|--------|--------|
| Initial safety factor SF_{prior} (step 1) | 0.93 | 1.06 | 1.1 | 1.06 |
| Initial reliability index β_{prior} (step 1) | -0.59 | 0.25 | 0.50 | 0.25 |
| Reliability index after including survived loads $\beta_{posterior;survived\ load}$ (step 2) | 3.12 | 3.29 | 3.34 | 3.29 |
| Subsidence observation | severe | light | severe | severe |
| Relative reduction on safety factor [%] | 15 | 7.5 | 15 | 15 |
| Reliability index after including degradation observations $\beta_{posterior;after\ degradation}$ (step 3) | 2.94 | 3.19 | 3.13 | 3.08 |
| Target reliability index $\beta_{required}$ | 3.21 | 2.47 | 2.47 | 3.54 |
| Failure probability (1/return period) | 1/620 | 1/1380 | 1/1130 | 1/980 |

An overview of the effect of observations from levee inspections on the reliability index is shown in Table 4.7. It becomes clear that step 2 (reliability updating through survived load observations) significantly increases the reliability index. This is also the case for the other 10 initially rejected levee sections that are not presented in this table. Even after inclusion of levee degradation observations, the reliability indices of levee section 12 and 26 exceed the required reliability index, whereas with the traditional semi-probabilistic approach they were rejected. For levee section 1 and 9 the reliability indices after including degradation observations do not exceed the required reliability index, but still a significant increase in the reliability index is obtained through inclusion of observed levee performance. Repairs of the levee degradation will increase the levee strength, although for levee section 1 and 29 repairs will not be sufficient to meet the safety standard.

4.4.6 Result of comparison of both approaches

A comparison of both methods is presented in Table 4.8, which contains the initial factor of safety (using the traditional approach), the posterior reliability index (including survived loads and, if available, observations from levee inspections) and the required reliability index, and a new judgement, following from the observed levee strength approach. We have only included the levee sections that were rejected in the traditional approach. From the initially 14 levee sections (16.1 km) that were rejected using the traditional approach, 9 sections (11.0 km) can be considered safe, when the observed levee strength approach is applied. Important to note is that the approach from this pilot study quantifies the reliability indices (and failure probabilities), which show how far the outcome of the safety assessment is from the target reliability index.

4.5 Discussion

In this study, a new approach for levee safety assessment was developed in such a way that the effects of observations of survived loads and levee degradation on the levee's failure probability could be taken into account in a pragmatic way. The loading conditions consisted of combinations of the canal water level and the phreatic line. Traffic loads were not included in the assessment, which means that the calculated reduction in failure probability is overestimated. In a follow-up study, the proposed methods could be extended by including traffic loads in a probabilistic way.

In the case study, the 14 levee sections that initially did not meet the safety requirements according to the semi-probabilistic approach, were reduced to 5 different representative levee sections. For these 5 sections, the relation between the estimated safety factor and the levee reliability was established. Due to the limited number of levee sections treated in this study, we have compiled all results from our safety assessments (factors of safety and reliability indices) into a single plot to find the relation between β and SF . However, and this can also be seen in Figure 4.13 and Figure 4.14, there are several important variations in levee characteristics, such as the presence or absence of a berm and the variations in retaining height. It is likely that the SF - β relation becomes more accurate if more levee sections are assessed, and the levees are grouped, based on individual levee characteristics, such as retaining height, presence of a berm, inner slope, crest width, and sub soil composition. Then, a SF - β relation can be established per levee typology, which should, ideally, lead to a distinctive SF - β relation per levee type.

There are several performance indicators, which all affect the levee reliability

Table 4.8

Results of both the traditional approach (safety factor) and the observed levee strength approach (β_{final}), the required reliability index ($\beta_{required}$), and the final judgement when the observed levee strength approach is used.

| Levee section | Safety factor traditional approach | $\beta_{posterior}$ | $\beta_{required}$ | New safety judgement |
|---------------|------------------------------------|---------------------|--------------------|----------------------|
| 1 | 0.68 | 2.94 | 3.21 | Unsafe |
| 7 | 0.83 | 3.62 | 2.88 | Safe |
| 12 | 0.90 | 3.19 | 2.47 | Safe |
| 13 | 0.87 | 3.62 | 2.47 | Safe |
| 14 | 0.93 | 3.62 | 2.47 | Safe |
| 15 | 0.87 | 3.62 | 2.47 | Safe |
| 16 | 0.83 | 3.62 | 2.47 | Safe |
| 17 | 0.87 | 3.62 | 2.47 | Safe |
| 18 | 0.82 | 3.16 | 3.54 | Unsafe |
| 20 | 0.88 | 3.16 | 3.54 | Unsafe |
| 21 | 0.88 | 3.29 | 2.47 | Safe |
| 24 | 0.87 | 3.29 | 3.54 | Unsafe |
| 26 | 0.79 | 3.13 | 2.47 | Safe |
| 29 | 0.88 | 3.08 | 3.54 | Unsafe |

in different ways. Several important examples are: animal burrows, cracks, and subsidence. Levee characteristics determine how a levee's reliability is affected by a levee performance indicator. In this study, we have focused only on levee subsidence, and have assumed that all levees are affected by subsidence in the same way. Further development of the observed levee strength approach should include performance indicators that are used in an inspection, and estimations of how levees are affected by these degradation types. A distinction should be made between levee types, based on levee characteristics.

The relation between β and SF after reliability updating shows a different, milder, slope than before updating, as can be seen in Figure 4.14. A possible explanation for this

change in slope is that reliability updating might have a larger effect on stability assessments that resulted in low safety factors (low values for β), than on high safety factors, especially if the lower safety factors are caused by high uncertainties. Observations of survived loads will then result in a large uncertainty decrease and, consecutively, in higher reliability indices. If uncertainties are smaller, reliability updating is expected to have a smaller effect, resulting in a decreased slope.

Not all inspection results have been included in this study, since many of them contain levee performance indicators of which the effect on the factor of safety is not yet known. Therefore, the results from this study may be seen as a proof-of-concept, and not as a complete safety assessment.

As the authors aimed to show how to determine the effect of subsidence on levee stability, not only the most recent inspection results (2018), but also results from older inspections (2016, and 2017) were used.

It is not possible to use the same probabilities of occurrence of different loading combinations for all types of levees, like we did in this study. In practice, it seems reasonable to derive probabilities of occurrence through a location-specific analysis of loads and their combinations. Another approach is to derive a table of probabilities of occurrence per levee type. These levee types should then be determined, based on levee characteristics, such as geometry, soil type and geotechnical properties. Whether this is a feasible approach, can be assessed by measuring the phreatic surface in levees with similar properties and compare the behaviour of the phreatic surface under varying conditions. Consequently, these measurements can be used to determine levee type specific probabilities of occurrence.

4.6 Conclusions and recommendations

4.6.1 Conclusions

In this study, we proposed an approach for the stability assessment of polder canal levees, with the aim to improve the accuracy of levee reliability analyses by including observations of survived loads and current levee performance observations from levee inspections.

The observed levee strength approach, proposed in this chapter, shows that it can significantly reduce the estimated failure probability of levees by optimally utilizing information on actual levee performance and performance under observed extreme conditions. Through inclusion of observed levee behaviour, the estimated failure probabilities become significantly lower, which is more in line with the estimation of Rikkert and Kok (2019). In this study, this has resulted in approval of 11.0 of the 16.1 km of levees that was rejected initially. This emphasizes the value of proper levee performance observations and the importance of levee monitoring and inspection.

The proposed approach leads to estimations of levee failure probabilities, whereas the current semi-probabilistic approach is only able to assess whether or not the levee meets the safety requirement, without giving further estimation of the actual failure probability. While a probabilistic approach requires an additional effort in terms of levee stability calculations, it allows for the inclusion of survived loads and levee inspection results, with major improvement of the safety assessment as a result. The additional effort is therefore often rewarded in more accurate estimations of failure probabilities, which give insight into how

much room there is left between the actual levee strength and the requirements, and possibly how much degradation can be allowed, before reparations become urgent. Estimations of levee failure probabilities provide opportunities to assess the failure probability and corresponding risk of a flood defence system, and prioritize interventions based on their (cost) effectiveness in terms of risk reduction.

4.6.2

Recommendations

The currently used approach for stability analysis of polder canal levees calculates the safety factor, following a semi-probabilistic approach: one extreme loading scenario is considered. The proposed approach follows a probabilistic approach and determines the failure probability of a levee, expressed as the reliability index. The approach we propose in this paper does not comply with the current safety standard system, which is based on exceedance probabilities of the water level and prescribes a required factor of safety. For the observed levee strength approach to be directly applicable, safety standards should be expressed in probabilities of failure. In a future study, it can be explored how observations of past performance could be included in such a way that it complies with current safety assessment practices.

We recommend to further investigate a levee typology classification in which levee sections can be divided, so that levee type-specific $SF-\beta$ relations can be determined. A larger number of levee sections should be included in an advanced study in such a way, that the sample set is representative for all canal levees in the Netherlands and includes all levee typologies.

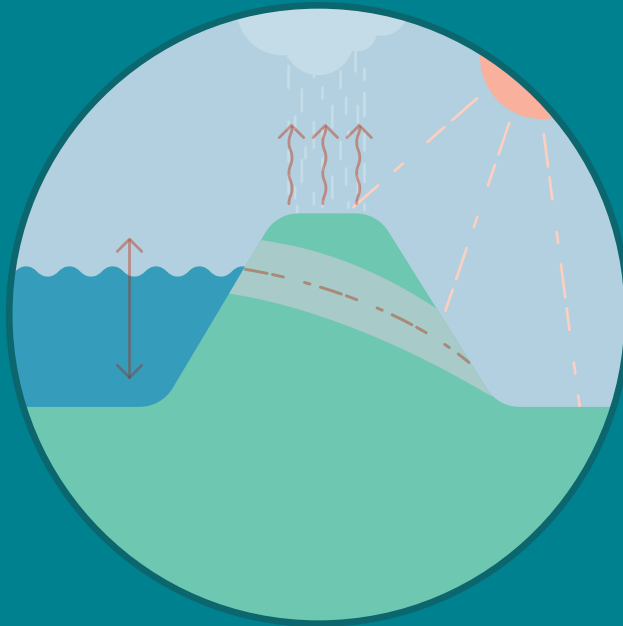
In this study, reasonable assumptions of survived loads allowed us to perform reliability updating. However, more evidence of survived load conditions is

essential to further improve levee strength estimations. This pleads for ongoing monitoring of hydraulic loads (canal water level and phreatic water level), especially under extreme circumstances. Monitoring is also recommended to further improve and justify the estimation of probability of occurrence of specific combinations of loading conditions. Due to a lack of measurements, we had to assess these probabilities by expert judgment (Table 4.4), and applied them to each levee section, while in practice these probabilities might be location-specific.

For further research into the effects of levee performance indicators on levee failure mechanisms, it is recommended to select the levee performance indicators that are actually included in levee inspections. In this way, actual levee conditions can easily be included in the analysis of levee safety.

Finally, as our approach has shown, optimally utilizing the information from observed levee performance, significantly reduces the estimated failure probability by reducing uncertainty. Levee performance observations can be obtained relatively easy and at low cost. Especially, when compared to the high costs of reinforcement of (unnecessary) rejected levees. Therefore, further development and improvement of the observed levee strength approach requires a shift of focus towards monitoring and inspection, but potentially saves money.

5



**Conceptual hydrological
modelling of phreatic
water levels in polder
drainage canal levees**

5.1 Introduction

5.1.1 Problem analysis

One of the most important failure mechanisms in assessments of canal levees is instability of the inner slope (also referred to as macro-stability). This mechanism occurs when the active strengths of soil particle movement exceed the resistant strengths, resulting in sliding along a shear surface within the levee embankment and/or foundation soils that damage the levee (CIRIA, 2013). In the Dutch design guidelines for canal levees, 80% of the total failure probability is allocated for this type of failure mechanism (Van der Meer et al., 2009).

For this type of failure, there are three important variable loads considered in the levee stability assessment: the polder canal water level, the resulting phreatic line inside the levee and the expected traffic loads (if there is a road present on the levee) (STOWA, 2015a). The canal water level is regulated, and water level changes

are kept at a minimum. The extreme water level is relatively close to normal conditions. The difference between normal and extreme conditions is often in the order of decimeters. The loads induced by traffic and the phreatic line therefore govern the overall failure probability of canal levees (Lendering, Jonkman & Kok, 2015). While the canal water level and traffic load are easily observable, the phreatic line is situated below the surface, which makes it difficult to predict. Therefore, the extreme phreatic line for stability assessments for canal levees is currently based on predictions of extreme canal and polder water levels (see Figure 5.1). Clearly, the canal water level plays a central role in this approach, while other factors, such as meteorological conditions, are not taken into account explicitly.

A measurement campaign by Flanagan and Tigchelaar (2016) has shown that the assumed phreatic line used in stability calculations sometimes underestimated the measured phreatic line. In other cases, the measured phreatic lines were significantly lower than the estimate used in the stability assessment. The main cause for the

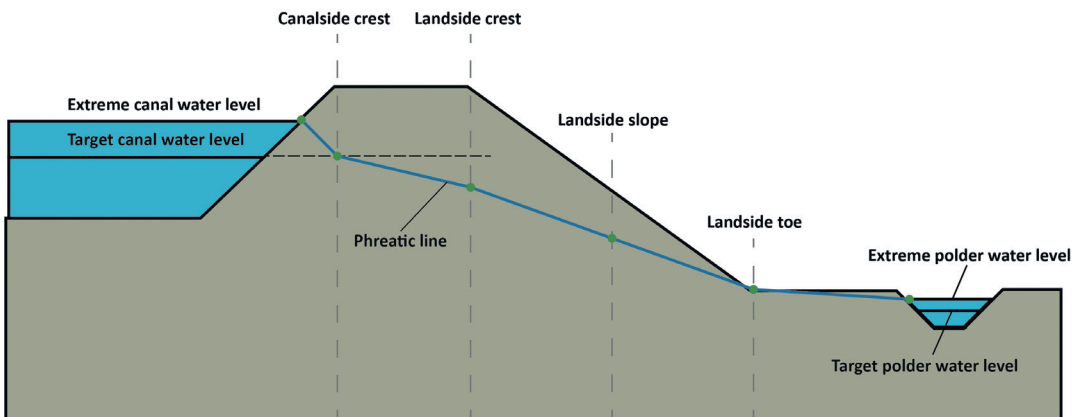


Figure 5.1 Graphical representation of current approach to predict the phreatic line in a levee under extreme conditions (based on Expert workshop, 2008). The phreatic line is shown as the blue line within the levee body.

94

variations in the phreatic line seemed to be rainfall and evaporation, since the canal water level stay within a relatively small range. Attempts to model the effects of rainfall and evaporation on the phreatic line have shown to be difficult. Several studies have focused on an idealized homogenous levee (Jamalinia et al, 2019; De Loor, 2018). These studies showed how meteorological conditions influence the phreatic line and levee stability, but since idealized situation were used, validation of the results with measurements was not possible. Monden, van Opstal and Zwartendijk (2020) compared observed phreatic lines with results of their model, in which they modelled constant rainfall over multiple days, rather than using the actual rainfall. Van Esch (2012) modelled how an existing levee responded to varying meteorological inputs, using two modelling approaches (a finite element and a finite volume model). An intercomparison between the model results was made, but the results were not validated with actual measurements. Other studies have used field measurements to compare their model outcomes with, but heterogeneity in soil composition and behaviour resulted in large uncertainties (Dorst, 2019; Ten Bokkel-Huinink, 2016). Their models heavily relied on information of soil characteristics, such as soil layer thickness and hydraulic conductivity, while this information is often lacking. Our hypothesis is that precipitation and evaporation processes play a key role in the fluctuations of the phreatic lines inside the Dutch polder drainage canal levees, which are not accounted for in the current methods for levee stability assessments.

5.1.2

Objective

The objective of this chapter is to investigate whether the estimation of the phreatic line in a levee can be improved, by taking into account the hydrological processes in the levee. We develop a

hydrological model of a levee that can be calibrated on hydraulic head measurements and uses precipitation and evaporation as input data for the determination of the phreatic line. This allows for location-specific phreatic line predictions, which in turn may enhance the accuracy of levee stability assessments.

5.1.3

Outline

This chapter starts with an explanation of the research approach in Section 5.2. The steps presented in this approach are all carried out using data from a measurement campaign, which is presented in Section 5.3. Section 5.4 tests the hypothesis that rainfall and evaporation play a key role in the fluctuations of the phreatic line. Then, in Section 5.5 hydrological models are developed and applied for the levees in the measurement campaign. An in-depth discussion of the results is included in Section 5.6, followed by the conclusions and recommendations in Section 5.7.

5.2

Approach

In this chapter, we first tested our hypothesis that the variations in the phreatic line are mainly dominated by meteorological inputs: precipitation and evaporation. We use data analysis techniques to test our hypothesis. Once the relation between meteorological inputs and phreatic line changes was established, we developed and applied a physically-based hydrological model. Hence, the approach consists of 2 parts, for which data from a measurement campaign is used:

Part 1. Hypothesis testing: establishing the relation between meteorological, canal water level and the phreatic line measurements

First, the relation between the phreatic line and meteorological inputs (i.e. precipitation and evaporation) was analysed through a) cross-correlation and b) linear regression analysis. We used measured time series of 5 levee locations, where the hydraulic head is measured at 3 positions in the levee cross-section.

a. Cross-correlation analysis

In signal processing, cross-correlation is a measure of similarity of two waveforms as a function of a time lag applied to one of them. In this chapter, we used the cross-correlation method to analyse the similarity between measured time series of the phreatic line on the one hand, and rainfall, evaporation, and the canal water level on the other hand. This analysis resulted in an optimal time lag, that describes how much one time series should be shifted (or lagged), to get the highest (absolute) correlation with the other time series.

b. Linear regression analysis

Using the optimal lag found in the cross-correlation analysis, a linear regression analysis was performed to investigate if there is a linear relation between the

phreatic line and the lagged time series of the canal water level, rainfall and evaporation.

Part 2. Hydrological modelling of the phreatic line

After the relation between the meteorological inputs and the phreatic line is established, the focus will be on simulating the effects of the phreatic line as a response to the meteorological inputs. This part consists of developing, testing and comparing different hydrological model set-ups.

a. Development of the hydrological models

Multiple process-based hydrological models are developed, so that rainfall and evaporation effects on the phreatic line are taken into account. The models developed in this chapter are of the type Explicit Soil Moisture Accounting (ESMA) models, often called conceptual models (O'Connell, 1991). The models consist of a varying number of storage elements, and functions and parameters that control the exchange between the elements (Beven, 2011).

While these models are usually applied in catchment-runoff modelling, we developed them to represent the hydraulic head in the subsurface. The first model is a relatively simple model, with a limited number of hydrological processes included and has a limited number of parameters. New models were iteratively developed by including more hydrological processes, by applying the model to five real cases and visually interpreting the model results.

b. Calibration of the hydrological models

The Nash-Sutcliffe efficiency (NSE) was used to determine the model performance. The NSE is calculated as follows:

$$NSE = 1 - \frac{\sum_{i=1}^n (y_i^{obs} - y_i^{mod})^2}{\sum_{i=1}^n (y_i^{obs} - y_{mean})^2} \quad (\text{Eq. 5.1})$$

In which y_i^{obs} is the observed value at time i , y_i^{mod} is the modelled value at time i , and y_{mean} is the mean of the observed data. In theory, an NSE score can go from minus infinity (lowest performance) to 1 (highest performance). A score < 0.0 indicates that the mean of the observed data is a better predictor than the model, which means that the model performance is unacceptable. The interpretation of the NSE-scores varies in the literature, but Moriasi et al. (2007) give the following interpretation: $NSE \leq 0.5$ is considered unsatisfactory, $0.50 < NSE \leq 0.65$ is considered satisfactory, $0.65 < NSE \leq 0.75$ is considered good, and $0.75 < NSE \leq 1.00$ is considered very good.

c. *Comparison and validation of the hydrological model results*

As a final step, the performance of the calibrated models, developed in the previous step, was compared to each other, based on the NSE-scores that were found in the calibration. Finally, the model results are compared to a linear regression model from part 1, to evaluate if a model including hydrological processes better reproduces the measurements.

5.3 Measurement data

In this study, hydraulic head measurement data provided by the Hollands Noorderkwartier water board (regional water authority) were used. This data consists of phreatic line measurements inside levees at several locations for the period between November 2013 until April 2015. Due to sensors failing at several locations, only 5 out of 10 measurement locations were used for analysis (see Figure 5.2). Sensors were placed in the landside crest, landside slope, landside toe of the levee and in the hinterland (as specified in Figure 5.1).

The rainfall data is obtained from HydroNET/KNMI (Royal Netherlands Meteorological Institute) with a 1 km x 1 km spatial resolution and a 1 hour temporal resolution. This data is produced, based on satellite imagery, and calibrated with ground measurements (STOWA, 2015c). The potential evaporation data was obtained from the nearest KNMI meteorological station. The KNMI uses the Makkink (1957) equation to calculate this potential evaporation.

To get an impression of the available measurement data, a sample of the collected time series is shown in Figure 5.3. Here, the observations of precipitation, potential evaporation, the canal water level and the measured hydraulic head for the period between January of 2014 and mid April of 2015 in the landside crest of location 2 are shown.

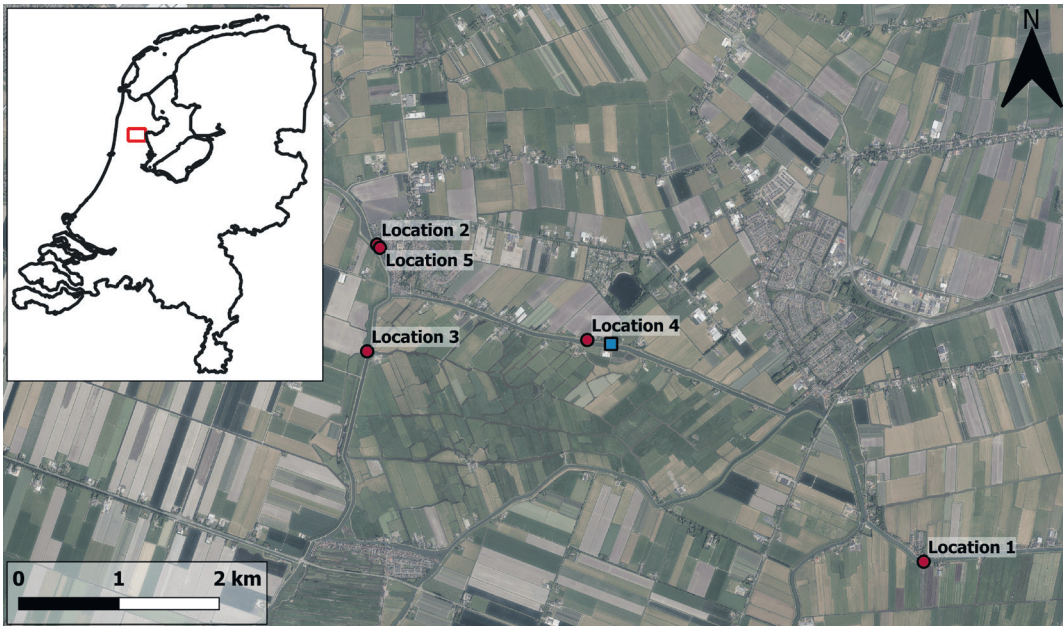


Figure 5.2

Overview of measurement locations. Red squares indicate location of levee cross-sections, blue squares indicate canal water level measurement locations.

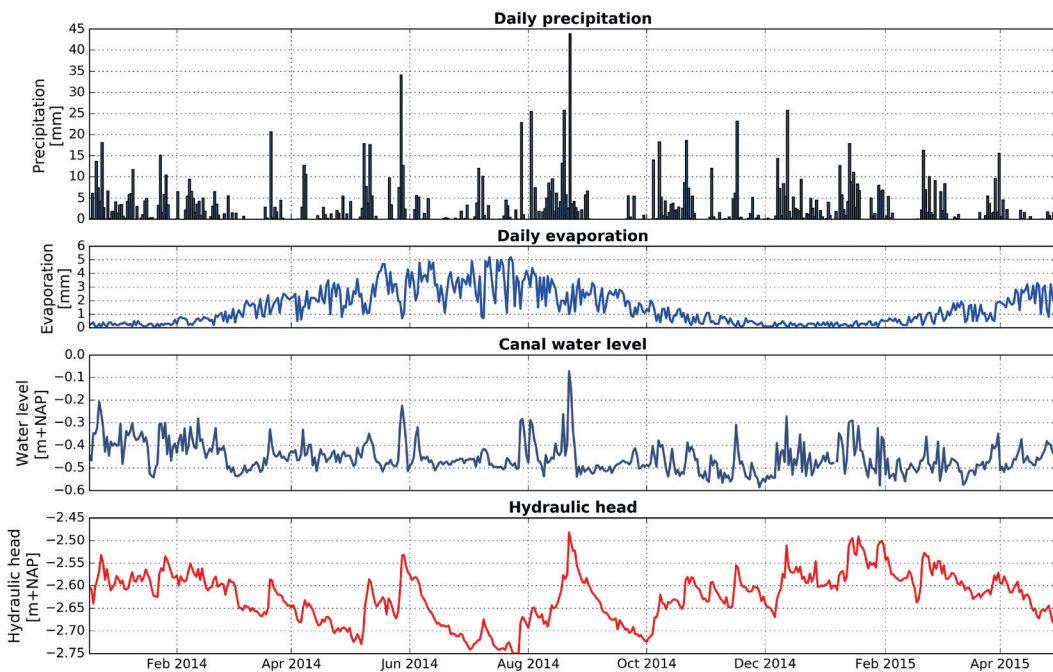


Figure 5.3

Overview of available measurement data. From top to bottom: hyetograph on a daily scale [mm]; daily potential evaporation [mm]; canal water level [m +NAP], and; the hydraulic head measurement in the landside crest (see Figure 5.1) of location 2.

5.4

Hypothesis testing: establishing the relation between meteorological, canal water level and the phreatic line measurements

In this first part, we compare time series of observed rainfall, evaporation, and canal water level with the hydraulic head to establish whether there is a relation between the different time series.

5.4.1

Cross-correlation analysis

Time series of the following variables were compared to the observed hydraulic head:

- Accumulated rainfall in one hour (P (h));
- Accumulated rainfall in one day (P (d));
- Accumulated rainfall in 2 days (P (2d));
- Accumulated rainfall in 5 days (P (5d));
- Accumulated rainfall in 10 days (P (10d));
- Accumulated rainfall excess (rainfall – evaporation) in 5 days (RE (5d));
- Accumulated rainfall excess (rainfall – evaporation) in 10 days (RE (10d));
- Instantaneous canal water every hour (CWL).

The optimal Pearson correlation coefficient r and lag were calculated per levee cross-section. Since the results show quite similar patterns for each levee, Figure 5.4 shows only the results obtained for levee location 2. Results for the other measurement locations can be found in Appendix A. What becomes directly clear from the correlation coefficients is that rainfall over one or multiple days outperforms the hourly rainfall and the hourly canal water level in terms of the correlation coefficient. Including also evaporation, by calculating the rainfall excess, increases the similarity further. The lag (Figure 5.4; right) indicates that the phreatic line responds to the rainfall (and rainfall excess) with some delay. This lag decreases when the rainfall (and rainfall excess) over multiple days is used, since rainfall from earlier events might have already reached the hydraulic head. Because rainfall excess over 10 days in some cases lead to a negative lag, the rainfall excess over 5 days is included in the linear regression analysis. The optimal lag times found for the crest and slope of levee 9 are very high (order of magnitude is 1000–2000 hours). This might indicate that there were problems with these measurements.

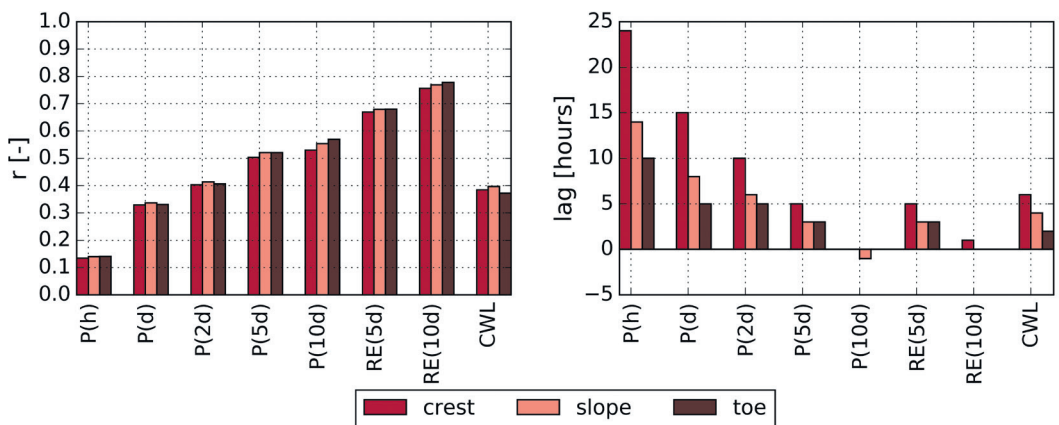


Figure 5.4

Results of the cross-correlation analysis for levee location 2, showing the Pearson correlation coefficient r on the left and the lag [in hours] on the right.

5.4.2

Linear regression analysis

Linear regression analysis was used to analyse whether there is a linear relation between the variables. We used 2 predictor variables:

- (Rainfall P – evaporation E) per 5 days (with lag);
- Canal water level (CWL) per hour (with lag).

Three linear regression models were developed, using each predictor variable individually, and the combination of both. The initial time series were shifted using the optimal time lag, as calculated in the cross-correlation analysis.

Model 1:

$$hh_t = \alpha_{RE(5d)} \times RE(5d)_{t+lag} + c$$

Model 2:

$$hh_t = \alpha_{CWL} \times CWL_{t+lag} + c$$

Model 3:

$$hh_t = \alpha_{RE(5d)} \times RE(5d)_{t+lag} + \alpha_{CWL} \times CWL_{t+lag} + c$$

In which hh_t = the hydraulic head inside the levee [m +NAP], $RE(5d)_{t+lag}$ = the rainfall excess over 5 days with lag [m], CWL_{t+lag} = the hourly canal water level with lag [m +NAP], $\alpha_{RE(5d)}$ and α_{CWL} are the regression coefficients of the rainfall excess and the canal water level [-], respectively, and c is a constant [m]. The least squares method was used to determine the best fit between the predicted and the observed hydraulic head. The corresponding coefficient of determination R^2 of each model is presented in Figure 5.5.

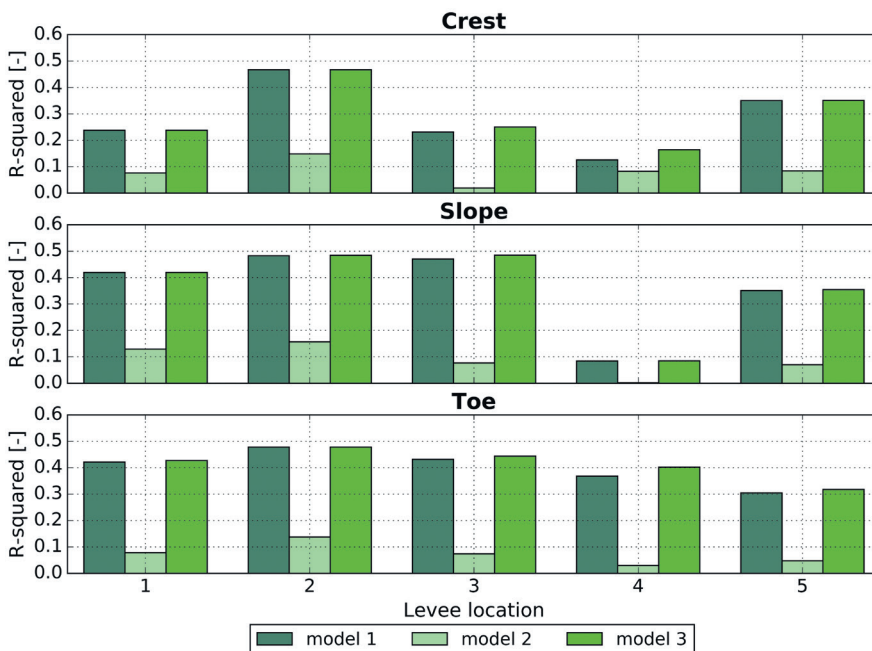


Figure 5.5
Coefficient of determination R^2 for prediction the hydraulic head in the landside crest, landside slope, and landside toe at different levee locations, using linear regression.

As can be seen from the results of the linear regression analysis, model 1 always outperforms model 2, in terms of the coefficient of determination. This suggests that the rainfall excess over 5 days, as used in model 1, is a better predictor for the phreatic line, than the canal water level, as used in model 2. Combining both predictor variables (model 3), hardly gives any improvement compared to using only the rainfall excess. In almost all cases the predictor variables have p-values $\ll 0.05$, meaning that the predictor variables have a significant effect on the phreatic line. The p-value was only larger than 0.05 for the canal water level in model 3. This means that the water level for these cases had no significant contribution to the predicted outcome. This was the case for the crest and landside slope at location 1, and the landside toe at location 2. Including the canal water level as predictor variable (model 3) led to no significant improvement, compared to using only the rainfall excess over 5 days as predictor variable (model 1). This indicates that the changes in the phreatic line are best explained by the meteorological inputs.

5.5 Hydrological modelling of the phreatic line

5.5.1

Development of the hydrological model

Now that we have established the strong relation between rainfall and evaporation and the phreatic line in the previous part, hydrological modelling was used to predict the behaviour of the phreatic line in a levee. Several attempts to use sophisticated geohydrological models to predict the phreatic line showed good results for idealized situations (De Loor, 2018; Van Esch, 2012), but failed to reproduce a good fit for actual measurement locations (Dorst, 2019; Ten Bokkel Huinink, 2016). In Dorst (2019) it was concluded that the heterogeneity of the soil is very high, which made it almost impossible to reproduce the measurements with a geohydrological model. Only if unrealistic parameter combinations were chosen (e.g., a much higher hydraulic conductivity for clay than for sand), the model results were approaching the observed hydraulic head. These higher hydraulic conductivities could have been a result of animal burrows, cracks in the cover layer, and root canals. However, the models was not able to include these effects. This calls for a less complex modelling approach.

Therefore, we applied an Explicit Soil Moisture Accounting model, which is often applied in hydrology. It is important to note that such models often rely heavily on parameter calibration. Therefore, the number of model parameters is kept at a minimum. This low number of parameters also reduces the equifinality problem: where different model parameter sets could result in equally good model results (Beven, 2011). The 4 models developed have a minimum of 2 and a maximum of 4 parameters. The first model started with a simple structure: the benchmark model (Model A). From

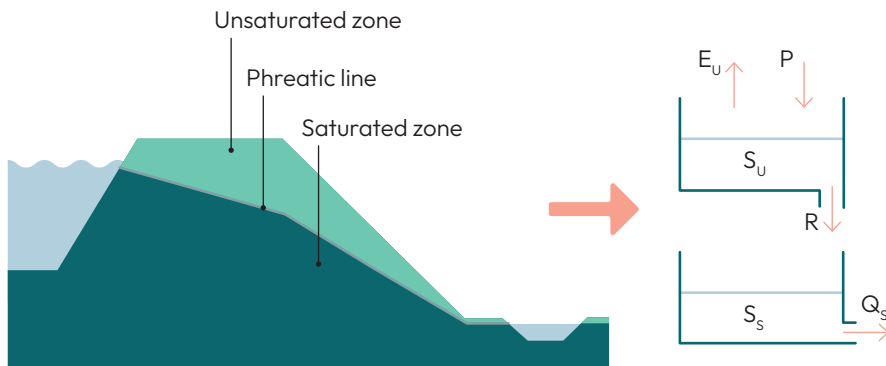


Figure 5.6
Schematic representation of how the levee is translated to a conceptual hydrological model.

here, the model was adjusted in steps based on visual interpretation of the differences between measured and predicted hydraulic heads. The benchmark model A, and the improved models (B, C, and D) are described here:

Model A: benchmark

The levee was divided into two zones: an unsaturated and a saturated zone. In this simplification, the phreatic line is located at the interface between the unsaturated and saturated zone (Figure 5.6). These zones are represented as reservoirs. As rainfall falls on the ground, it can infiltrate into the unsaturated reservoir. From the unsaturated reservoir only vertical movement of water takes place. Upward, water can leave the reservoir through transpiration by vegetation. Downward, water percolates to the saturated reservoir. Outflow from this reservoir is represented as a linear function. The structure of this model and used equations are shown in Table 5.1 and Table 5.2. The model needs only 2 parameters: the retention times of water in the unsaturated zone k_u [d], and in the saturated zone k_s [d].

Model B: interception

Model B is an extension of model A: an interception reservoir was added. For small rainfall events, water is intercepted by vegetation before it reaches the surface. From this vegetation it evaporates. The structure of this model and used equations are shown in Table 5.1 and Table 5.2. Model B needs 3 parameters: the retention times of water in the unsaturated zone k_u [d], and in the saturated zone k_s [d], and the maximum interception capacity I_{max} [mm/d].

Model C: preferential flow

Model C is another extension of model A: a shortcut was added to the unsaturated reservoir, representing preferential flow (fast response with respect to the unaffected average soil matrix) to the saturated reservoir. These preferential flow paths can be present due to cracks in the clayey cover layer of the levee, or by tunnels, burrowed by animals. The addition of preferential flow paths enables the phreatic line to respond faster to heavy rainfall events. The structure of this model and used equations are shown in

Table 5.1

Overview of the model structures applied in this paper. For each model the model parameters and total number of free parameters are given. The equations used in each model are also given. These equations refer to the equations given in Table 5.2, and the symbols are explained in Table 5.3.

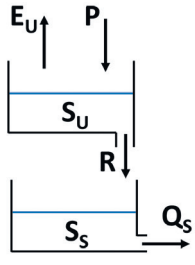
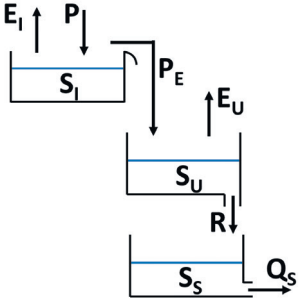
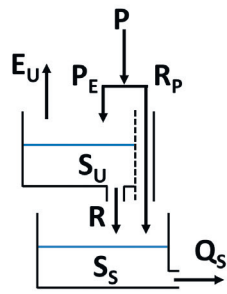
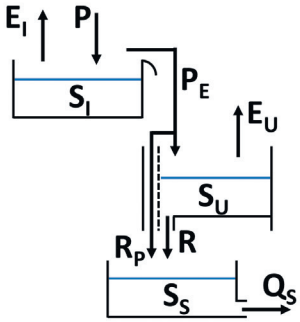
| Model | Model structures | Parameters and used equations |
|-----------------------|---|--|
| <p>Model A</p> |  | <p>Total number of parameters = 2: k_U, k_S</p> <p>Equations used: W5, W8, W12, W16, W17, W19, W21</p> |
| <p>Model B</p> |  | <p>Total number of parameters = 3: I_{max}, k_U, k_S</p> <p>Equations used: W1, W2, W3, W4, W6, W9, W13, W14, W17, W19, W21</p> |
| <p>Model C</p> |  | <p>Total number of parameters = 3: k_U, k_S, C</p> <p>Equations used: W7, W9, W11, W12, W14, W15, W18, W20, W21</p> |
| <p>Model D</p> |  | <p>Total number of parameters = 4: I_{max}, k_U, k_S, C</p> <p>Equations used: W1, W2, W3, W4, W7, W10, W13, W16, W18, W20, W21</p> |

Table 5.1 and Table 5.2. Model C needs 3 parameters: the retention times of water in the unsaturated zone k_u [d], and in the saturated zone k_s [d], and the preferential flow coefficient C [-].

Model D: interception and preferential flow

Model D is an extension of model A, but now both the interception from model B and the bypass for preferential flow from

model C were included. The structure of this model and used equations are shown in Table 5.1 and Table 5.2. Model D needs 4 parameters: the retention times of water in the unsaturated zone k_u [d], and in the saturated zone k_s [d], the maximum interception capacity I_{max} [mm/d], and the preferential flow coefficient C [-].

Table 5.2

Overview of the formulas used by the models. The symbols are explained in Table 5.3.

| Process | Water balance | Eq. | Flux state equations, constitutive relationships | Eq. |
|------------------------|---|------|--|-------|
| Interception reservoir | $\frac{dS_I}{dt} = P - P_E - E_I$ | (W1) | $S_{I;in} = S_I + P \times dt$ | (W2) |
| | | | $P_E = \min\left(\frac{S_{I;in}}{dt} - I_{max}, S_{I;in}\right)$ | (W3) |
| | | | $E_I = \min\left(\frac{S_{I;in}}{dt} - P_E, E_P\right)$ | (W4) |
| Unsaturated reservoir | $\frac{dS_U}{dt} = P - E_U - R$ | (W5) | $S_{U;in} = S_U + P \times dt$ | (W8) |
| | $\frac{dS_U}{dt} = P_E - E_U - R$ | (W6) | $S_{U;in} = S_U + P_E \times dt$ | (W9) |
| | $\frac{dS_U}{dt} = P_E - E_U - R - R_P$ | (W7) | $S_{U;in} = S_U + (1 - C) \times P_E \times dt$ | (W10) |
| | | | $P_E = (1 - C) \times P$ | (W11) |
| | | | $E_U = \min\left(\frac{S_{U;in}}{dt}, E_P\right)$ | (W12) |
| | | | $E_U = \min\left(\frac{S_{U;in}}{dt}, E_P - E_I\right)$ | (W13) |
| | | | $R = \frac{S_{U;in} - E_U \times dt}{k_U}$ | (W14) |

| Process | Water balance | Eq. | Flux state equations, constitutive relationships | Eq. |
|---------------------|-----------------------------------|-------|--|-------|
| | | | $R_p = C \times P$ | (W15) |
| | | | $R_p = C \times P_E$ | (W16) |
| Saturated reservoir | $\frac{dS_S}{dt} = R - Q_S$ | (W17) | $S_{S;in} = S_S + R \times dt$ | (W19) |
| | $\frac{dS_S}{dt} = R + R_p - Q_S$ | (W18) | $S_{S;in} = S_S + (R + R_p) \times dt$ | (W20) |
| | | | $Q_S = \frac{S_{S;in}}{k_S}$ | (W21) |

Table 5.3

Explanation of symbols
(L=length, T=time).

| Fluxes | |
|------------|---|
| P | Rainfall [L/T] |
| P_E | Effective rainfall [L/T] |
| E_I | Evaporation from interception reservoir [L/T] |
| E_p | Potential evaporation [L/T] |
| E_U | Evaporation from unsaturated reservoir [L/T] |
| R | Recharge to saturated reservoir [L/T] |
| R_p | Preferential flow to saturated reservoir [L/T] |
| Q_S | Groundwater flow [L/T] |
| Storages | |
| S_I | Storage in interception reservoir [L] |
| S_U | Storage in unsaturated reservoir [L] |
| S_S | Storage in saturated reservoir [L] |
| Parameters | |
| I_{max} | Maximum interception capacity [L/T] |
| k_U | Retention time coefficient for unsaturated zone [T] |
| k_S | Retention time coefficient for saturated zone [T] |
| C | Coefficient determining preferential flow [-] |

Table 5.4
Initial parameter range.

| Parameter | Min | Max | Used in model |
|----------------|--------|-----|---------------|
| k_U [day] | 1 | 100 | A, B, C, D |
| k_S [day] | 1 | 100 | A, B, C, D |
| l_{max} [mm] | 0.5 | 2.5 | B, D |
| C [-] | 0.0001 | 1 | C, D |

5.5.2

Model calibration and results

In this study, we assumed that the saturated reservoir storage represents the phreatic line. As part of the model calibration, this storage was compared to the phreatic line measurements for a large number of model parameter sets. Both observed hydraulic heads and reservoir storage were normalized, so that calibration could be performed on their normalized signals. Normalizing was necessary, since the measured hydraulic head and the modelled reservoir storage have different units. Afterwards, the optimized reservoir storage was rescaled to hydraulic head.

For each levee location and measuring position each model was optimized, using Monte Carlo analysis. The initial parameter range is shown in Table 5.4, and the number of runs is 10,000. For each run, we calculated the NSE score, and we are interested in the combinations of parameter values that give the highest NSE values.

Figure 5.7 shows the measurements and simulation results for the landside crest at location 2, using the 4 different models. Since different combinations of parameter values may produce a high NSE score, we consider the normalized parameter sets of the 2.5% best performing solutions.

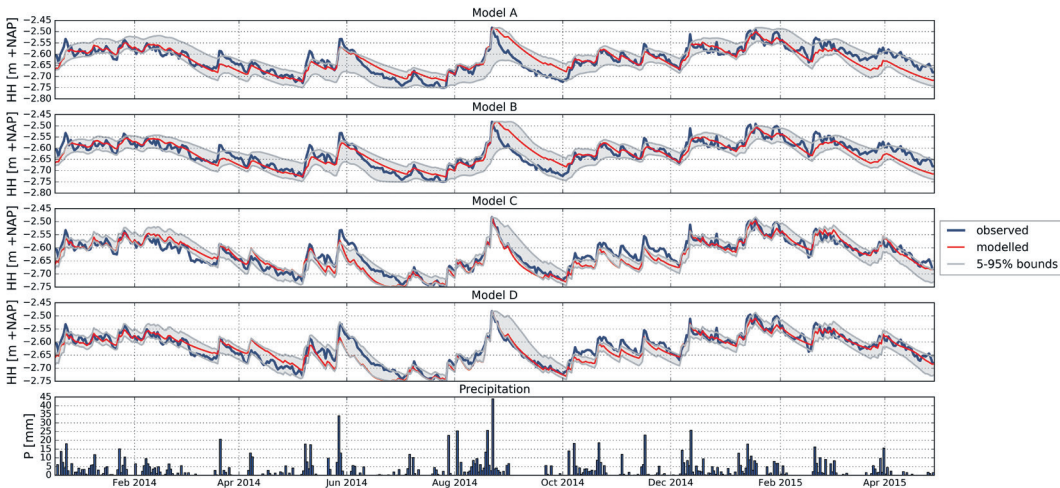


Figure 5.7

Results of optimized models for landside crest at location 2. The observations are shown in blue, the red line shows the highest NSE-value, and the grey bounds represent the 5%-95% boundaries of the parameter sets resulting in the top 2.5% NSE values. Optimal NSE-values can be found in Table 5.5.

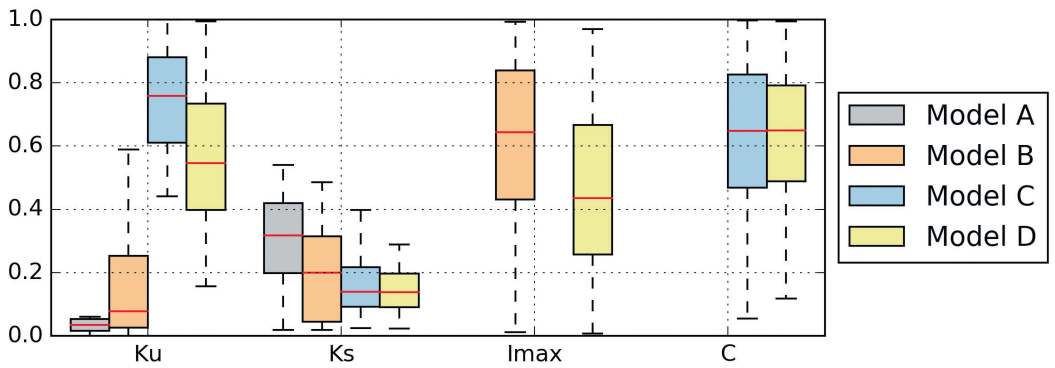


Figure 5.8

Normalized parameter range of the 2.5% highest NSE-scores for the landside crest at location 2. The horizontal red line represents the median, the boxes are representing the interquartile range (IQR): all values within the 25th (Q1) till the 75th (Q3) quantile. The whiskers represent the minimum ($Q1-1.5 \cdot IQR$) and maximum ($Q3+1.5 \cdot IQR$).

From these 2.5% of best performing solutions, both the optimal and the 5%-95% confidence bounds have been included in the figure.

The hydraulic head at the landside crest at location 2 is modelled relatively well with all models, as can be seen from Figure 5.7. However, when preferential flow is included (models C and D) the model can recreate sharper increases and decreases in the hydraulic head, which is more similar to the observed behaviour at this location. Figure 5.8 shows the parameter range of the 2.5% best solutions for the landside crest at location 2. What is most notable is the different retention coefficient of the unsaturated zone k_u for model A and B compared to model C and D. The relatively low k_u values in model A and B with respect to the initial parameter range, mean that water is only retained in the unsaturated zone for a brief period, which is required for a fast response of the hydraulic head to rainfall. When preferential flow is included (model C and D), the k_u values increase significantly, compared to the k_u values in model A and B. The same behaviour could be seen at location 1 and 3. At location 4, the measured response of the hydraulic head to rainfall events is much slower and less

pronounced than for the other locations, which is reflected in that all models have a relatively high value for k_u . At location 5, all models seem to have comparable parameter values, and no significant improvement to model results are achieved by including more hydrological processes.

The highest NSE-values for each model at each location and position are shown in Table 5.5. As can be seen from the table, good model performance, with NSE-values > 0.65 , can be obtained at 10 out of 15 measurement locations. Especially, at locations 1, 2 and 3 it seems that including preferential flow is more important than interception, and with model C and D higher NSE-scores were obtained than with model A and B for these locations. At locations 4 and 5 no significant improvements were obtained by including preferential flow (model C and D).

Table 5.5

Overview of the highest NSE-scores for each location and position per model. The highest NSE-scores are in bold.

| Location | Position | Model | | | |
|----------|----------|-------------|-------------|-------------|-------------|
| | | A | B | C | D |
| 1 | Crest | 0.11 | 0.12 | 0.09 | 0.18 |
| | Slope | 0.66 | 0.64 | 0.71 | 0.76 |
| | Toe | 0.40 | 0.39 | 0.51 | 0.57 |
| 2 | Crest | 0.70 | 0.70 | 0.81 | 0.84 |
| | Slope | 0.72 | 0.72 | 0.80 | 0.84 |
| | Toe | 0.74 | 0.74 | 0.80 | 0.82 |
| 3 | Crest | 0.54 | 0.54 | 0.59 | 0.62 |
| | Slope | 0.59 | 0.57 | 0.64 | 0.68 |
| | Toe | 0.60 | 0.60 | 0.60 | 0.72 |
| 4 | Crest | 0.65 | 0.68 | 0.69 | 0.70 |
| | Slope | 0.51 | 0.64 | 0.47 | 0.63 |
| | Toe | 0.53 | 0.59 | 0.55 | 0.61 |
| 5 | Crest | 0.90 | 0.88 | 0.90 | 0.77 |
| | Slope | 0.87 | 0.87 | 0.87 | 0.74 |
| | Toe | 0.77 | 0.76 | 0.76 | 0.62 |

5.6 Discussion

The model results show that relatively simple hydrological models are able to reproduce the observed hydraulic head in a levee, based on the available data. However, hydraulic head measurements in levees are scarce; especially for long and continuous periods. In this study, we used the data set that contained measurements over a period of about 15 months. While hydraulic head measurements of such a duration are quite unique, they are still not long enough for proper validation of the proposed hydrological models. If a part of the data would have been used for validation, then the calibration set would hardly contain a full year, while ideally all 4

seasons need to be included, and preferably for multiple years.

Even in the limited number of measurement locations, there are significant differences between how levees respond to rainfall. An important example is the different ranges of measured hydraulic heads: while at location 2 the difference between minimum and maximum measured hydraulic head is close to 1 m, this range is smaller than 0.2 m at location 5. Also the speed with which the hydraulic head rises and drops differs per location. This can be due to local differences in geometry, vegetation, and soil characteristics. A factor that is not considered in this article is concentrated flow, which can occur in the case of an asphalt road over the crest with a

foundation layer containing sand. Rainfall on the road might completely runoff without infiltrating and ending up as extreme ponding in side ditches of the road.

The 'unsaturated reservoir' component in the model represents the unsaturated zone of the levee. This means that the actual moisture content in the soil is reflected by the amount of water in the modelled unsaturated reservoir. Unfortunately, comparison is not possible, because there are no moisture content measurements.

The temporal resolution of the model is daily, which might not be sufficient to detect the difference between a uniform low-intensity rainfall event and a high-intensity rainfall event with a short duration. Especially a high-intensity rainfall event might trigger a hydrological process that is currently not included in the models: overland flow. If the rainfall intensity exceeds the infiltration capacity of the levee, excess rainwater might flow overland from the crest towards the toe, where it will accumulate and eventually infiltrate.

The models proposed in this study represent the hydraulic head as a saturated reservoir component. Because the model is run separately for the crest, slope, and toe of the levee, no interaction takes place between these areas. Therefore, the models are currently not able to deal with (horizontal) groundwater flow between crest, slope and toe. In reality, the head difference between the canal and the polder water level result in a continuous groundwater flow through the levee. This could be improved by connecting the models in a way that interaction between the crest, slope and toe can take place.

5.7 Conclusions and recommendations

5.7.1 Conclusions

In this study, we analysed the relation between meteorological conditions, i.e. rainfall and evaporation, and the phreatic line within polder drainage canal levees. Through cross-correlation analysis it was found that the rainfall excess over multiple days has higher influence on the variations of the phreatic line than the canal water level. When using both rainfall excess and the canal water level as predictor variables in a linear regression model, the variations of the phreatic line were dominated by rainfall and evaporation.

Building further on this relation between meteorological conditions and the phreatic line, 4 relatively simple hydrological reservoir models were developed. To counter the complexity and degrees of freedom that conventional geohydrological models have, the developed models only contained a parsimonious number of parameters: 2 for the benchmark model, up to 4 for the most complex model, making the models relatively easy to calibrate.

In general, all models perform quite well, with maximum NSE-scores ≥ 0.5 in 88% of the locations. Model D gives the best results overall: 60% show at least a good fit with NSE-scores ≥ 0.64 , and 33% show a very good fit with NSE-scores ≥ 0.75 (see Table 5.5). If scores of model A and B are compared, no significant improvement in NSE-score is observed. The interception seems to be relatively unimportant. A possible explanation is that the levees are covered mainly by grass. For locations 1, 2 and 3, it can be seen from the NSE-scores, that the inclusion of preferential flow (model C and D) improve the model results.

This chapter shows that simple hydrological models are able to better reproduce the variations in the phreatic line, whereas this seems very difficult with more complex geohydrological models (Ten Bokkel Huinink, 2016; Dorst, 2019). This allows for the prediction of extreme values for the phreatic line, which can increase the accuracy of levee stability analyses.

5.7.2

Recommendations

To allow for longer calibration and validation data sets, longer measurement campaigns are necessary, so that all seasons are included and also wet and dry years. Besides hydraulic head, also the soil moisture content should be measured, so that the water content of the modelled unsaturated reservoirs can be compared to physical measurements of the soil moisture content. The relation between the determined retention coefficients should be compared to local measurements of the hydraulic conductivity to analyse the physical meaning of these model parameters.

The models are all data-driven, and can only be applied to locations where data is available. Unfortunately, measuring the hydraulic head for longer periods is expensive. To collect data on a large scale, it might be interesting to investigate the possibility to monitor other indicators of the wetness of the levee, and further investigate how these indicators are related to the phreatic line. For example, Özer et al. (2019) show how levee deformations, observed with satellites, represent the seasonal swelling and shrinking of levees under wetting and drying conditions.

Conclusions and recommendations

A large part of the regional flood defences in the Netherlands consists of canal levees (boezemkaden), which are levees along drainage canals (boezemkanalen), which all together form a complex water system, called the boezem. Often, such systems also include lakes. The levees are assessed periodically to ensure that they meet the required safety standard. There is a clear discrepancy between observations of actual levee failures and model predictions of levee safety. In the period 1960 – 2020, only 2 actual failure cases of regional flood defences that lead to flooding have occurred in the Netherlands. However, a large part of these flood defences are labelled as ‘unsafe’, based on calculations. The main causes seems to be the conservatism in the calculation (“better safe than sorry”), a lack of sufficient and reliable data, and a lack of understanding of the processes contributing to failure. This dissertation focusses on improvement of the current methods for safety assessments through solutions not only on the scale of the individual levee, but also on the scale of the entire water system. The system scale is important, because changes in the system, such as a levee breach, or a drain stop, significantly influence the hydraulic loads elsewhere in the system. The main conclusions and recommendations are presented in this chapter.

6.1

Conclusions

This dissertation contributes to improvement of levee reliability and flood risk assessments through methods developed for the scale of a levee section, the scale of multiple levee sections protecting a polder and on the scale of the entire system.

Research question 1: How do hydraulic load interdependencies in polder systems influence flood risk?

Drainage canal levees are assessed individually in safety assessments, and potential failure of other levee sections in the system is not taken into account. However, a levee breach affects the canal water level in the entire system, and thus indirectly affects the safety of other levees in the system. This is referred to as hydraulic load interdependency.

In this dissertation, an approach is developed that takes into account these hydraulic load effects in polder canal levee systems. Application of this approach on two case studies showed that, on the system level, the estimated levee failure probabilities for most levees were significantly reduced, compared to the current practice, where these system effects are not taken into account. On the individual levee section, the reduction in failure probability was the highest for levee sections that are relatively strong, compared to nearby levee sections. A smaller reduction in failure probability was found for the weaker levee sections (levee sections with a relatively high probability of failure, compared to nearby connected levee sections), since they are more likely to fail. This has several consequences for current practice:

- On the one hand, strengthening of a weaker levee section, reduces flood risk locally, but might result in an increased flood risk elsewhere in the system.
- On the other hand, strengthening of a relatively strong levee (failure probability lower than that of surrounding levee sections) might have negligible results on the failure probability, and hence flood risk, since

the failure probability was already low in the first place.

Chapter 3 clearly shows that the effects of hydraulic load interdependency significantly reduce the flood risk in the system, and can therefore not be neglected in flood risk assessments. By taking hydraulic load interdependency explicitly into account, the impact of flood risk reduction measures can be assessed on a system level.

Research question 2: How can evidence of survived loads and observations of the actual levee condition be included in safety assessments of polder canal levees?

Levees are often functioning well for years, often even for many decades. Existing levees have therefore already survived combinations of hydraulic loading without showing any signs of losing structural integrity. These survived loading conditions contain information that can significantly reduce uncertainty in levee reliability assessments, resulting in significant reductions in the estimated failure probability. Important information on the actual state of the levee can be obtained from regular levee inspections. These inspections give an impression of the actual state of the levee. Levee inspectors often find the levee in similar conditions as during previous inspections. Sometimes however, signs of levee degradation are observed. This levee degradation influences the structural integrity of a levee in a negative way.

The pragmatic approach that is developed in Chapter 4 improves the credibility of levee reliability analyses by including observations of survived loads and current levee performance observations from levee inspections. Application of the developed approach on a case study demonstrated that taking into account such information can significantly improve the reliability assessment and prevent unnecessary levee strengthening.

Research question 3: How do meteorological inputs influence the phreatic line in polder canal levees?

On a levee section scale, levee stability is influenced by external and internal loading variables. In current practice, the focus is mainly on water levels in the canal. However, precipitation and evaporation also influence levee stability, because they influence the pore pressures within the levee body. In current methods, this effect of rainfall and evaporation is not explicitly taken into account.

In Chapter 5, the relation between rainfall and evaporation and the phreatic line was established through time series analysis. The analysis showed that the variability in the phreatic line was mainly dominated by rainfall and evaporation, rather than water level changes. Conceptual hydrological modelling was then used to reproduce the phreatic line over a time period of 15 months. In most cases, the best fit was obtained if the process of preferential flow was included in the model. In conclusion, the phreatic line in levees responds differently to rainfall and evaporation, depending on local levee characteristics. Not taking this into account in safety assessments, leads to inaccurate results of the levee safety assessment

6.2 Recommendations for future studies

To further improve on the methods and concepts proposed in this dissertation, the following recommendations are made:

Develop a pragmatic and practically feasible method for determining flood probabilities for canal levees. As this dissertation shows, moving towards failure probabilities creates opportunities for including many aspects that are currently not included in safety assessments of regional levees. The effects of hydraulic

load interdependencies, evidence of survived loads, and current levee conditions on the failure probability are demonstrated in this dissertation. Another important aspect not dealt with in this dissertation is the length effect: the effect that the longer the levee section, the more likely it contains a weak spot. Incorporating these components into levee reliability assessments results in more accurate levee reliability and flood risk estimations. These flood risk estimations are crucial for cost-benefit analysis, which help prioritize and compare flood risk reducing measures. Therefore, a pragmatic method should be further developed, so that water authorities can determine flood probabilities in a practically feasible way.

Expand the set of possible load conditions to estimate hydraulic load interdependency. During an event, the amount of rainfall, rainfall pattern, and timing of the event vary in space and time. Also wind direction and velocity can change. Preliminary conditions influence the storage capacity of the canals and water levels on the water bodies where the canal system is discharging to, influence how much water can be discharged. This will result in a more complete estimation of the effect of hydraulic load interdependency.

Further develop fragility surfaces for levees in the system. Each levee section has a different response to rainfall, depending on its soil composition, geometry, and initial conditions. This means that local, extreme rainfall might cause a critical situation within a levee section locally, while other levee sections in the system are less affected. A critical situation can even occur without a high canal water level. The accuracy of reliability estimations can be improved by combining the levee's response to the canal water level and to rainfall in a fragility surface. A pragmatic approach would be to derive fragility surfaces for different levee typologies, based on relevant

levee characteristics, such as geometry, soil composition, and water retaining height. This means that for different levee typologies the relation between the Safety Factor (SF) and reliability index (β) need to be determined. Therefore, this relation between SF and β has to be further investigated and validated on large data sets, so that practitioners can easily make use of the found relations.

Investigate effects of degradation on levee stability. Degradation reduces the levee's strength. The reduction factor not only depends on the extent of the degradation, but also on the local levee conditions, such as soil composition and characteristics and geometry. To estimate the relative effect of degradation on the levee's reliability, detailed reliability estimations are needed with and without the effects of degradation. Possibly, a generalized reduction factor can be found per type of degradation for levees with similar characteristics. If degradation is observed in levee sections with similar characteristics, this reduction factor can be directly applied to estimate levee reliability, without doing additional reliability calculations.

Extensive measurement campaigns on phreatic lines. Changes in the phreatic line in canal levees are dominated by rainfall and evaporation. But how the phreatic line responds to these meteorological inputs, can vary significantly per location, as a consequence of heterogeneity in the subsoil. Therefore, the current one-size-fits-all approach, that is used to determine the extreme phreatic line, is not an accurate estimation of the phreatic line. As we have seen in measurements, the observed phreatic line can even exceed the estimated phreatic line. Unfortunately, detailed measurement campaigns of hydraulic heads in a levee section, and rainfall, evaporation and water levels at a levee section are lacking. If these measurements exist, their measurement period is usually too short

to cover a large variety of circumstances: normal, dry and wet years. A measurement period of at least 5 to 10 years is recommended to ensure that a range of circumstances has been measured. Besides the length of the measurement period, a large variety of measurement locations should be included in the measurement campaign, to be representative for the canal levees in the Netherlands. Eventually, this contributes to a better insight into how the phreatic line behaves under normal and extreme conditions, which will improve the levee stability estimations.

6.3

Recommendations for current practice

Based on the topics researched in this dissertation, recommendations are made for current practice that will help improving the outcomes of flood risk assessments:

Express flood protection standards in failure probabilities instead of exceedance probabilities. This means that a shift is necessary, moving from the current approach towards a new approach: that of flood probabilities, in which a levee failure probability has a central place. The methods derived in this dissertation have proven applicable and valuable. Further elaborating them and incorporating them into levee design and safety assessment procedures will significantly improve the accuracy of flood risk estimations, and enhances cost-effectiveness in flood management.

Include hydraulic load interdependencies in levee reliability assessments. The effects of hydraulic load interdependencies significantly influence the failure probabilities of levees, and hence the flood risk in the system. These effects must be taken into account for levee safety assessments, and also in assessment of flood risk reduction measures. This ensures

that the most cost-effective measures are taken.

Include hydraulic load interdependencies in the design of polder systems. The principles of system behaviour have to be implemented in the design and management of the polder system. This means that strengthening levees so that it meets a higher safety standard, could have a counter-intuitive negative effect on the system risk. To further exploit the system behaviour effects, overflow structures can be implemented at locations where flooding causes relatively low damage, to reduce the hydraulic loads in the system.

More emphasis on levee inspection and monitoring. Levees have often proven their strength over the past decades, due to survived loads. In this dissertation, plausible assumptions for survived loads are used, because observations were lacking. Ideally, actual observations are available. Water levels in the system and rainfall are already monitored at many locations in the system. If the resolution is increased to the levee section level, data can be obtained from all the load combinations the levee survived during its lifetime, or at least for the period where the data is available.

More frequent levee inspections: increases the amount of information the levee manager has on the actual levee condition. Visual inspections are often carried out by professional levee inspectors, but are time consuming and costly. Remote sensing techniques are a promising complement. For example, Özer et al. (2019) showed a way to monitor levee deformation on the system scale.

Include the effect of rainfall in reliability estimations. The effect of rainfall on the phreatic line differs per levee section, and is dependent on local conditions. By acknowledging this and properly account for this in stability assessments,

more accurate reliability estimations can be made. This requires on the one hand, an additional effort to obtain local information on levee characteristics, such as soil composition and characteristics. On the other hand, it requires monitoring of the hydraulic head, soil moisture and deformation.

Appendix A - Derivation of fragility surfaces

This appendix contains the fragility surfaces developed and used in Chapter 3. Fragility curves are often used to represent the failure probability of a levee section as a function of a hydraulic load variable, usually the water level (in 2D). In this appendix, it is explained how the fragility surfaces that were used in Chapter 3 were developed: the failure probability of a levee section expressed as a function of two hydraulic load variables.

Different loading variables determine the probability of failure of a levee. The water level is often considered as the dominant loading variable. However, precipitation can also be important, as it can lead to saturation of the levee. In this appendix, 4 fragility surfaces are presented for different types of levees. For the fragility surfaces presented here, the relationship between the failure probability and the water level is based on the width of the levee, whereas the relationship between the failure probability and precipitation is based on the thickness of the clay cover layer. The assumption is that levees with a narrow crest become are more sensitive to water level increases than levees with a wider crest. Levees with a thin or absent clay

cover layer are more sensitive to rainfall than levees with a thick clay cover layer. The fragility surface is determined using the following equation:

$$P(F | P, h) = \alpha_p \left(\frac{P}{\gamma_p} \right)^{\beta_p} + \alpha_h \left(\frac{h - h_{target}}{\gamma_h - h_{target}} \right)^{\beta_h}$$

In which P is the amount of rainfall during the event [mm], h is the local water level [m+NAP], h_{target} is the target water level in the canal [m+NAP]. In the case study of the Schermerboezem the target water level was -0.5m + NAP. Parameters α , β , and γ are fitting parameters that determine the shape of the fragility surface. It should be noted that the values in this study are assumed and are not based on any kind of safety assessment. The fragility surfaces do, however, reflect the sensitivity of the levee to the water level and rainfall, based on levee characteristics. The parameter values used in this study are presented in Table A.1 and Table A.2.

Table A.1

Parameters that determine the sensitivity of the levee to the water level based on the width of the levee crest.

| | α_h [-] | β_h [-] | γ_h [m+NAP] |
|---------------|----------------|---------------|--------------------|
| Narrow | 1.0 | 0.5 | 1.5 |
| Wide | 0.2 | 0.8 | 2.0 |

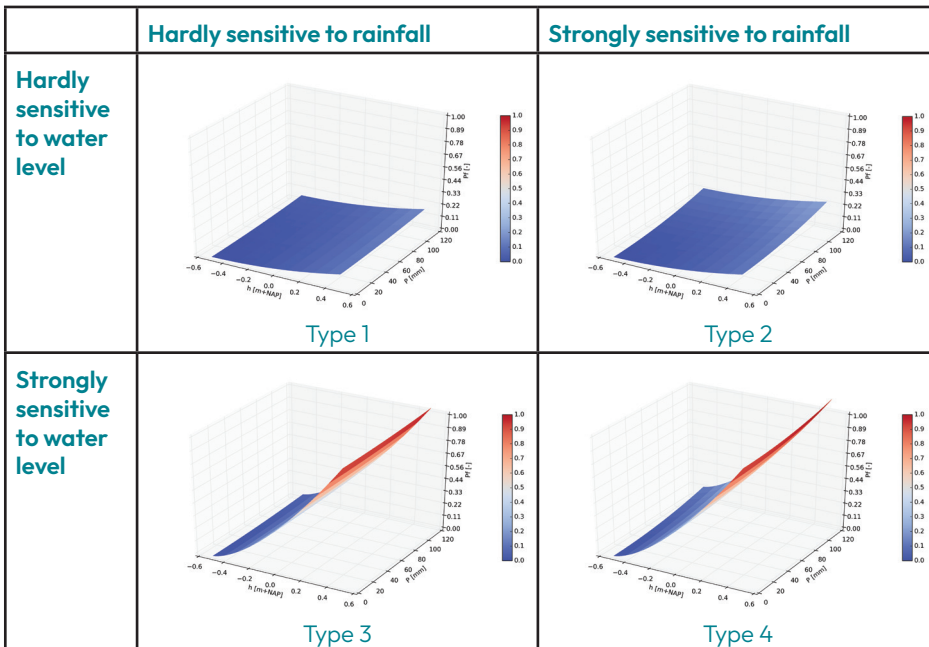
Table A.2

Parameters that determine the sensitivity of the levee to rainfall based on the thickness of the clay cover layer.

| | α_r [-] | β_r [-] | γ_r [mm] |
|-------------------------------|----------------|---------------|-----------------|
| Thin clay cover layer | 0.3 | 200.0 | 2.0 |
| Thick clay cover layer | 0.1 | 200.0 | 2.0 |

Figure A.1

Fragility surfaces which show per levee the failure probability as function of the outer water level and the cumulative precipitation.



Appendix B - Results of cross-correlation analysis

This appendix contains the results of the cross-correlation analysis performed for hypothesis testing in Chapter 5: meteorological inputs dominate changes in the phreatic line. The figures in this appendix show in the left plot the Pearson correlation coefficient when the different variables are compared to the hydraulic head in the crest, landside slope and landside toe of the levee. Time series of the following variables were compared to the observed hydraulic head:

- Accumulated rainfall in one hour (P (h));
- Accumulated rainfall in one day (P (d));
- Accumulated rainfall in 2 days (P (2d));
- Accumulated rainfall in 5 days (P (5d));
- Accumulated rainfall in 10 days (P (10d));
- Accumulated rainfall excess (rainfall – evaporation) in 5 days (RE (5d));

- Accumulated rainfall excess (rainfall – evaporation) in 10 days (RE (10d));
- Instantaneous canal water every hour (CWL).

The right plot of the figures in this appendix shows the optimal lag time [hours] for which the optimal Pearson correlation coefficient was found.

Note: at location 4 we see very large lags (up to 3800 hours). Further analysis has shown that when the rainfall excess over longer periods was used in the analysis, the Pearson coefficient could go up to 0.51 in the crest (rainfall excess over previous 40 days, with a lag of 91 hours). For the slope the Pearson coefficient could go up to 0.756 (rainfall excess over previous 100 days, with a lag of 487 hours).

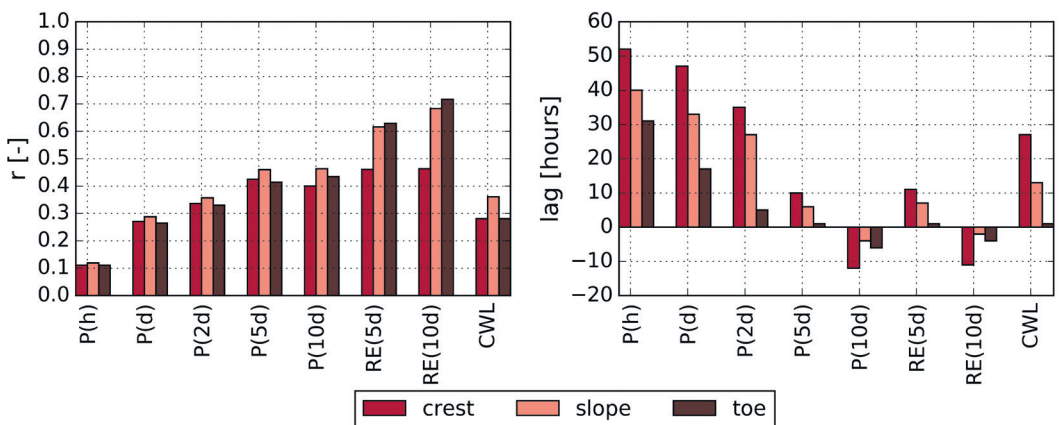


Figure B.1

Results of the cross-correlation analysis for location 1, showing the Pearson correlation coefficient r on the left and the lag [in hours] on the right.

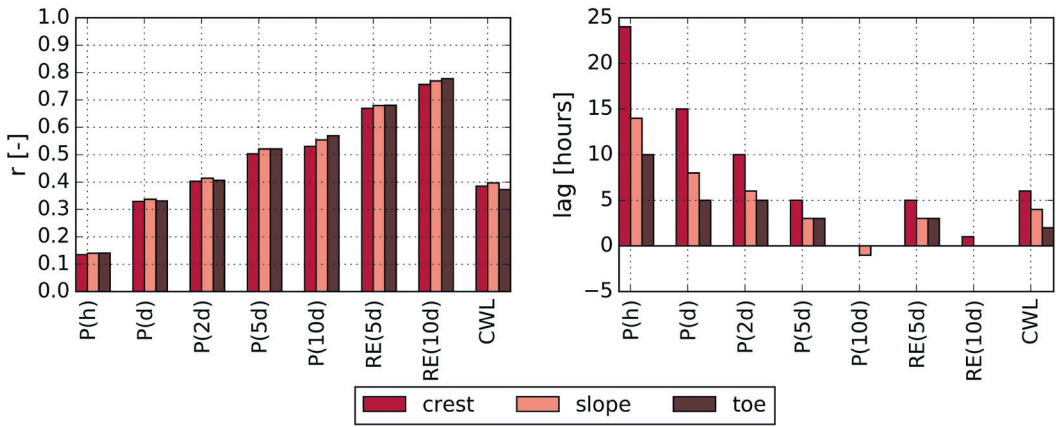


Figure B.2

Results of the cross-correlation analysis for location 2, showing the Pearson correlation coefficient r on the left and the lag [in hours] on the right.

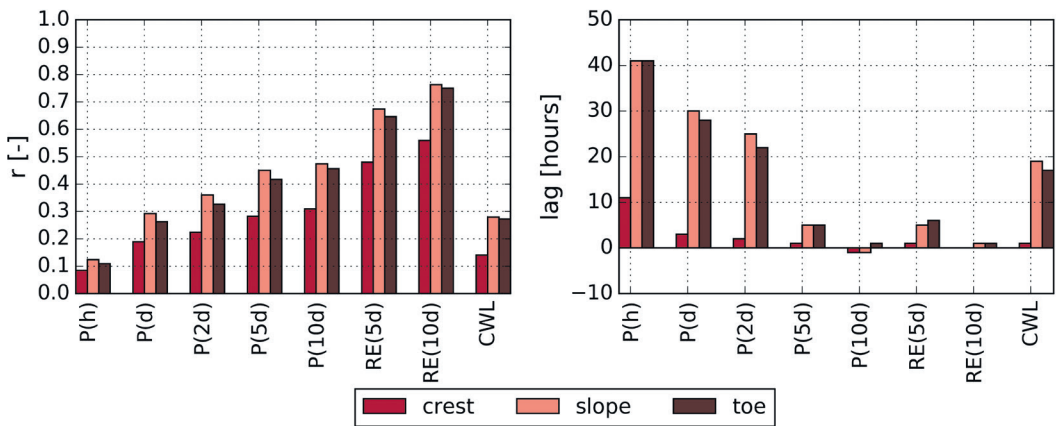


Figure B.3

Results of the cross-correlation analysis for location 3, showing the Pearson correlation coefficient r on the left and the lag [in hours] on the right.

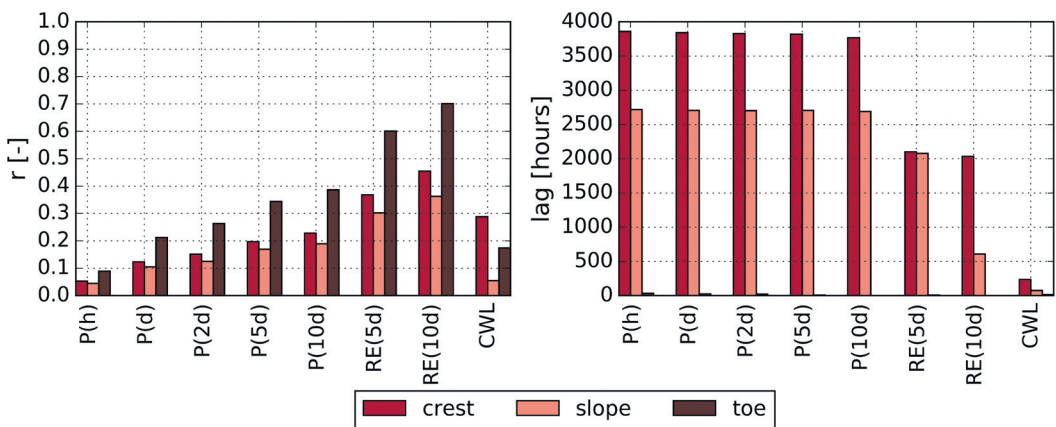


Figure B.4

Results of the cross-correlation analysis for location 4, showing the Pearson correlation coefficient r on the left and the lag [in hours] on the right.

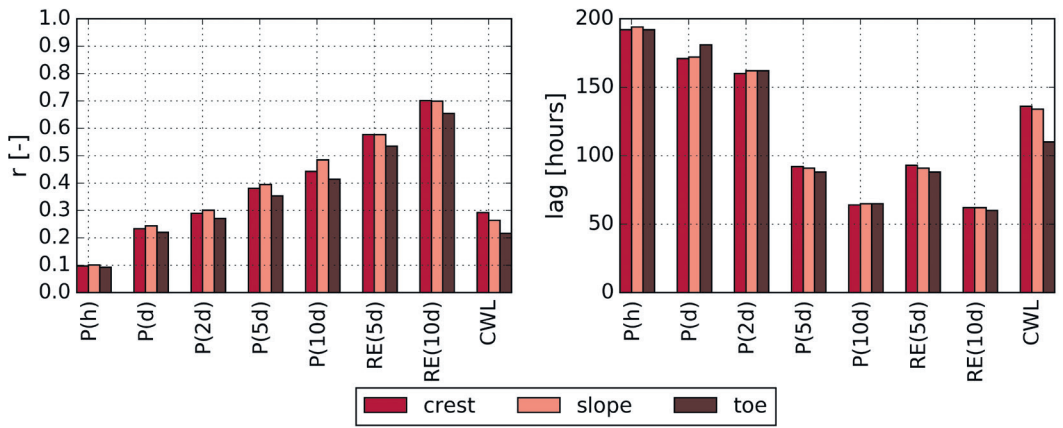


Figure B.5
Results of the cross-correlation analysis for location 5, showing the Pearson correlation coefficient r on the left and the lag [in hours] on the right.

Note: at location 5 we see large lags, although much smaller than at location 4. If the rainfall excess over 30 days is used, the Pearson coefficient reaches its maximum in the crest, slope and the toe: 0.82, 0.813, and 0.779, respectively. The corresponding lag times are 5, 6, and 5 hours, respectively.

References

- Apel, H., Thielen, A.H., Merz, B., & Blöschl, G. (2004). Flood risk assessment and associated uncertainty. *Natural Hazards and Earth System Science*, 4(2), 295-308.
- Apel, H., Thielen, A.H., Merz, B., & Blöschl, G. (2006). A probabilistic modelling system for assessing flood risks. *Natural hazards*, 38(1), 79-100.
- Apel, H., Merz, B., & Thielen, A.H. (2009). Influence of dike breaches on flood frequency estimation. *Computers & Geosciences*, 35(5), 907-923.
- Beven, K. J. (2011). *Rainfall-runoff modelling: the primer*. John Wiley & Sons. p20.
- Bishop, A. W. (1955). The use of the slip circle in the stability analysis of slopes. *Géotechnique*, 5(1), 7-17.
- CIRIA (2013). *The International Levee Handbook*. CIRIA.
- Courage, W., Vrouwenvelder, T., van Mierlo, T., & Schweckendiek, T. (2013). System behaviour in flood risk calculations. *Georisk: Assessment and Management of Risk for Engineered Systems and Geohazards*, 7(2), 62-76.
- De Bruijn, K.M., Diermanse, F.L.M., & Beckers, J.V.L. (2014). An advanced method for flood risk analysis in river deltas, applied to societal flood fatality risk in the Netherlands. *Natural Hazards and Earth System Sciences*, 14(10), 2767.
- De Bruijn, K., Slager, K., Piek, R., Riedstra, D., Slomp, R. (2018). *Leidraad voor het maken van overstromingssimulaties*.
- De Vriend, H. J., Kok, M., Pol, J. & Hegnauer, M. (2016). *Heeft de Rijnafvoer bij Lobith een maximum? Expertisenetwerk Waterveiligheid*.
- Deltares (2015). *Basisstochasten WTI-2017. Statistiek en statistische onzekerheid*.
- Deltares 2016. *D-Geo Stability. Slope stability software for soft soil engineering: User Manual*. Delft: Deltares.
- Deltares (2018). *SOBEK - 1D/2D modelling suite for integral water solutions, User Manual 2.16, versie 1.00*. Delft, Nederland.
- De Kok, J.L., & Grossmann, M. (2010). Large-scale assessment of flood risk and the effects of mitigation measures along the Elbe River. *Natural hazards*, 52(1), 143-166.
- De Loor, D. (2018). *An Analysis of the Phreatic Surface of Primary Flood Defences*. Delft University of Technology (MSc thesis).
- Dorst, P. (2019). *Modelling the phreatic surface in regional flood defences*. Delft University of Technology (MSc thesis).

Flanagan, M. and Tigchelaar, J. (2016). Waterspanningen in regionale en overige keringen. Analyse 4,5 jaar metingen Delfland. (In Dutch)

Fugro (1998). Methodiek voor de bepaling van het vereiste veiligheidsniveau van boezemkaden. Opdrachtnummer M-0293.

Geuze, A., Feddes, F. (2005). Polders! Gedicht Nederland. NAI Uitgevers - IABR, Rotterdam. ISBN: 90-5662-444.

HHNK (2015). Veiligheidstoets Boezemkaden Starnmeer. Technisch oordeel + Beheerdersoordeel.

HHNK (2019a). Toetsing boezemkades Eilandspolder.

HHNK (2019b). Bestuurlijke voortgangsrapportage regionale keringen over het jaar 2018. Version 1.3, Report number: 19.0237729.

Hieselaar, L. (2010). Tuindorp Oostzaan onder water. Overstroming maakte 11.000 mensen tijdelijk dakloos. Geraadpleegd van: <https://onsamsterdam.nl/tuindorp-oostzaan-onder-water>

Historisch Archief Tuindorp Oostzaan, z.d. Watersnood 1960. Geraadpleegd van: <http://www.historischarchief-toz.nl/350-2/>

Hoes, O.A.C., Van de Giessen, N.C. (2018). Polders. Lecture notes. Delft University of Technology.

IPO (1999). IPO-richtlijn ter bepaling van het veiligheidsniveau van boezemkaden.

Jamalinia, E., Vardon, P., & Steele-Dunne, S. (2019). The effect of soil-vegetation-atmosphere interaction on slope stability: a numerical study. *Environmental Geotechnics*, 1-10.

Jamalinia, E., Vardon, P. J., & Steele-Dunne, S. C. (2020). The impact of evaporation induced cracks and precipitation on temporal slope stability. *Computers and Geotechnics*, 122, 103506.

Jongejan, R. B., Maaskant, B., Ter Horst, W. L. A., Havinga, F. J., Roode, N., & Stefess, H. (2013). The VNK2-project: a fully probabilistic risk analysis for all major levee systems in the Netherlands. In *The 5th international conference on flood management (ICFM5)*, Tokyo, Japan (pp. 75-85). IAHS press.

Kanning, W., Vastenburger, E., Kames, J., Van der Heijden, E. (2017). Bewezen sterkte regionale keringen. Deltares. Technical Report (in Dutch).

Klerk, W.J. (2013). Load interdependencies of flood defences. A new methodology for incorporating load interdependencies in flood risk analysis of lowland. TU Delft, MSc thesis.

Klerk, W.J., Kok, M., De Bruijn, K.M., Jonkman, S.N., & van Overloop, P.J. (2014). Influence of load interdependencies of flood defences on probabilities and risks at the Bovenrijn/ IJssel area, The Netherlands. In Proceeding of the 6th international conference on flood management-ICFM6, 1-13.(2014). Brazilian Water Resources Association and Acquacon Consultoria.

Kok, M. (2006). Schade na een overstroming. Taak van overheid of eigen verantwoordelijkheid? *Externe Veiligheid*, 4, 15-17.

Kok, M., Jongejan, R., Nieuwjaar, M., & Tanczos, I. (2017). Fundamentals of Flood Protection. Ministry of Infrastructure and the Environment and the Expertise Network for Flood Protection.

Konings, V., Van Hemert, H. (2020). Kwalitatief toetsen van de veiligheid van regionale keringen. Resultaten pilots – concept.

Kwakman, L., Van Loon, O. (2019). Rapportage studie invloed degradatiekenmerken.

Lanzafame, R. C. (2017). Reliability Analysis of the Influence of Vegetation on Levee Performance (Doctoral dissertation, UC Berkeley).

Leau, J. de, Bijnen, J., Fila, J. (2019). Toetsing boezemkades Eilandspolder. Uitgangspunten en toetsing. IV-Infra report number: INFR180772 R-01

Lendering, K.T., Jonkman, S.N., Kok, M. (2015). Flood risk of regional flood defences. Technical report.

Lendering, K.T., Schweckendiek, T., & Kok, M. (2018). Quantifying the failure probability of a canal levee. *Georisk: Assessment and Management of Risk for Engineered Systems and Geohazards*, 12(3), 203-217.

Lendering, K.T., Van der Krogt, M., Rikkert, S.J.H., Kok, M. (2018). Faalkans updating o.b.v scenario's voor stabiliteit van regionale keringen. Amersfoort: STOWA.

Lendering, K.T. (2018). Advancing Methods For Evaluating Flood Risk Reduction Measures (Doctoral dissertation, Delft University of Technology).

LOLA Landscape Architects (2014). Dijken van Nederland.

Maaskant, B. (2021). Overschrijdingskans – overstromingskans regionale keringen. Technische vergelijking tussen de overschrijdingskans en overstromingskans. Technical report in Dutch. Amersfoort, 2021. ISBN: 978.90.5773.918.7.

Makkink, G.F. (1957a). "Examination of the formula by Penman." *Neth. J. Agric. Sci.*, 5, 290-305 (in Esperanto).

McClave, J. T., Benson, P. G., Sincich, T., & Sincich, T. (2014). *Statistics for business and economics*. Essex: Pearson.

Ministry I&E (2009) National water plan. Ministry of Infrastructure and the Environment, The Netherlands (in Dutch)

Monden, M., R. van Opstal, B. Zwartendijk (2020). Optimalisatie dijkversterkingen op basis van meting en modellering van het freatisch vlak. Civiele techniek.

Moriasi, D. N., Arnold, J. G., Van Liew, M. W., Bingner, R. L., Harmel, R. D., & Veith, T. L. (2007). Model evaluation guidelines for systematic quantification of accuracy in watershed simulations. *Transactions of the ASABE*, 50(3), 885-900.

Nicolai, R., Kok, M., Rikkert, S.J.H. (2017). Kosten baten afweging versterken regionale waterkeringen. Analyse effect van versterkingskosten op kadeverbetering van gestileerde cases. PR3565.10. August, 2017. (In Dutch).

Nieuwjaar, M.W.C. (2020). De veiligheidsbenadering regionale keringen. Ontstaan, achtergronden en toepassing van de huidige veiligheidsbenadering voor regionale keringen. Amersfoort, 2020. Technical Report (in Dutch). ISBN 978.90.5773.864.7

NOS, z.d. 100 jaar strijd tegen het water. Geraadpleegd van: <https://app.nos.nl/evenementen/droge-voeten/>

O'Connell, P.E. (1991). A historical perspective. In Bowles, D.S., & O'Connell, P.E. (Eds.). *Recent advances in the modeling of hydrologic systems*, p3-30.

Özer, I.E., Rikkert, S.J.H., van Leijen, F.J., Jonkman, S N., & Hanssen, R.F. (2019). Sub-seasonal levee deformation observed using satellite radar interferometry to enhance flood protection. *Scientific Reports*, 9(1), 1-10.

OECD (2012). *OECD Environmental Outlook to 2050*, OECD Publishing. <http://dx.doi.org/10.1787/9789264122246-en>

Pleijster, E.J. & van der Veeke, C. (2015), *Dikes of the Netherlands*, LOLA Landscape Architects, The Netherlands.

Province of South Holland (2019). *Samenvatting voortgangsrapportages regionale keringen 2018*. Voortgang van de verbeteropgave aan de regionale waterkeringen van de in Zuid-Holland gelegen waterschappen. Report number: PZH-2019-697784228.

Rikkert, S.J.H., Kok, M. (2019). The failure probability of canal levees from a statistical perspective. *H2O - Water Matters*. Edition 1, 2019.

Schweckendiek, T. (2014). *On reducing piping uncertainties: A Bayesian decision approach*. Delft: Delft University of Technology.

Schweckendiek, T., Vrouwenvelder, A.C.W.M., & Calle, E.O.F. (2014). Updating piping reliability with field performance observations. *Structural Safety*, 47, 13-23.

- Schweckendiek, T., Teixeira, A., Krogt, M.G. van der, & Kanning, W. (2016). "Reliability updating for slope stability of dikes - Test cases report." Deltares report number 1230090-037-GEO-0001.
- Sellmeijer, H., de la Cruz, J. L., van Beek, V. M., & Knoeff, H. (2011). Fine-tuning of the backward erosion piping model through small-scale, medium-scale and IJkdijk experiments. *European Journal of Environmental and Civil Engineering*, 15(8), 1139-1154.
- STOWA (2004). Overzicht normen waterveiligheid en wateroverlast. Utrecht. ISBN: 90.5773.236.X
- STOWA (2008). Richtlijn – Normering keringen langs regionale rivieren. Amersfoort. ISBN 978.90.5773.401.4.
- STOWA (2009). Materiaalfactoren boezemkaden. Amersfoort. ISBN: 978.90.5773.420.5.
- STOWA (2015a). Leidraad toetsen op veiligheid regionale waterkeringen. Amersfoort
- STOWA (2015b). Actualisatie meteogegevens voor waterbeheer 2015. Deel 2: Statistiek van de extreme neerslag. Rapport: 2015-10. ISBN 978.90.5773.706.0.
- STOWA (2015c). Vergelijking landsdekkende neerslagproducten. Amersfoort.
- STOWA (2016) - Visie op regionale waterkeringen 2016. Verder bouwen op een goed fundament.
- STOWA (2018). Handboek Dijkbewaking. Waarnemen 2018.
- TAW (1993). Systematisch kade-onderzoek: de resultaten. Delft, 1993. Technical report. In Dutch.
- Ten Bokkel Huinink, J.G.F. (2016). Assessment of the probability distribution of the phreatic surface in a regional flood defence: Finite element computation for a better understanding of the influence of precipitation on the phreatic surface. Delft University of Technology (MSc thesis).
- Tsuchida, T., & Athapaththu, A. M. R. G. (2014). Practical slip circle method of slices for calculation of bearing capacity factors. *Soils and Foundations*, 54(6), 1127-1144.
- USACE (2015). Levee Screening Tool – Technical Manual.
- Verheij, H.J. (2003). Aanpassen van het bresgroeimodel in HIS-OM. WL-Delft Hydraulics. Q3299.
- Vrouwenvelder, A.C.W.M., Van Mierlo, M.C.L.M., Calle, E.O.F., Markus, A.A., Schweckendiek, T., & Courage, W.M.G. (2010). Risk analysis for flood protection systems. Main report, TNO and Deltares, Delft, the Netherlands.

Van Baars, S. (2005). The horizontal failure mechanism of the Wilnis peat dyke. *Géotechnique*, 55(4), 319-323.

Van Beek, V. M. (2015). Backward erosion piping: initiation and progression.

Van Esch, J. M. (2012). Modeling groundwater flow through embankments for climate change impact assessment. In *Proceedings, 19th International Conference on Computational Methods in Water Resources (CMWR 2012)*. University of Illinois at Urbana-Champaign, USA.

Van der Meer, M.T., Kapinga, H.S.O., Jonkman, L.N., Lam, K.S., Calle, E.O.F. (2009). *Materiaalfactoren boezemkaden*. STOWA, Amersfoort, the Netherlands. (Report in Dutch). ISBN: 978.90.5773.420.5.

Curriculum Vitae

Stephanus Johannes Hendrikus Rikkert

30-08-1990 Born in Almelo, the Netherlands.

Education

- Master Civil Engineering, track: Water Management at Delft University of Technology, graduated in 2015. Specialisation: Hydrology. MSc-thesis topic: Improving model consistency and process realism in conceptual rainfall-runoff models.
- Bachelor Civil Engineering and Management at the University of Twente, graduated in 2012. BSc-thesis topic: Modelling the urban drainage system in Hanoi, Vietnam for flood predictions.
- High school, track: Nature and Technology, and Nature and health, graduated in 2008.

Work

2020 – current

Delft University of Technology, Faculty of Civil Engineering and Geosciences, Hydraulic Engineering, Coastal Engineering

Researcher

In this period I participated on behalf of the Delft University in the international Polder2C's project. This project aimed, among other, at increasing knowledge of the levee resistance against continuous overflow and wave overtopping conditions. Over 3 kilometers of levee was available for full-scale testing. I have contributed mainly to performing the tests in the field and modelling of the hydrodynamic conditions and erosion.

2016 – 2022

Delft University of Technology, Faculty of Civil Engineering and Geosciences, Hydraulic Engineering, Hydraulic Structures and Flood Risk

PhD-researcher

My research focused on improving methods to assess flood risk in regional flood defences, with this dissertation as a result. Other responsibilities were the guidance and supervision in of students in their BSc and MSc thesis projects, and contributing to courses, such as Flood Defences.

List of publications

Journal publications

Özer, I.E., Rikkert, S.J.H., van Leijen, F.J., Jonkman, S N., & Hanssen, R.F. (2019). Sub-seasonal levee deformation observed using satellite radar interferometry to enhance flood protection. *Scientific Reports*, 9(1), 1-10.

Rikkert, S.J.H., Kok, M., Lendering, K.T., Jongejan, R. Jongejan (2021). A pragmatic, performance-based approach to levee safety assessments. (submitted, under review)

Conference contributions

Rikkert, S.J.H., Kok, M. (2017). Consequences of breaches in canal systems on flood risk. 7th International Conference on Flood Management (ICFM7), Leeds, UK, 15-17 September 2017. Book of Abstracts – Poster presentation.

Van Damme, M., Ozer, I.E., Rikkert, S.J.H., & van Leijen, F. (2018, June). Preliminary Results of the Safelevee Project. In ICOLD World Congress 2018: 1-7 July 2018, Vienna, Austria.

Rikkert, S.J.H., Kok, M. (2019). Importance of rainfall events on levee stability. European Geosciences Union conference 2019 (EGU2019). Vienna, Austria, 7-12 April 2019. Geophysical Research Abstracts, Vol. 21. EGU2019-9638. Oral presentation.

Rikkert, S.J.H., Kok, M. (2019). Hydraulic load interdependencies: a case study on a regional flood defence system in the Netherlands. System Risk – ETN. Flood risk: Interactions, temporal changes and System approaches. Potsdam, Germany, 17-19 September 2019. Oral presentation.

Rikkert, S.J.H., Alleon, C., Khaldi, I., Shaiek, S., Verelst, K., Ebrahimi, M., Soares-Frazão, S., Kaidi, S., Smaoui, H., Sergent, P. (2021). How strong are our levees? Hydraulic analysis based on Polder2C's project in-situ testing. SimHydro 2021: Models for complex and global water issues - Practices and expectations. Sophia Antipolis, France, 16-18 June 2021. Oral presentation.

Professional magazines

Rikkert, S.J.H., Kok, M. (2019). The failure probability of canal levees from a statistical perspective. H2O - Water Matters. Edition 1, 2019.

Özer, I.E., Rikkert, S.J.H., van Leijen, F.J., Jonkman, S N., & Hanssen, R.F. (2019). Dijkinspecties vanuit de ruimte: droom of werkelijkheid? Land+Water, nr.5, May 2019. (in Dutch)

Reports

Lendering, K., Van der Krogt, M., Rikkert, S.J.H., Kok, M. (2018). Faalkans updating o.b.v scenario's voor stabiliteit van regionale keringen. Amersfoort: STOWA. (In Dutch).

Nicolai, R., Kok, M., Rikkert, S.J.H. (2017). Kosten baten afweging versterken regionale waterkeringen. *Analyse effect van versterkingskosten op kadeverbetering van gestileerde cases*. PR3565.10. August, 2017. (In Dutch).